Author: **F. Belloni**
Reviewer: **Cyrille Thomas, ESS**
Jacques Marroncle, CEA
Date: January 23, 2017
Version: 1.0

Space Charge based model of an IPM

CEA SACLAY document number: CEA-ESS-DIA-RP-0018 v0.1

Contents

Chapter 1

Space charge effects

1.1 Introduction

In 2015 CEA engaged in the construction of five Non invasive Profile Monitors (NPMs) in the frame of the in-kind contribution agreement signed with ESS.

Based on requirement of level 4 for the measurement of the beam profile and beam size, on both horizontal and vertical axis, and for any pulse delivered, the preliminary studies concluded that no interceptive instrument can achieve this. For very small beam current, and limited up to 50 µs pulse, a very well established instrument is sensitive enough to deliver a reliable beam transverse profile, and beam transverse size, a so-called Wire-Scanner[1]. For pulses that are longer than 50 µs, another instrument has to be chosen. Therefore the studies concluded that Non-invasive Profile Monitors shall be built, covering the range of charge per pulse from 10^{13} - corresponding to a 50 µs full peak current pulse - and up to the maximal beam charge. In the Cold Linac section of the accelerator, the residual gas pressure is expected to be 10^{-9} mbar. As a result, the best candidate to read a beam profile is based on ionization of the gas interaction with the beam. The instrument to measure the ionization based beam profile is called a Ionization Profile Monitor (IPM). Every NPM is thus composed of two IPMs, which can be pictured as two cubes of approximately $10 \times 10 \times 10$ cm^3 and separated by few cm. Each box will be equipped with two electrodes setting a uniform electric field inside its volume. The two electric fields will be orthogonal to each other and both perpendicular to the beam direction.

One of the main issues the beam profile monitors will be confronted with is the space charge effect. ESS will deliver proton pulses 2.86 ms long with a duty cycle of 4% and a peak current equal to 62.5 mA. The beam beam bunch frequency will be 352 MHz, which translates into 1.1 10^9 protons per bunch. Besides, the r.m.s beam size dimension is typically $\sigma_{x,y,z} = 3 \times 3 \times 1$ mm^3.

Such intense proton bunches will generate not negligible electromagnetic fields and may modify the trajectories of the photoelectrons and ions created via the ionization of the residual gas and deriving towards the electrodes. This may lead to a distortion of the projected initial distribution of the ions/electrons, and thus the read profile may not represent an image of the beam transverse profile.

Understanding and eventually correcting for the distortion is essential to validate a measurement delivered by the NPM. To this aim, we developed a numerical code modeling an NPM, taking into account the 3D spatial distribution of moving bunches.

[1] No wire can withstand the interaction with ESS full peak current pulses longer than 50 µs without breaking

The code has been benchmarked against other codes and also against real IPM measurements from the PS (CERN)[1]

From the code, we will see in the following that there are two cases: either the distortion is less than 10% and thus negligible, or it is larger than 10%, in which case possible correction can be implemented to recover the initial distribution. The possible corrections methods are:

- application of larger electric fields between the two electrodes of each box
- application of a magnetic field parallel to the electric field direction in order to force the e^-/ion pairs to move in spiral along the electric field direction
- simulations to reconstruct the non-distorted beam profile

The first two possibilities listed above are "in flight" corrections allowing to avoid software treatment on the collected data. Space constraints in the LWUs where the NPM are installed makes the second correction method impracticable. However, the first and the last possibilities listed above apply. A high difference of potential between the electrodes of the IPM will limit the space charge effects and a systematic study of the output beam profile as a function of the input proton beam parameters and applied electric fields can be used to retrieve the initial beam widths on the basis of the obtained final ones.

1.2 Simulations

A simulation to reproduce the space charge effects experienced by the ionization particles has been implemented in MATLAB[2] on the basis of [2] and translated into C++ coupled to ROOT[3].

The code creates an electron or an ion with the desired mass and charge according to the user request. This particle is generated around the center of one IPM box following a Gaussian distribution in x and y with sigmas equal to σ_x and σ_y of the incident proton beam and following a uniform distribution along the z dimension. Such procedure allows to correctly reproduce the ionization process since, for a fixed gas composition and pressure and for a certain kinetic beam energy, its probability is higher where the proton beam density is higher. Moreover, given the extremely low density of the residual gas (10^{-9} mbar), the proton beam is not really likely to interact with the gas molecules and be slowed down. Therefore the ionization process can be considered linear along the z axis and hence the choice of a uniform distribution.

The charged particle generated, known as test particle, will start moving under the influence of the uniform electric field established between the two electrodes of the IPM as well as following the electromagnetic field induced by the moving proton beam. The motion equation in an interval dt is solved by applying the adaptive step size Runge-Kutta-Fehlberg algorithm. The test particle is therefore displaced by dx and the fields to whom it is subjected in the new position are computed. A new displacement dx is performed in the time dt and step by step the particle reaches the electrode, where its position is recorded.

At this point another test particle, with the same mass and charge as the previous one, is generated in the center of the IPM box following the space distributions seen before. Its trajectory is reconstructed step by step and its final coordinates on the electrode stored.

[2]Work performed by C. Thomas

[3]Work performed by F. Belloni

This procedure is repeated 10000 times, in order to achieve a statistical uncertainty on the results of 1%.

Generally speaking, it is expected that the lower the applied electric field, the higher the space charge effect. In the same way, the lighter the deriving ion and the more important the modification of its trajectory. Finally, the denser the proton beam distribution, the more severe the space charge effect.

1.3 Results

The code has been run considering a proton beam of 90 MeV kinetic energy in one case, 200 MeV in a second case and 1 GeV in a third case. For every kinetic energy, more simulations have been launched, each one with a different uniform electric field imposed in the detector (50 kV/m, 100 kV/m, 200kV/m, 300kV/m, 600 kV/m and 1000 kV/m). Finally, for each electric field, the code has been run for a certain set of proton beam widths. The nominal r.m.s bunch sizes values for the ESS accelerator, σ_x, σ_y and σ_z, can be found in [3], where the reported maxima are σ_x = 3.0 mm, σ_y = 3 mm and σ_z = 2.8 mm. Nevertheless the simulations were run for the following root mean square configurations: σ_x = 0.5 mm, 1.4 mm, 3.2 mm, 4.1 mm, 5 mm or 10 mm, σ_y = 0.5 mm, 1.4 mm, 3.2 mm, 4.1 mm, 5 mm or 10 mm, and σ_z = 0.75 mm, 2 mm and 10 mm. Given the residual gas composition (79 % H_2, 10% CO_2, 10% CO and 1% N_2) the code have been launched both for electrons and for H_2^+ as test particles. Other ions created via ionization of the residual gas are CO^+, CO_2^+... Being heavier than H_2^+, these ions will be less affected by the presence of the proton beam.

The graphs reported in the next pages summarize the main features of the results for these simulations (for detailed results of all simulations run, see the Appendix), where the test particles were created at rest (speed = 0 m/s). In all simulations, the test particles were generated according to the following distributions:

- ALONG X: Gaussian distribution centered around 0 and with width equal to σ_x of the proton beam
- ALONG Y: Gaussian distribution centered around 0 and with width equal to σ_y of the proton beam
- ALONG Z: Uniform distribution between -2.5 mm and +2.5 mm

  This last condition implies that, when σ_z = 0.75 mm the portion of area scanned along the z direction represents 6.6 σ_z, but reduces to 2 σ_z for σ_z = 3.2 mm and to 0.5 σ_z when σ_z = 10 mm. As a consequence, a test scanning the whole z direction was performed to check the impact of such choice on the root mean square calculated by the code and is reported at the end of this chapter.

1.3.1 Trend of the final σ_x (σ_{xf}) as a function of the beam energy

The plot reported in Fig. 1.1 shows that, given a fixed electric field and beam widths along the y and z direction, the space charge effects diminish when the proton beam energy increases. This depends on the particular cases studied.

It is possible to develop the mathematical formulae used to calculate the space charge effects to extract a general rule, but this rule results to have limited validity. Following [2], let a Gaussian bunch with total charge Q_b move with the velocity v_b along the z-axis of the laboratory frame K. The Lorentz-Force on a point charge Q_0 is calculated from the

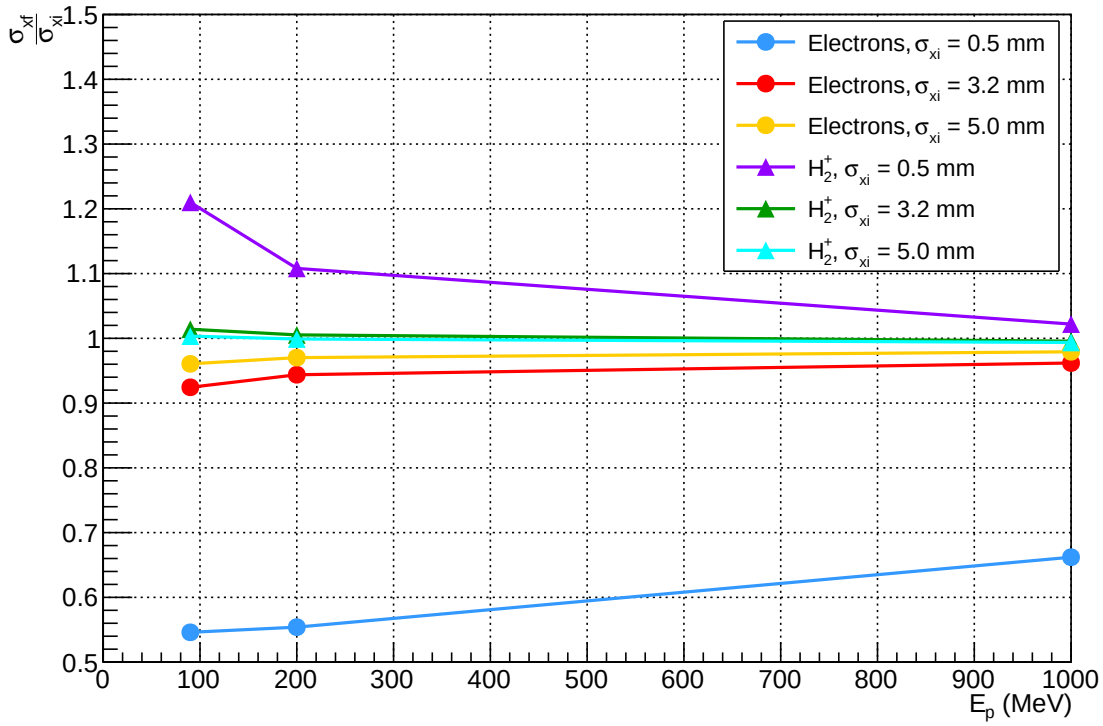

Figure 1.1: Trend of the final σ_x (σ_{xf}) to initial σ_x (σ_{xi}) as a function of the proton beam energy for an applied electric field equal to 300 kV/m, and initial proton beam widths along the y and z direction equal to σ_{yi} = 3.2 mm and σ_{zi} = 2 mm.

electric field of the bunch computed in the co-moving frame $\overline{K}$ and transformed back to the laboratory frame K (see Fig. 1.2).

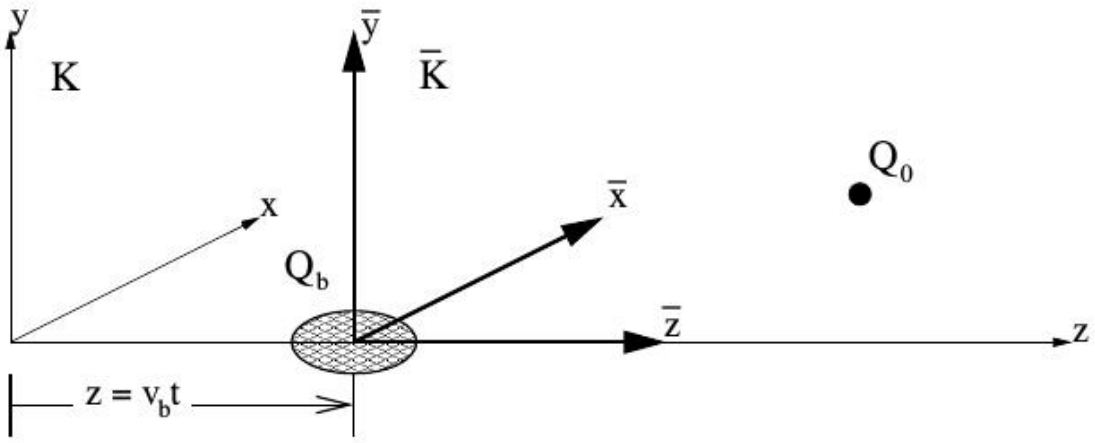

Figure 1.2: Laboratory frame K and rest frame $\overline{K}$ of a Gaussian bunch. Picture taken from [2].

From the velocity of the beam v_b the normalized velocity β_b and the relativistic factor γ_b are calculated as:

$$\beta_b = \frac{v_b}{c}, \qquad \gamma_b = \frac{1}{\sqrt{1-\beta_b^2}}$$

The electric field in the co-moving frame $\overline{\mathbf{E}}$ is linked to the electric (**E**) and magnetic field (**B**) in the laboratory frame by the following relations:

$$\boldsymbol{E} = \begin{pmatrix} E_x \\ Ey \\ Ez \end{pmatrix} = \begin{pmatrix} \gamma_b \overline{E}_x \\ \gamma_b \overline{E}_y \\ \overline{E}_z \end{pmatrix}, \qquad \boldsymbol{B} = \begin{pmatrix} -\gamma_b \beta_b \overline{E}_y / c \\ \gamma_b \beta_b \overline{E}_x / c \\ 0 \end{pmatrix} = \frac{\beta_v}{c} \begin{pmatrix} -E_y \\ E_x \\ 0 \end{pmatrix}$$

The Lorentz force on a point charge Q_0 with velocity **u** is:

$$\boldsymbol{F} = Q_0(\boldsymbol{E} + \boldsymbol{u} \times \boldsymbol{B}) = Q_0 \begin{pmatrix} (1 - \beta_b u_z/c) E_x \\ (1 - \beta_b u_z/c) E_y \\ Ez + \beta_b (E_x u_x/c + E_y u_y/c) \end{pmatrix}$$

For really low proton beam energies, $\beta = 0$, while for relativistic energies $\beta \to 1$. Moreover let $E_x = E_z = 0$. The Lorentz force, for $\beta = 0$, becomes:

$$\boldsymbol{F}_{\boldsymbol{\beta=0}} = \begin{pmatrix} 0 \\ Q_0 E_y \\ 0 \end{pmatrix}$$

while the Lorentz force for $\beta = 1$ becomes:

$$\boldsymbol{F}_{\boldsymbol{\beta=1}} = \begin{pmatrix} 0 \\ Q_0 E_y (1 - v_z/c) \\ Q_0 E_y v_y / c \end{pmatrix}$$

From the two previous relations it is already visible that, if the charge Q_0 is not moving ($v_x = v_y = v_z = 0$), the force it feels **at a certain time t** is independent of the proton beam energy. If the test charge is instead moving, the force it feels in the laboratory system is higher for low proton beam energies than for a relativistic proton beam if $\boldsymbol{F}_{\boldsymbol{\beta=0}} > \boldsymbol{F}_{\boldsymbol{\beta=1}}$:

$$\sqrt{(Q_0 E_y)^2} > \sqrt{(Q_0 E_y)^2} \sqrt{(1 - v_z/c)^2 + (v_y/c)^2}$$

This means when:

$$1 > \sqrt{1 + \frac{v_z^2}{c^2} - 2\frac{v_z}{c} + \frac{v_y^2}{c^2}}$$

The root square of the member in the right side of the inequality exists whenever $v_y^2 \geq -(c - v_z)^2$. This is always the case. The inequality reported above is satisfied for:

$$c - \sqrt{c^2 - v_y^2} < v_z < c + \sqrt{c^2 - v_y^2}$$

The right part of the inequality is always true for $v_y < c$, while the left part is true for $v_z > c - \sqrt{c^2 - v_y^2}$. All this holds only when the particle Q_0 has the same v_y and v_z for $\beta = 0$ and $\beta = 1$. In other words, if we take the case $\beta = 0$ and and at the time t the particle is in the position x1, y1, z1 and has speed $v_y = v_{y1}$ and $v_z = v_{z1}$ and then we take the case $\beta = 1$ and and at the time t the particle is in the same position x1, y1, z1 and has the same speeds $v_y = v_{y1}$ and $v_z = v_{z1}$, then the previous discussion applies.

Since in the simulations the initial location of the electrons (or ions) created by ionizing the gas is randomly sampled, it is unlikely that, for two different runs (one with a proton energy equal to 90 MeV and another with proton energy equal to 200 MeV) these particles are in same position at the same time. On the other side it is possible to observe the collective behavior of the electrons (or ions) at specific times while they move towards the collection electrode (see Fig. 1.3 and Fig. 1.4).

The two pictures here above (Fig. 1.3 and Fig. 1.4) show the result of two simulation whose initial conditional differ only for the value of the considered proton beam energy. Every ellipse in the plots above is a snapshot of the electron cloud at a certain time. As visible from the pictures, the electromagnetic field generated by the proton beam passing by acts as a lens, first focusing and then defocusing the electron cloud. The coordinates of the focus (i.e. where the electron cloud is more compact) change with the beam parameters and applied external electric field.

1.3.2 Trend of the final σ_x (σ_{xf}) as a function of the applied electric field

Intuitively, the higher the difference of potential applied between the electrodes of the IPM, the more the ionized particles (electrons and H_2^+) will tend to follow the field lines of the imposed electric field. Moreover, the higher the mass of the considered test particle, the less its trajectory is deviated by the presence of a charged proton beam passing by.

In Fig. 1.5 one can see the final beam size at the collection electrodes as function of the electric field strength, and for several initial beam size values. The deviation from the initial beam size value, σ_{xi}, decreases in absolute value for increasing strength. Also, the absolute deviation seems to be less for ions than for electrons. So the general rule of the thumb seems to apply. For ions, and for beam size 3.2 mm, the deviation is less than 10% for a field strength larger than 100 kV/m. For electrons, the same initial beam size value is less than 10% for 200 kV/m.

For very the small initial beam size 0.5 mm, the deviation for ions is still around 20%. But in the case of ions, the trend shows that the deviation get smaller for higher field strength.

For electrons, there seems to be no intuitive trend. This could be explained by the focusing effect of the proton beam on opposite charged particles. The focus point position seems to be a function of the field strength and also beam density compactness. These two effects may move the focus point in opposite directions. With high field, the points may be moved towards infinity. With high beam density, the focus point may moves towards the center of the beam. At this point, this partial analysis is based on the observation of the trajectories [1]. Further analysis is required to eventually conclude for the case of electrons.

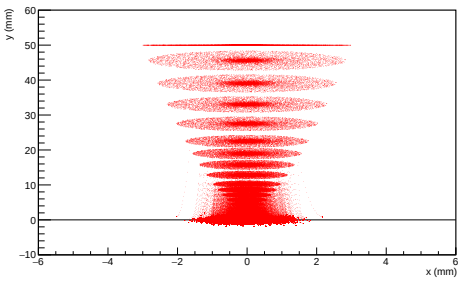

Figure 1.3: Snapshot of the electron cloud moving towards the electrode at y = 5 cm for different times. The simulation was run in the following conditions: electric field 600 kV/m, proton energy = 90 MeV, $\sigma_{xi} = \sigma_{yi} = 0.5$ mm and $\sigma_{zi} = 0.75$ mm.

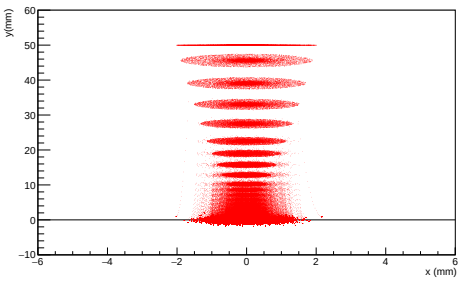

Figure 1.4: Snapshot of the electron cloud moving towards the electrode at y = 5 cm for different times. The simulation was run in the following conditions: electric field 600 kV/m, proton energy = 200 MeV, $\sigma_{xi} = \sigma_{yi} = 0.5$ mm and $\sigma_{zi} = 0.75$ mm.

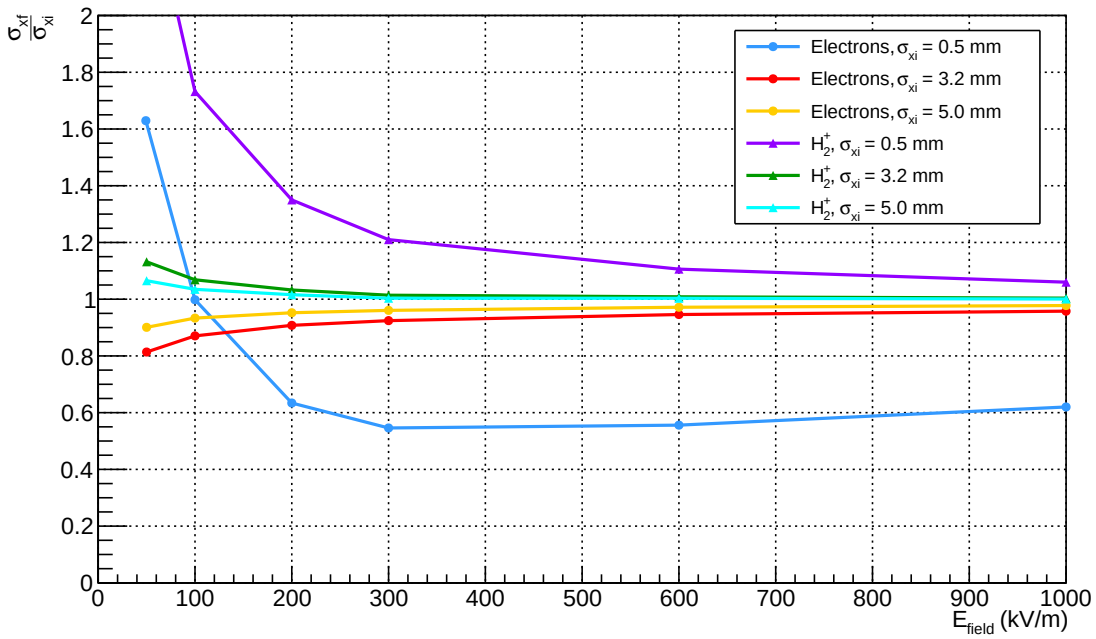

Figure 1.5: Trend of the final beam size (σ_{xf}) relative to the initial beam size (σ_{xi}) as a function of the applied electric field for a proton beam energy equal to 90 MeV, and initial proton beam widths along the y and z direction equal to σ_{yi} = 3.2 mm and σ_{zi} = 2 mm.

1.3.3 Trend of the final σ_x (σ_{xf}) as a function of the initial σ_y (σ_{yi})

The space charge effect depends on the beam distribution density. So the influence of the beam size measured on one axis by the beam size on the orthogonal axis should be understood. Fig. 1.6 shows the influence of the initial beam size along the orthogonal direction on the final beam size. The extreme case of an initial beam size of 0.5 mm is shown here. In the case of protons, the variation of the orthogonal beam size from 0.5 mm to 5 mm, shows the final relative beam size to decrease form 80% to 20% and for an electric field equal to 200kV/m. The same trend is to be observed with other values of the field strength. In the case of electrons, the trend is more difficult to comprehend. However, a larger orthogonal beam size seems also to induce less deviation to the final beam size.

1.4 Example of simulated beam profile at the collecting electrode

The following pictures 1.7, 1.8 and 1.9 compare the initial proton beam profile with the final ones at the collected electrode in three particular conditions. In all cases the initial beam is round with its size equal in both dimensions, but it is varied from 0.5 mm to 3.2 mm.The beam size along the propagation axis is 0.75 mm; the electric field is equal to 300 kV/m and the proton beam energy is 90 MeV.

Looking at the profiles for ions, the profiles look somehow slightly blown out from the Gaussian. And the calculated beams size by means of Moments analysis deviated from the original one from 40% to less than 3%. Besides, the final beam size is always larger, due to the defocusing effect. So the initial profile is always enlarged. In the cases of extremely small beam sizes a transformation may be used to regularise the distribution

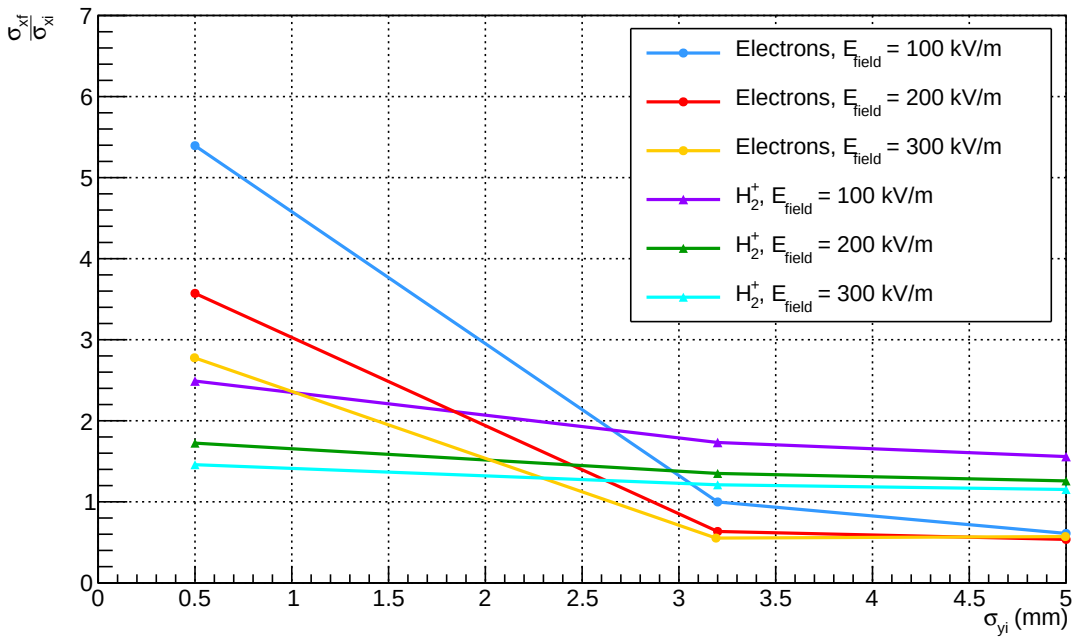

Figure 1.6: Trend of the final beam size (σ_{xf}) relative to the initial beam size (σ_{xi} = 0.5 mm) as a function of the initial orthogonal beam size (σ_{yi}) for a proton beam energy equal to 90 MeV; the reported values are also shown for different applied electric fields. The initial proton beam size along the z direction equal to σ_{zi} = 2 mm.

profile. This may be done by mean of a transform operator. This operator which can compensate for the defocusing may be a regular operator, in the sense that no pole may appear in the transform operator. This is a favorable case which make any correction trustful.

The profile of the electrons is compressed, highly peaked, and with large feet for smaller initial beam sizes. The distortion seems to be stronger for electrons. Besides, the focusing effect, which depends on the initial beam size, can be an issue for the regularisation of the profile. Indeed, the focus point may lead to the existence of poles in the transform operator, which makes the problem Ill-defined.

For the NPM, the information on the profile is a requirement with error less than 10%. In order to match this requirement, a detector based on ions collection seems to be preferable. Indeed, the correction appears to be minimum with ions that with electrons, and the regularisation of the profiles may be based on a more robust transform operator.

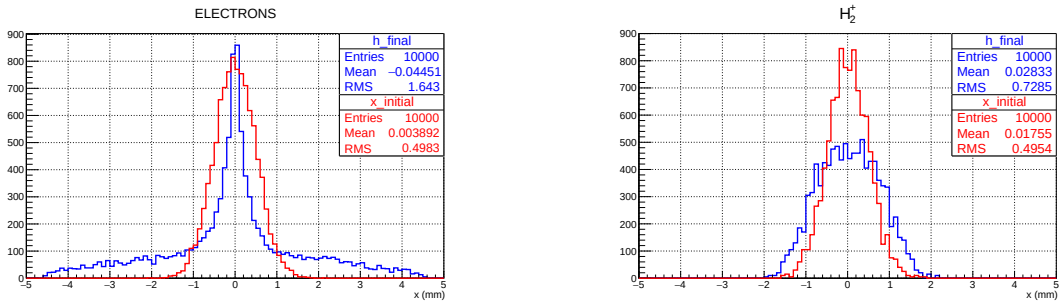

Figure 1.7: Comparison between initial and final the beam profile from electrons (left plot) and H_2^+ ions with an applied electric field equal to 300 kV/m; the proton beam energy is 90 MeV and for the case of an extremely small beam, $\sigma_{xi} = \sigma_{yi} = 0.5$ mm and $\sigma_{zi} = 0.75$ mm.

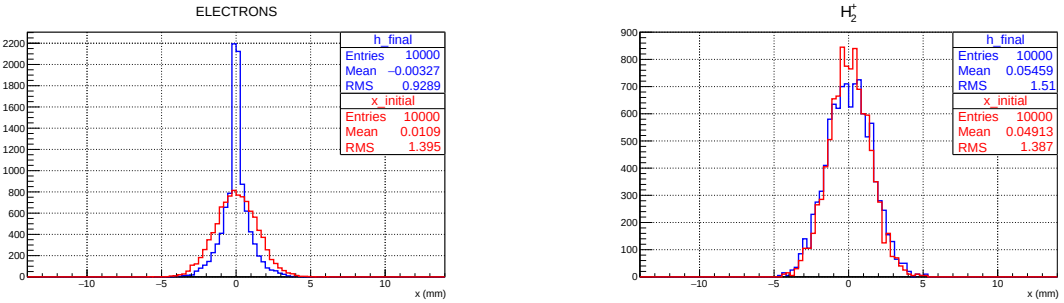

Figure 1.8: Comparison between initial and final the beam profile from electrons (left plot) and H_2^+ ions with an applied electric field equal to 300 kV/m; the proton beam energy is 90 MeV and for the case of a nominal beam size, $\sigma_{xi} = \sigma_{yi} = 1.4$ mm and $\sigma_{zi} = 0.75$ mm.

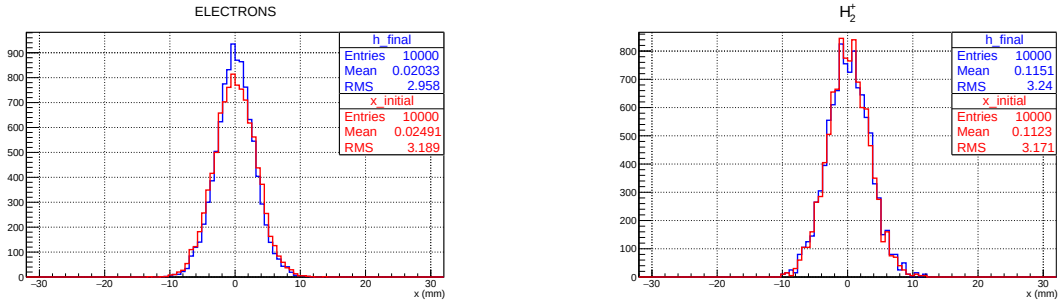

Figure 1.9: Comparison between initial and final the beam profile from electrons (left plot) and H_2^+ ions with an applied electric field equal to 300 kV/m; the proton beam energy is 90 MeV and for the case of a nominal beam size, $\sigma_{xi} = \sigma_{yi} = 3.2$ mm and $\sigma_{zi} = 0.75$ mm.

1.5 Preliminary conclusions

We have been investigating the space charge effects on to the distributions of ions and electrons generated by the ESS proton bunches and collected by the electrode of the IPMs. For this purpose, a numerical code modeling the IPM have been written and benchmarked. The results from the code can predict the performance of an IPM and in particular, the IPM planned for the case of the ESS Cold Linac NPM.

The space charge effect as function of initial conditions, beam size in 3-D, electric field strength, beam energy have been investigated for the case of the ESS beam, and at locations between the beginning of the Spoke section to the end of the High Beta section. The investigation on the space charge effect showed that for the nominal beam conditions, the profiles given by an IPM are not noticeably distorted in shape, and the beam size measured on the final distribution has less than 10% error. This represents the majority of the case that will be seen by the NPMs. Indeed, the NPM might not be sensitive to very small beam current as planned for the initial tuning. However, for increasing current and pulse duration, the beam will have to meet nominal parameters and minimum beam loss. So the use of the NPM may be relevant to check out-of-nominal condition while tuning the beam from 50 µs pulse to full pulse duration.

For extremely small beam sizes, typically less than 1 mm, the space charge effect induced by a full ESS peak current is significant. In these cases, a strategy will have to be developed so that the beam size and profile shape can be retrieved with the required accuracy. However, these extremely small beam sizes far from nominal values should not be seen in the accelerator at full peak current and long pulses, as out-of-nominal beam parameters at nominal peak current and a pulse of the order of 10 µs may be qualified as errant beam condition. Any errant beam condition with such a beam power can induce too large beam loss than acceptable (>1W/m) or even causes damage to the machine. Since the number of particle threshold to perform of profile measurement with the NPM is 10^{13} proton/bunch, which correspond to a 30 µs pulse at full peak current, the expected range of beam sizes seen by the NPM in the Cold Linac is in a small range around the nominal beam size, i.e. between 2 mm and 3 mm.

Finally, an IPM collecting ions seems to be a better choice than using electrons. Indeed, the distortion seems to be stronger for electrons. In addition, the regularisation may appear to be more difficult due to the focusing effect of the opposite charged beam.

Chapter 2

Initial electron conditions

In the previous chapter it was assumed that the electrons and ions are created at rest. In reality such approximation is quite good for ions, given their mass, but not for electrons. The GARFIELD++ [4] code was used to calculate the kinetic energy of electrons at their creation.

2.1 Speed

The considered geometry for the GARFIELD++ simulation is the following: a cube of 10 cm × 10 cm × 10 cm centered in the origin of a Cartesian frame was filled with 79% H_2, 10% CO_2, 10% CO and 1% N_2[1]. A uniform electric field of 30 kV/m was set along the Y direction. A pencil-like monochromatic protons beam of 90 MeV kinetic energy started in the position (x_0, y_0, z_0) = (0.0, 0.0, -4.99 cm) and was directed towards the z axis. The beam intensity is 1.6 10^{-19} A, therefore only one proton at a time is shot.

The nominal residual gas pressure is 10^{-9} mbar. With such low gas molecules concentration and beam intensity it would take months to acquire a distribution with some statistics. On the other hand, already at a gas pressure of 1 mbar, not more than one ionization (if any at all) per incident proton is expected in the best case scenario[2]. Therefore it is foreseen that at low enough gas pressures, the distribution of the kinetic energy of electrons at their generation will be practically constant.

A test with different gas densities was performed and the results are shown in Fig. 2.1 All curves are scaled so that their integral is the same. As seen in the figure, all lines referring to a gas pressure ≤ 1 mbar superimpose. At higher pressures, more than 1 e^-/ion pairs are expected to be created by a single proton passing through 10 cm of residual gas. Following every ionization, the proton looses some energy, therefore the n^{th} electron will not be created by 90 MeV protons, but by lower energy ones. As a consequence the electron kinetic energy will peak around a lower value. This physical explanation can not be applied to our case, since the difference between the proton energy before and after collision is of the order of the 10 eV to 100 eV, which is about 10^{-4} % - 10^{-5} % of the incident proton energy. Such percentage applied to the energy with which a first electron is emitted, will give the amount by which the kinetic energy of a second electron differs from that of the first one. And this difference is too small (100 eV · 10^{-4} %) to provoke a visible change in the distribution of the kinetic energy with which electrons are generated. What in reality happens in Fig. 2.1 is a matter of sampling. In Garfield++, when an electron is emitted, its energy is sampled from the kinetic energy distribution

[1] Source of the vacuum composition is provide by ESS vacuum group

[2] A proton of 90 MeV creates 1 e^-/ion pairs in 1 cm of 79 % H_2, 10% CO_2, 10% CO and 1% N_2 at a pressure of 1 mbar (Bethe-Bloch formula).

corresponding to a gas pressure ≤ 1 mbar. If a second electron is emitted, again the same distribution is sampled. Sampling twice the same distribution increases the probability that an electron is emitted at lower energies (it is almost as sampling from the result of the distribution corresponding to a gas pressure ≤ 1 mbar convoluted with itself).

Another feature visible in Fig. 2.1 is the presence of some lines: around 13 eV, 256 eV and 378 eV. The first can be easily identified as the hydrogen line. The other two are respectively the Auger carbon peak and the Auger nitrogen peak (see Fig. 2.2) . The ratio between the peak contents is roughly constant for gas pressures ≤ 1 mbar, but changes above such threshold.

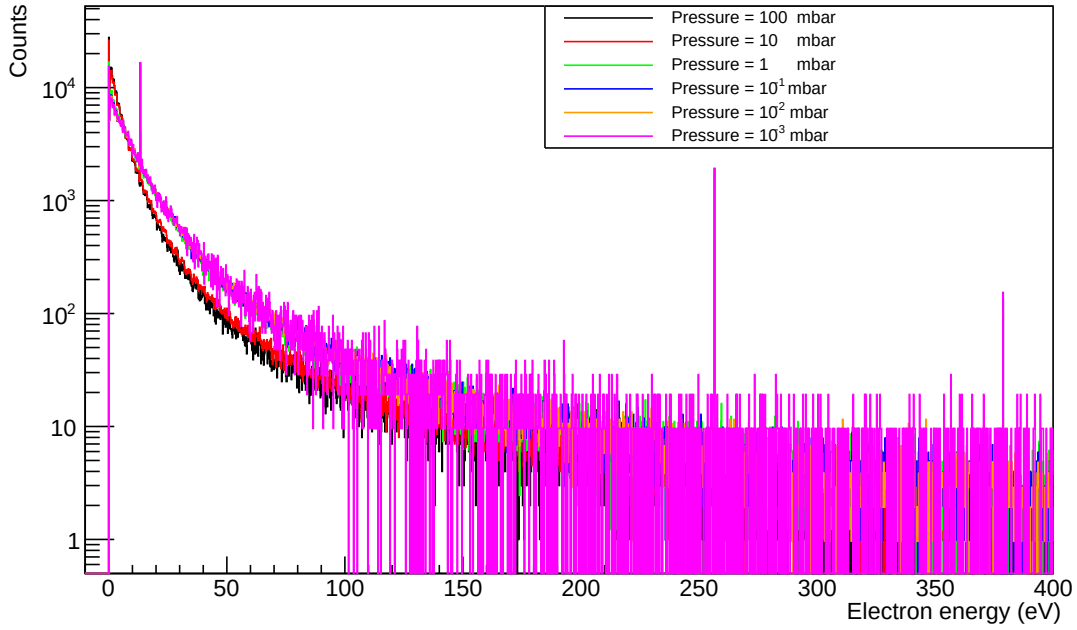

Figure 2.1: Kinetic energy distribution of electrons at their creation for different gas pressures.

2.2 Angular distribution

Garfield++ was used also to obtain the angular distribution of the primary electrons created through ionization of the residual gas. 90 MeV protons shot one by one along the Z axis are the incident particles. The projections along the X, Y and Z axis of the electron momentum normalized to 1 are plotted in Fig. 2.3, Fig. 2.4 and Fig. 2.5.

In GARFIELD++ first the ϕ (azimuthal) angle is uniformly sampled between 0 and 2π [5], and the X projection is obtained simply by creating a histogram filled with $\cos(\phi)$. This produces the plot shown in Fig. 2.3, where it is also evident that the sampling is independent of the gas pressure. The two curves in this pictures are normalized to the same integral. The only difference between the two lines is visible at x=0. The electrons emitted at 0 angle are the ones emitted at rest and therefore, following the discussion reported in the previous paragraph, they are more for higher gas densities.

The Y projection is obtained as $\sin(\phi)$, and the same arguments reported above hold.

The polar angle is "approximated by the angle of momentum transfer at the collision with a free electron, in which the given energy is transferred" [5]. In this case there is a light dependency on the gas pressure, which in reality can be traced back to the same sampling bias seen for the distribution of the speed with which electrons are emitted.

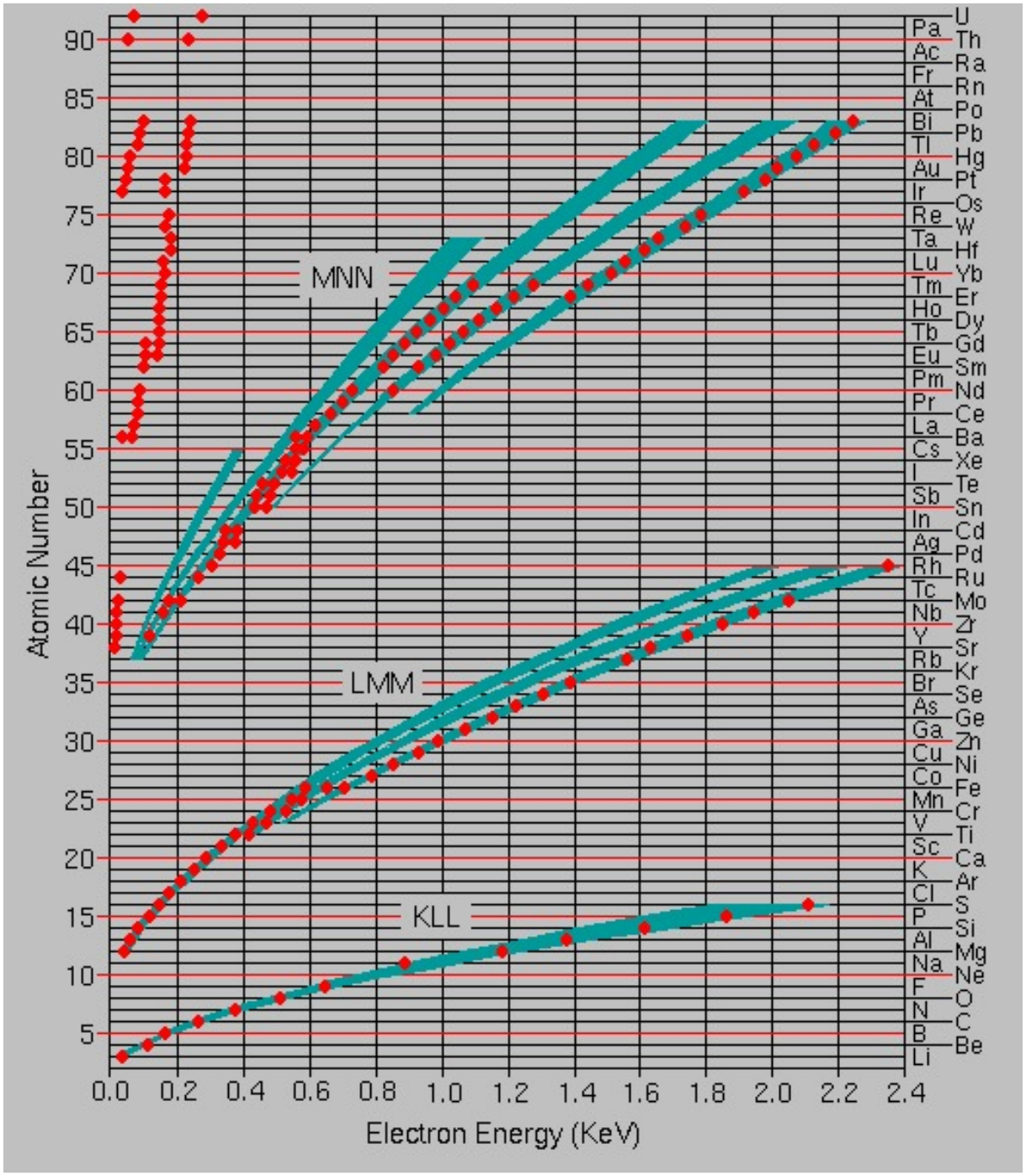

Figure 2.2: Auger electron energies.

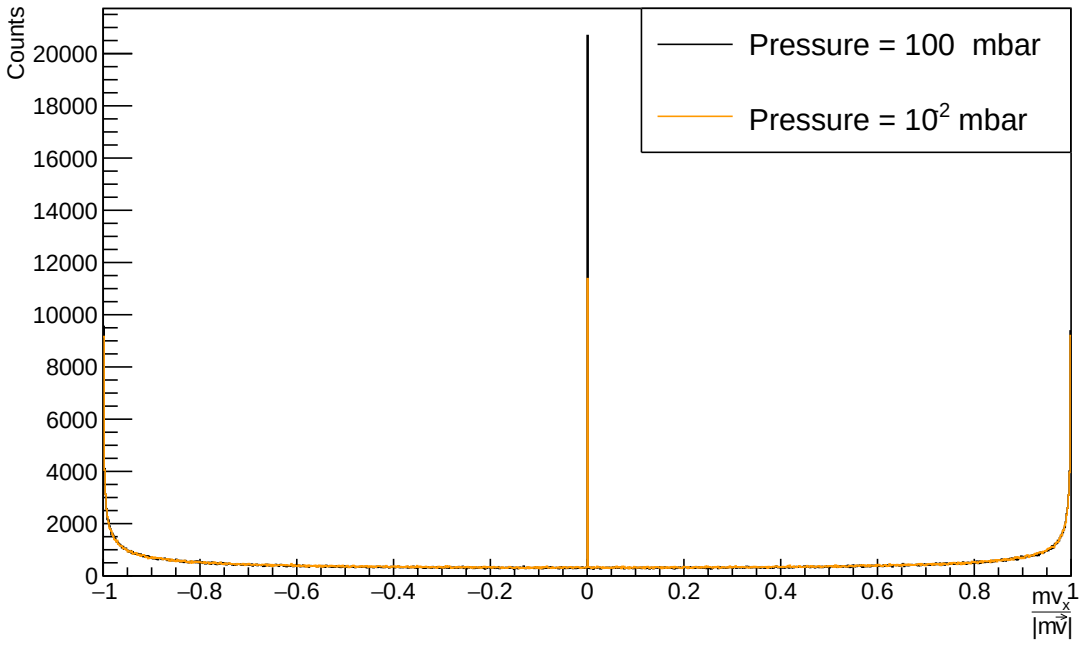

Figure 2.3: Electron momenta projected along the X axis.

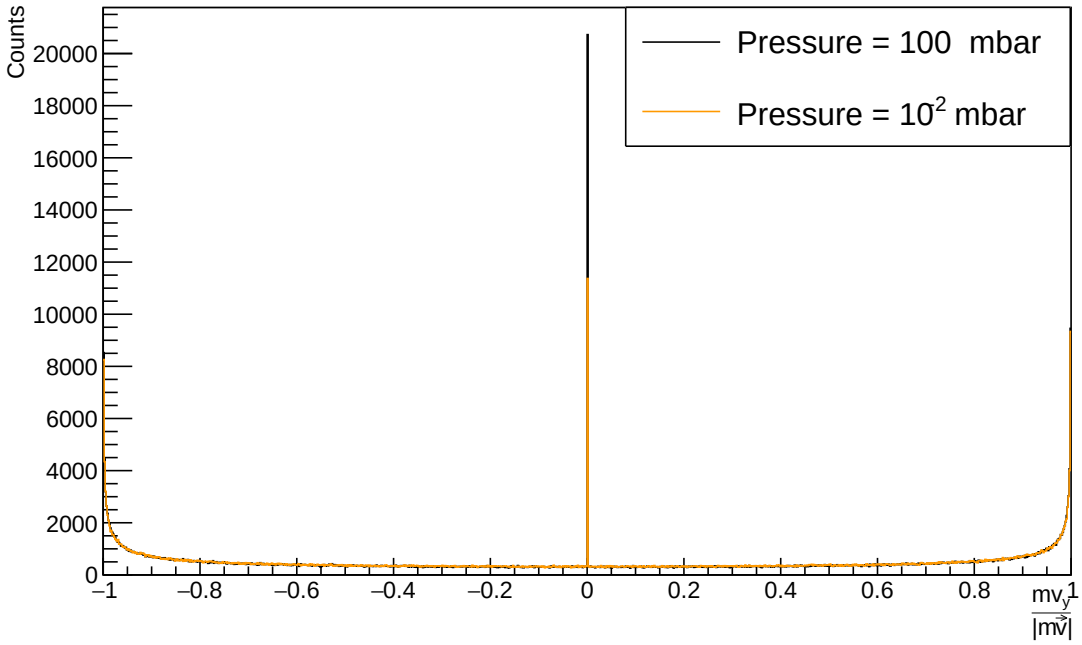

Figure 2.4: Electron momenta projected along the Y axis.

The picture reported in Fig. 2.5, as already said, corresponds to the case of 90 MeV protons ionizing the considered gas. All distributions are peaked around $\frac{mv_z}{|m\vec{v}|} = 0$, which corresponds to 90° with respect to the proton incident direction. This is due to the fact that the emission energy of most electrons is quite small. Fig. 2.5 shows also that the higher the gas pressure, the lower the number of electrons emitted isotropically. In order to understand this result, it is necessary to look at Fig. 2.6. This plot shows the emission angle of electrons of different energies for the same gas pressure. When the energy transferred to electrons is small, they tend to be emitted orthogonal to the incident proton beam direction. For intermediate electron energies, the angular distribution becomes isotropic, while at high energies the electrons are emitted at forward angles [6]. Coming back to Fig. 2.5 it is now possible to explain the difference in the plots referring to low and high gas pressures. If the gas pressure is low, only one electron is created in the whole gas volume and the polar emission angle distribution will have the shape reported for pressure equal to 10^{-3} mbar. When the gas pressure is high, on the other hand, more electrons are created. The polar emission angle distribution found for a single electron is therefore called more times. As a result, the polar emission angle distribution of a number "x" of electrons in high gas pressure is obtained by convoluting the single electron polar emission angle distribution for itself "x" times.

For a fixed gas pressure, the higher the proton energy, the lower the energy transferred to the e^-/ion pairs and (because of total momentum conservation) the more the emission angle is close to 90° with respect to the proton incident direction. Fig. 2.7 reports the polar angle distribution (acos($\frac{mv_z}{|m\vec{v}|}$)) for two different incident proton energies.

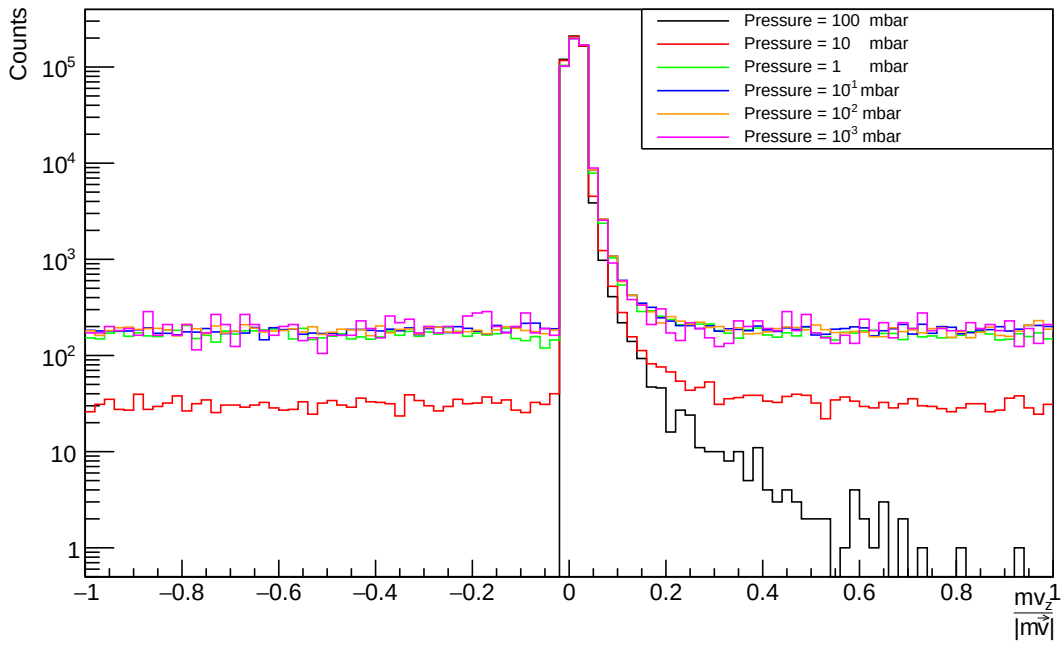

Figure 2.5: Electron momenta projected along the Z axis.

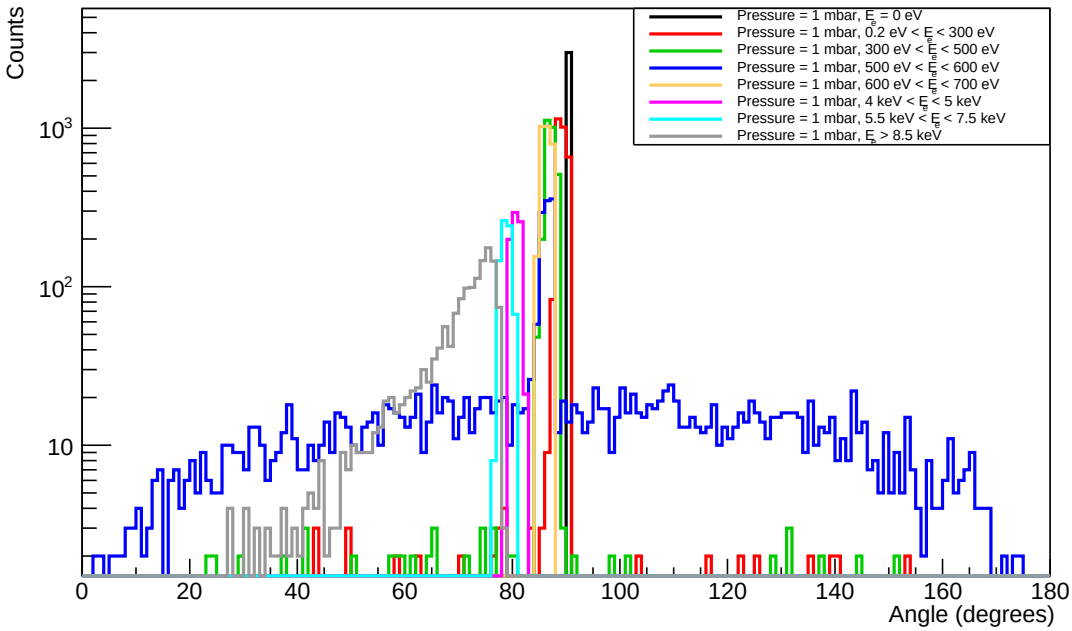

Figure 2.6: Polar angular distribution of electrons of different energies.

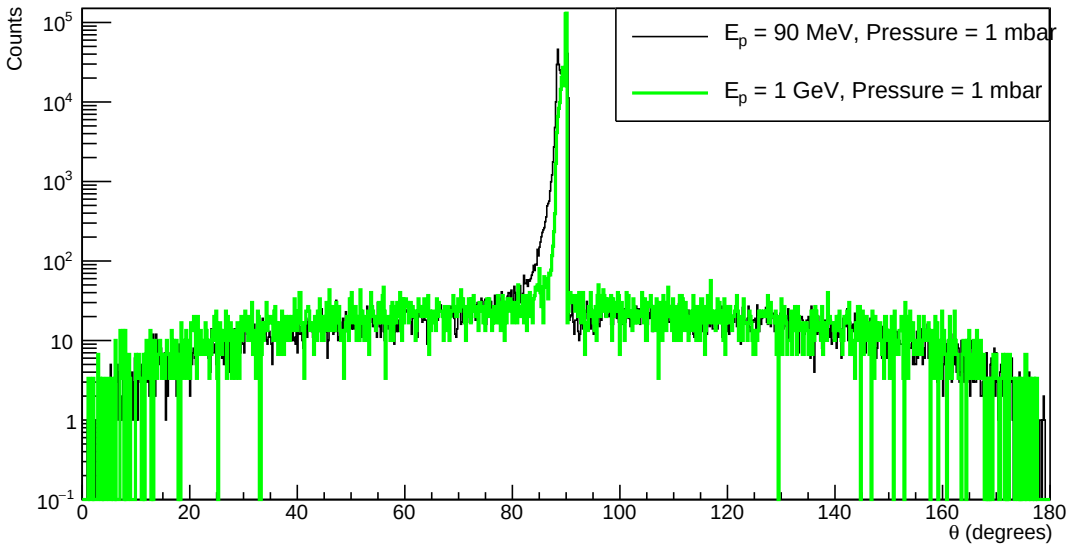

Figure 2.7: Polar angular distribution of electrons created through ionization of the gas by protons of different energies.

2.3 Spatial coordinates of the generated electrons

GARFIELD++ can give also the coordinates and time at which the electrons are generated. As a matter of fact it does so relying on the basic assumption that the incident particle beam is relativistic. Therefore, independently on the kinetic energy of the proton beam entered by the user, the instant at which the last electron is created is always the same and corresponds to the time taken by relativistic protons to travel the length of the detector.

As a consequence the x, y and z coordinates of the electrons at generation are biased by this assumption and the information was not used.

2.4 Simulations

The same type of simulations that were performed in chapter 1 were run once more for electrons and H_2^+ molecules, this time considering that the mentioned ionized particles are created with a non zero speed. For the electrons, the speed and angular distributions obtained by GARFIELD++ were used as initial values. For the H_2^+ ions it was decided, as a first approximation, to consider a total momentum of the system ion + electron equal to zero. Mathematically:

$$m_{ion}v_{ion} = m_{electron}v_{electron}$$

From the above relation, the speed of the generated ion was calculated every time as a function of the electron speed given by GARFIELD++. The emission angle of the ions was considered to be the same as the one of the electrons.

Evidently the initial speed of the electrons reach quite high values (see Fig.2.1), while the one of the ions remain low, given the multiplicative factor $v_{ion} = v_{electron}\frac{m_{electron}}{m_{ion}} = v_{electron} \cdot 2.72\ 10^{-4}$. Therefore it is expected that the introduction of an initial speed different from zero in the simulations will affects more the beam profile obtained by following electrons than ions.

The results of last set of simulations are reported in Appendix C, and point out once more the advantage of detecting ions instead than electrons.

2.5 Preliminary conclusions

In the first chapter it was assumed for simplicity that, following the passage of the ESS proton beam in the vacuum pipe, the electrons and ions created through the ionization process were emitted with zero momentum. This assumption is close to reality for ions, but not for electrons. As a second step to better approach reality, the program GARFIELD++ was used to determine the kinetic energy and angular distribution with which electrons are created when 90 MeV protons cross the sensitive volume of an IPM. From such quantities, and considering a total momentum of the system ion + electron equal to zero (condition introduced for simplicity), the speed with which H_2^+ molecules are emitted was also calculated.

A subset of the simulations run in the first chapter was relaunched, this time taking account the initial momenta of electrons and ions and their emission angle. The impact of such parameters on the final simulated beam profile was investigated (see Appendix C). As expected, the results of this new set of simulations agree with the results of the set of simulations run in the first chapter for ions. For electrons the introduction of an initial speed different from zero instead leads to a significant change of the simulation results producing a higher discrepancy between the initial and final beam width.

The IPMs can be used in ”electron mode” (the particles detected being electrons) or ”ion mode” (the particles detected been the ionized molecules) indifferently. As already pointed out, if used in ”ion mode”, smaller corrections need to be introduced for accounting for the space charge effects. In this chapter it is now shown that, if the IPMs are used in ”ion mode”, the developed MATLAB/ROOT codes alone can be used to simulate the beam profile, while if the ”electron mode” is selected, the GARFIELD++ program

needs to be run before in order to calculate the electron speed and angular distribution with which these particles are generated.

Chapter 3

Final conclusion

Being non-interceptive devices the proposed ionization profile monitors are not subjected to material vaporization caused by the high peak temperatures generated by the 1.1 10^9 protons/bunch delivered at a frequency of 352.21 MHz with a duty cycle of 4% at the ESS facility. The radiation damage induced in a detector not directly hit by the beam is moreover much smaller than the one received by a device intercepting the proton bunches. The proposed detector is therefore robust and technically represents the only viable solution to measure transverse profiles in the Cold Linac sections when the ESS beam is delivered at full peak power and longer pulses than 50 μs.

The document "Ion-Electron pairs production in the ESS Cold Linac (ESS-0092071)" assures that enough electron/ion pairs will be produced by ionization of the residual gas, and this report demonstrates the capability of the IPM to measure the beam profile and size within the required accuracy. It shows the space charge effect to be noticeable in condition far from nominal beam parameters, i.e. for extremely small beam sizes. In this cases, which may be considered as errant beam conditions, retrieving the beam profile and beam size can possibly be done, and the accuracy of the method to be used as to be specified yet. Nonetheless, the measured beam distribution is so characteristic that it could be use to qualify extremely small beam sizes, and thus acknowledge errant beam conditions.

Independently of the instrument operated mode ("ion mode" or "electron mode") it was remarked that, in the simulated cases, for the same beam width parameters and applied electric field, the intensity of the space charge effects decreases when the proton energy increases. Also, as a rule of thumb, for a fixed beam condition (energy and widths), the higher the electric field, the more similar to the initial beam profile the simulated beam profile results. However in this case more caution is needed. If the assertion is always true in "ion mode", in "electron mode" an the general trend for the final beam size is less linear than with ions, which leads us to a discussion of the results for the two different operation mode separately.

As a first thing, it was demonstrated that larger corrections need to be applied to pass from the measured beam profile (in this report that's the expected simulated final beam profile) to the real one when detecting electrons than when detecting ionized molecules. As a second step not only the size, but also the shape of the expected simulated final beam profile (what should be obtained by direct measurements) was investigated. In this respect it was noted that, when the beam width is smaller than 1 mm and the detector is operated in "electron mode", a significant distortion may prevent a full recovery of the beam profile and size. This is not the case when the detector is operated in "ion mode". As a matter of fact the nominal ESS beam is of the order of 2 mm. For nominal beam size, the simulation conclude that the distortion is within the requirements, and no correction

may have to be done to the measurement. For the cases with extremely small beam sizes, a correction will have to be done, but these cases may not be measured with an NPM. Indeed, the range of current over which the NPM will be used may be already to high to allow significant deviation to the nominal beam parameters, without causing errant beam conditions.

Working in ”ion mode” would simplify things with respect to the space charge effect issues, since the detected beam profile would already have the right shape and almost the right dimensions. Moreover the initial speed and angular distribution of the ionized molecules would not significantly affect the results.

Summarizing, both options (”ion mode” and ”electron mode”) are viable, each with their pros and cons. A test will have be carried out at the IPHI accelerator in CEA-Saclay to determine which option is the most suitable for the Cold Linac NPMs. In this test, all the aspects linked to the performance of the NPM will be carried out.

Appendix A

IPM 5 mm long, electrons/ions initially at rest

A.1 Electric field: 50 kV/m

A.1.1 Proton energy: 90 MeV

E_p MeV	E kV/m	σ_{x_0} mm	σ_{y_0} mm	σ_{z_0} mm	$\sigma_{x_{el}}$ mm	$\frac{\sigma_{x_{el}}-\sigma_{x_0}}{\sigma_{x_0}}$ %	$\sigma_{x_{H_2^+}}$ mm	$\frac{\sigma_{x_{H_2^+}}-\sigma_{x_0}}{\sigma_{x_0}}$ %
90.0	50	0.50	0.50	0.75	4.542	808.382	2.010	302.010
90.0	50	0.50	0.50	2.00	3.974	694.882	2.010	302.075
90.0	50	0.50	0.50	10.00	3.405	580.931	2.010	302.062
90.0	50	0.50	1.40	0.75	2.179	335.783	1.589	217.775
90.0	50	0.50	1.40	2.00	1.902	280.414	1.590	217.957
90.0	50	0.50	1.40	10.00	1.615	222.902	1.589	217.879
90.0	50	0.50	3.20	0.75	0.960	92.065	1.234	146.756
90.0	50	0.50	3.20	2.00	0.813	62.549	1.242	148.389
90.0	50	0.50	3.20	10.00	0.653	30.594	1.246	149.237
90.0	50	0.50	4.10	0.75	0.723	44.610	1.132	126.334
90.0	50	0.50	4.10	2.00	0.599	19.886	1.146	129.259
90.0	50	0.50	4.10	10.00	0.463	-7.428	1.154	130.844
90.0	50	0.50	5.00	0.75	0.573	14.528	1.048	109.684
90.0	50	0.50	5.00	2.00	0.465	-6.933	1.073	114.643
90.0	50	0.50	5.00	10.00	0.345	-31.072	1.085	117.036
90.0	50	0.50	10.00	0.75	0.307	-38.641	0.761	52.117
90.0	50	0.50	10.00	2.00	0.257	-48.531	0.841	68.146
90.0	50	0.50	10.00	10.00	0.209	-58.221	0.880	75.945
90.0	50	1.40	0.50	0.75	1.563	11.642	2.323	65.908
90.0	50	1.40	0.50	2.00	1.307	-6.660	2.324	65.974
90.0	50	1.40	0.50	10.00	0.989	-29.361	2.324	65.966
90.0	50	1.40	1.40	0.75	0.903	-35.531	2.166	54.731
90.0	50	1.40	1.40	2.00	0.751	-46.385	2.168	54.863
90.0	50	1.40	1.40	10.00	0.541	-61.365	2.169	54.949
90.0	50	1.40	3.20	0.75	0.778	-44.432	1.974	41.023
90.0	50	1.40	3.20	2.00	0.732	-47.688	1.981	41.524

90.0	50	1.40	3.20	10.00	0.679	-51.524	1.984	41.741
90.0	50	1.40	4.10	0.75	0.831	-40.625	1.907	36.244
90.0	50	1.40	4.10	2.00	0.804	-42.601	1.921	37.232
90.0	50	1.40	4.10	10.00	0.775	-44.650	1.924	37.448
90.0	50	1.40	5.00	0.75	0.886	-36.718	1.851	32.197
90.0	50	1.40	5.00	2.00	0.868	-37.989	1.872	33.745
90.0	50	1.40	5.00	10.00	0.851	-39.197	1.877	34.105
90.0	50	1.40	10.00	0.75	1.069	-23.635	1.660	18.567
90.0	50	1.40	10.00	2.00	1.065	-23.895	1.722	23.004
90.0	50	1.40	10.00	10.00	1.064	-24.010	1.723	23.098
90.0	50	3.20	0.50	0.75	2.248	-29.758	3.761	17.520
90.0	50	3.20	0.50	2.00	2.230	-30.307	3.763	17.596
90.0	50	3.20	0.50	10.00	2.216	-30.754	3.764	17.632
90.0	50	3.20	1.40	0.75	2.402	-24.928	3.706	15.820
90.0	50	3.20	1.40	2.00	2.395	-25.143	3.709	15.920
90.0	50	3.20	1.40	10.00	2.392	-25.257	3.711	15.977
90.0	50	3.20	3.20	0.75	2.606	-18.558	3.613	12.903
90.0	50	3.20	3.20	2.00	2.604	-18.618	3.622	13.196
90.0	50	3.20	3.20	10.00	2.605	-18.582	3.625	13.293
90.0	50	3.20	4.10	0.75	2.673	-16.469	3.575	11.711
90.0	50	3.20	4.10	2.00	2.672	-16.505	3.590	12.182
90.0	50	3.20	4.10	10.00	2.674	-16.446	3.592	12.261
90.0	50	3.20	5.00	0.75	2.726	-14.824	3.543	10.708
90.0	50	3.20	5.00	2.00	2.725	-14.847	3.563	11.341
90.0	50	3.20	5.00	10.00	2.727	-14.780	3.564	11.369
90.0	50	3.20	10.00	0.75	2.880	-9.995	3.436	7.362
90.0	50	3.20	10.00	2.00	2.880	-9.998	3.467	8.345
90.0	50	3.20	10.00	10.00	2.882	-9.938	3.459	8.106
90.0	50	4.10	0.50	0.75	3.283	-19.923	4.569	11.449
90.0	50	4.10	0.50	2.00	3.278	-20.047	4.572	11.502
90.0	50	4.10	0.50	10.00	3.278	-20.058	4.574	11.558
90.0	50	4.10	1.40	0.75	3.402	-17.015	4.531	10.514
90.0	50	4.10	1.40	2.00	3.400	-17.065	4.535	10.609
90.0	50	4.10	1.40	10.00	3.402	-17.017	4.537	10.658
90.0	50	4.10	3.20	0.75	3.560	-13.159	4.460	8.789
90.0	50	4.10	3.20	2.00	3.560	-13.171	4.469	9.009
90.0	50	4.10	3.20	10.00	3.563	-13.107	4.472	9.071
90.0	50	4.10	4.10	0.75	3.614	-11.845	4.431	8.063
90.0	50	4.10	4.10	2.00	3.614	-11.852	4.444	8.398
90.0	50	4.10	4.10	10.00	3.617	-11.790	4.445	8.423
90.0	50	4.10	5.00	0.75	3.657	-10.795	4.404	7.423
90.0	50	4.10	5.00	2.00	3.657	-10.799	4.423	7.879
90.0	50	4.10	5.00	10.00	3.660	-10.738	4.423	7.868
90.0	50	4.10	10.00	0.75	3.788	-7.601	4.320	5.375
90.0	50	4.10	10.00	2.00	3.788	-7.600	4.340	5.859
90.0	50	4.10	10.00	10.00	3.790	-7.554	4.334	5.699
90.0	50	5.00	0.50	0.75	4.290	-14.194	5.401	8.027
90.0	50	5.00	0.50	2.00	4.289	-14.228	5.404	8.083
90.0	50	5.00	0.50	10.00	4.291	-14.171	5.406	8.123
90.0	50	5.00	1.40	0.75	4.380	-12.391	5.372	7.442

90.0	50	5.00	1.40	2.00	4.380	-12.404	5.377	7.539
90.0	50	5.00	1.40	10.00	4.383	-12.339	5.379	7.578
90.0	50	5.00	3.20	0.75	4.504	-9.915	5.316	6.317
90.0	50	5.00	3.20	2.00	4.504	-9.917	5.326	6.527
90.0	50	5.00	3.20	10.00	4.507	-9.859	5.328	6.555
90.0	50	5.00	4.10	0.75	4.548	-9.040	5.293	5.861
90.0	50	5.00	4.10	2.00	4.548	-9.041	5.306	6.121
90.0	50	5.00	4.10	10.00	4.551	-8.989	5.306	6.124
90.0	50	5.00	5.00	0.75	4.584	-8.327	5.273	5.465
90.0	50	5.00	5.00	2.00	4.584	-8.326	5.290	5.800
90.0	50	5.00	5.00	10.00	4.586	-8.279	5.287	5.741
90.0	50	5.00	10.00	0.75	4.695	-6.094	5.202	4.048
90.0	50	5.00	10.00	2.00	4.695	-6.092	5.217	4.349
90.0	50	5.00	10.00	10.00	4.697	-6.057	5.210	4.205
90.0	50	10.00	0.50	0.75	9.554	-4.457	10.187	1.867
90.0	50	10.00	0.50	2.00	9.554	-4.455	10.190	1.904
90.0	50	10.00	0.50	10.00	9.557	-4.428	10.192	1.915
90.0	50	10.00	1.40	0.75	9.582	-4.176	10.178	1.775
90.0	50	10.00	1.40	2.00	9.583	-4.174	10.183	1.827
90.0	50	10.00	1.40	10.00	9.585	-4.151	10.183	1.826
90.0	50	10.00	3.20	0.75	9.627	-3.733	10.159	1.588
90.0	50	10.00	3.20	2.00	9.627	-3.732	10.166	1.662
90.0	50	10.00	3.20	10.00	9.629	-3.713	10.163	1.632
90.0	50	10.00	4.10	0.75	9.644	-3.557	10.151	1.507
90.0	50	10.00	4.10	2.00	9.644	-3.555	10.158	1.580
90.0	50	10.00	4.10	10.00	9.646	-3.539	10.154	1.540
90.0	50	10.00	5.00	0.75	9.660	-3.404	10.143	1.430
90.0	50	10.00	5.00	2.00	9.660	-3.403	10.149	1.489
90.0	50	10.00	5.00	10.00	9.661	-3.388	10.145	1.452
90.0	50	10.00	10.00	0.75	9.714	-2.861	10.105	1.052
90.0	50	10.00	10.00	2.00	9.714	-2.860	10.108	1.084
90.0	50	10.00	10.00	10.00	9.715	-2.849	10.105	1.050

Table A.1: Simulations for an electric field of 50 kV/m and proton beam kinetic energy of 90 MeV.

A.1.2 Proton energy: 200 MeV

E_p MeV	E kV/m	σ_{x_0} mm	σ_{y_0} mm	σ_{z_0} mm	$\sigma_{x_{el}}$ mm	$\frac{\sigma_{x_{el}}-\sigma_{x_0}}{\sigma_{x_0}}$ %	$\sigma_{x_{H_2^+}}$ mm	$\frac{\sigma_{x_{H_2^+}}-\sigma_{x_0}}{\sigma_{x_0}}$ %
200.0	50	0.50	0.50	0.75	3.225	545.080	1.561	212.114
200.0	50	0.50	0.50	2.00	2.794	458.751	1.563	212.603
200.0	50	0.50	0.50	10.00	2.405	380.964	1.568	213.681
200.0	50	0.50	1.40	0.75	1.511	202.299	1.258	151.543
200.0	50	0.50	1.40	2.00	1.289	157.880	1.263	152.517
200.0	50	0.50	1.40	10.00	1.076	115.132	1.269	153.817
200.0	50	0.50	3.20	0.75	0.646	29.235	0.971	94.209
200.0	50	0.50	3.20	2.00	0.521	4.294	0.994	98.844
200.0	50	0.50	3.20	10.00	0.390	-21.942	1.027	105.313
200.0	50	0.50	4.10	0.75	0.491	-1.838	0.880	75.983
200.0	50	0.50	4.10	2.00	0.387	-22.591	0.907	81.411
200.0	50	0.50	4.10	10.00	0.275	-45.086	0.964	92.710
200.0	50	0.50	5.00	0.75	0.402	-19.599	0.809	61.870
200.0	50	0.50	5.00	2.00	0.315	-36.907	0.840	67.929
200.0	50	0.50	5.00	10.00	0.222	-55.611	0.916	83.209
200.0	50	0.50	10.00	0.75	0.310	-38.084	0.628	25.578
200.0	50	0.50	10.00	2.00	0.283	-43.342	0.660	31.908
200.0	50	0.50	10.00	10.00	0.262	-47.633	0.771	54.253
200.0	50	1.40	0.50	0.75	1.077	-23.087	2.046	46.143
200.0	50	1.40	0.50	2.00	0.861	-38.474	2.050	46.452
200.0	50	1.40	0.50	10.00	0.601	-57.092	2.060	47.128
200.0	50	1.40	1.40	0.75	0.793	-43.374	1.927	37.659
200.0	50	1.40	1.40	2.00	0.695	-50.383	1.935	38.241
200.0	50	1.40	1.40	10.00	0.583	-58.347	1.947	39.064
200.0	50	1.40	3.20	0.75	0.890	-36.449	1.768	26.280
200.0	50	1.40	3.20	2.00	0.866	-38.128	1.784	27.394
200.0	50	1.40	3.20	10.00	0.843	-39.764	1.817	29.768
200.0	50	1.40	4.10	0.75	0.953	-31.961	1.707	21.953
200.0	50	1.40	4.10	2.00	0.939	-32.963	1.727	23.391
200.0	50	1.40	4.10	10.00	0.926	-33.874	1.775	26.817
200.0	50	1.40	5.00	0.75	1.004	-28.294	1.662	18.686
200.0	50	1.40	5.00	2.00	0.995	-28.948	1.683	20.234
200.0	50	1.40	5.00	10.00	0.987	-29.495	1.742	24.418
200.0	50	1.40	10.00	0.75	1.153	-17.675	1.536	9.741
200.0	50	1.40	10.00	2.00	1.151	-17.816	1.561	11.536
200.0	50	1.40	10.00	10.00	1.150	-17.859	1.631	16.489
200.0	50	3.20	0.50	0.75	2.481	-22.468	3.578	11.817
200.0	50	3.20	0.50	2.00	2.472	-22.756	3.584	12.008
200.0	50	3.20	0.50	10.00	2.465	-22.966	3.599	12.481
200.0	50	3.20	1.40	0.75	2.604	-18.618	3.534	10.451
200.0	50	3.20	1.40	2.00	2.600	-18.735	3.543	10.721
200.0	50	3.20	1.40	10.00	2.599	-18.790	3.563	11.331
200.0	50	3.20	3.20	0.75	2.758	-13.815	3.458	8.054

200.0	50	3.20	3.20	2.00	2.757	-13.848	3.470	8.442
200.0	50	3.20	3.20	10.00	2.757	-13.831	3.501	9.410
200.0	50	3.20	4.10	0.75	2.807	-12.268	3.430	7.192
200.0	50	3.20	4.10	2.00	2.807	-12.288	3.442	7.564
200.0	50	3.20	4.10	10.00	2.808	-12.258	3.477	8.656
200.0	50	3.20	5.00	0.75	2.846	-11.056	3.406	6.439
200.0	50	3.20	5.00	2.00	2.846	-11.068	3.422	6.939
200.0	50	3.20	5.00	10.00	2.847	-11.032	3.456	8.015
200.0	50	3.20	10.00	0.75	2.960	-7.511	3.335	4.220
200.0	50	3.20	10.00	2.00	2.960	-7.513	3.354	4.799
200.0	50	3.20	10.00	10.00	2.961	-7.477	3.381	5.645
200.0	50	4.10	0.50	0.75	3.490	-14.870	4.410	7.566
200.0	50	4.10	0.50	2.00	3.488	-14.936	4.417	7.735
200.0	50	4.10	0.50	10.00	3.487	-14.940	4.433	8.114
200.0	50	4.10	1.40	0.75	3.580	-12.679	4.380	6.831
200.0	50	4.10	1.40	2.00	3.579	-12.706	4.387	6.995
200.0	50	4.10	1.40	10.00	3.580	-12.681	4.407	7.492
200.0	50	4.10	3.20	0.75	3.697	-9.829	4.323	5.447
200.0	50	4.10	3.20	2.00	3.697	-9.835	4.333	5.694
200.0	50	4.10	3.20	10.00	3.698	-9.803	4.360	6.345
200.0	50	4.10	4.10	0.75	3.737	-8.865	4.301	4.907
200.0	50	4.10	4.10	2.00	3.736	-8.868	4.314	5.208
200.0	50	4.10	4.10	10.00	3.738	-8.837	4.341	5.874
200.0	50	4.10	5.00	0.75	3.768	-8.097	4.283	4.452
200.0	50	4.10	5.00	2.00	3.768	-8.098	4.296	4.778
200.0	50	4.10	5.00	10.00	3.769	-8.066	4.325	5.493
200.0	50	4.10	10.00	0.75	3.864	-5.763	4.226	3.083
200.0	50	4.10	10.00	2.00	3.864	-5.763	4.245	3.537
200.0	50	4.10	10.00	10.00	3.865	-5.735	4.260	3.894
200.0	50	5.00	0.50	0.75	4.470	-10.604	5.259	5.174
200.0	50	5.00	0.50	2.00	4.469	-10.622	5.265	5.291
200.0	50	5.00	0.50	10.00	4.470	-10.591	5.282	5.647
200.0	50	5.00	1.40	0.75	4.537	-9.269	5.236	4.715
200.0	50	5.00	1.40	2.00	4.536	-9.276	5.242	4.849
200.0	50	5.00	1.40	10.00	4.538	-9.242	5.263	5.256
200.0	50	5.00	3.20	0.75	4.627	-7.452	5.193	3.852
200.0	50	5.00	3.20	2.00	4.627	-7.453	5.203	4.056
200.0	50	5.00	3.20	10.00	4.629	-7.423	5.226	4.513
200.0	50	5.00	4.10	0.75	4.659	-6.813	5.179	3.572
200.0	50	5.00	4.10	2.00	4.659	-6.813	5.188	3.755
200.0	50	5.00	4.10	10.00	4.661	-6.786	5.211	4.221
200.0	50	5.00	5.00	0.75	4.685	-6.293	5.163	3.262
200.0	50	5.00	5.00	2.00	4.685	-6.292	5.177	3.539
200.0	50	5.00	5.00	10.00	4.687	-6.268	5.197	3.936
200.0	50	5.00	10.00	0.75	4.767	-4.664	5.115	2.304
200.0	50	5.00	10.00	2.00	4.767	-4.664	5.132	2.649
200.0	50	5.00	10.00	10.00	4.768	-4.642	5.140	2.803
200.0	50	10.00	0.50	0.75	9.653	-3.473	10.098	0.984
200.0	50	10.00	0.50	2.00	9.653	-3.471	10.102	1.018
200.0	50	10.00	0.50	10.00	9.654	-3.456	10.115	1.149

200.0	50	10.00	1.40	0.75	9.673	-3.268	10.092	0.919
200.0	50	10.00	1.40	2.00	9.673	-3.267	10.097	0.966
200.0	50	10.00	1.40	10.00	9.675	-3.254	10.108	1.084
200.0	50	10.00	3.20	0.75	9.705	-2.946	10.080	0.800
200.0	50	10.00	3.20	2.00	9.705	-2.945	10.087	0.865
200.0	50	10.00	3.20	10.00	9.707	-2.935	10.094	0.940
200.0	50	10.00	4.10	0.75	9.718	-2.818	10.074	0.745
200.0	50	10.00	4.10	2.00	9.718	-2.817	10.082	0.822
200.0	50	10.00	4.10	10.00	9.719	-2.808	10.087	0.872
200.0	50	10.00	5.00	0.75	9.729	-2.707	10.069	0.690
200.0	50	10.00	5.00	2.00	9.729	-2.706	10.077	0.771
200.0	50	10.00	5.00	10.00	9.730	-2.698	10.081	0.809
200.0	50	10.00	10.00	0.75	9.769	-2.312	10.045	0.447
200.0	50	10.00	10.00	2.00	9.769	-2.312	10.049	0.493
200.0	50	10.00	10.00	10.00	9.769	-2.305	10.052	0.516

Table A.2: Simulations for an electric field of 50 kV/m and proton beam kinetic energy of 200 MeV.

A.1.3 Proton energy: 1000 MeV

E_p MeV	E kV/m	σ_{x_0} mm	σ_{y_0} mm	σ_{z_0} mm	$\sigma_{x_{el}}$ mm	$\frac{\sigma_{x_{el}}-\sigma_{x_0}}{\sigma_{x_0}}$ %	$\sigma_{x_{H_2^+}}$ mm	$\frac{\sigma_{x_{H_2^+}}-\sigma_{x_0}}{\sigma_{x_0}}$ %
1000.0	50	0.50	0.50	0.75	2.046	309.113	0.854	70.746
1000.0	50	0.50	0.50	2.00	1.703	240.544	0.881	76.193
1000.0	50	0.50	0.50	10.00	1.430	186.062	1.167	133.458
1000.0	50	0.50	1.40	0.75	0.936	87.205	0.689	37.861
1000.0	50	0.50	1.40	2.00	0.741	48.152	0.705	40.909
1000.0	50	0.50	1.40	10.00	0.570	14.099	0.970	93.915
1000.0	50	0.50	3.20	0.75	0.424	-15.244	0.593	18.551
1000.0	50	0.50	3.20	2.00	0.316	-36.754	0.600	19.916
1000.0	50	0.50	3.20	10.00	0.213	-57.472	0.803	60.677
1000.0	50	0.50	4.10	0.75	0.358	-28.378	0.573	14.581
1000.0	50	0.50	4.10	2.00	0.279	-44.102	0.580	16.083
1000.0	50	0.50	4.10	10.00	0.209	-58.177	0.761	52.179
1000.0	50	0.50	5.00	0.75	0.334	-33.248	0.560	11.921
1000.0	50	0.50	5.00	2.00	0.278	-44.466	0.565	12.999
1000.0	50	0.50	5.00	10.00	0.232	-53.641	0.736	47.203
1000.0	50	0.50	10.00	0.75	0.355	-28.949	0.525	4.990
1000.0	50	0.50	10.00	2.00	0.343	-31.459	0.529	5.779
1000.0	50	0.50	10.00	10.00	0.335	-33.095	0.655	31.048
1000.0	50	1.40	0.50	0.75	0.902	-35.540	1.582	12.988
1000.0	50	1.40	0.50	2.00	0.748	-46.577	1.597	14.077
1000.0	50	1.40	0.50	10.00	0.611	-56.391	1.806	28.973
1000.0	50	1.40	1.40	0.75	0.907	-35.205	1.524	8.831
1000.0	50	1.40	1.40	2.00	0.852	-39.178	1.531	9.373
1000.0	50	1.40	1.40	10.00	0.807	-42.365	1.727	23.349
1000.0	50	1.40	3.20	0.75	1.047	-25.218	1.474	5.296
1000.0	50	1.40	3.20	2.00	1.033	-26.232	1.481	5.766
1000.0	50	1.40	3.20	10.00	1.022	-26.994	1.640	17.126
1000.0	50	1.40	4.10	0.75	1.095	-21.771	1.459	4.241
1000.0	50	1.40	4.10	2.00	1.086	-22.399	1.466	4.688
1000.0	50	1.40	4.10	10.00	1.080	-22.854	1.611	15.071
1000.0	50	1.40	5.00	0.75	1.132	-19.134	1.451	3.645
1000.0	50	1.40	5.00	2.00	1.126	-19.555	1.455	3.957
1000.0	50	1.40	5.00	10.00	1.122	-19.845	1.594	13.823
1000.0	50	1.40	10.00	0.75	1.234	-11.868	1.423	1.670
1000.0	50	1.40	10.00	2.00	1.232	-11.972	1.427	1.942
1000.0	50	1.40	10.00	10.00	1.232	-12.013	1.534	9.579
1000.0	50	3.20	0.50	0.75	2.717	-15.107	3.290	2.812
1000.0	50	3.20	0.50	2.00	2.710	-15.305	3.298	3.058
1000.0	50	3.20	0.50	10.00	2.706	-15.430	3.432	7.252
1000.0	50	3.20	1.40	0.75	2.800	-12.485	3.270	2.197
1000.0	50	3.20	1.40	2.00	2.797	-12.579	3.278	2.445
1000.0	50	3.20	1.40	10.00	2.796	-12.630	3.406	6.428
1000.0	50	3.20	3.20	0.75	2.902	-9.312	3.248	1.505

1000.0	50	3.20	3.20	2.00	2.901	-9.346	3.253	1.656
1000.0	50	3.20	3.20	10.00	2.901	-9.351	3.369	5.278
1000.0	50	3.20	4.10	0.75	2.934	-8.297	3.241	1.270
1000.0	50	3.20	4.10	2.00	2.934	-8.317	3.247	1.460
1000.0	50	3.20	4.10	10.00	2.934	-8.315	3.355	4.859
1000.0	50	3.20	5.00	0.75	2.960	-7.503	3.235	1.083
1000.0	50	3.20	5.00	2.00	2.959	-7.516	3.241	1.268
1000.0	50	3.20	5.00	10.00	2.960	-7.510	3.345	4.520
1000.0	50	3.20	10.00	0.75	3.034	-5.180	3.218	0.566
1000.0	50	3.20	10.00	2.00	3.034	-5.185	3.223	0.709
1000.0	50	3.20	10.00	10.00	3.034	-5.175	3.301	3.158
1000.0	50	4.10	0.50	0.75	3.689	-10.022	4.165	1.588
1000.0	50	4.10	0.50	2.00	3.687	-10.071	4.172	1.745
1000.0	50	4.10	0.50	10.00	3.686	-10.089	4.287	4.570
1000.0	50	4.10	1.40	0.75	3.749	-8.569	4.154	1.317
1000.0	50	4.10	1.40	2.00	3.748	-8.593	4.160	1.467
1000.0	50	4.10	1.40	10.00	3.748	-8.596	4.269	4.128
1000.0	50	4.10	3.20	0.75	3.825	-6.703	4.138	0.921
1000.0	50	4.10	3.20	2.00	3.825	-6.710	4.142	1.025
1000.0	50	4.10	3.20	10.00	3.825	-6.704	4.242	3.455
1000.0	50	4.10	4.10	0.75	3.851	-6.073	4.133	0.801
1000.0	50	4.10	4.10	2.00	3.851	-6.077	4.137	0.911
1000.0	50	4.10	4.10	10.00	3.851	-6.070	4.232	3.213
1000.0	50	4.10	5.00	0.75	3.872	-5.571	4.128	0.680
1000.0	50	4.10	5.00	2.00	3.871	-5.573	4.133	0.796
1000.0	50	4.10	5.00	10.00	3.872	-5.565	4.222	2.976
1000.0	50	4.10	10.00	0.75	3.934	-4.042	4.113	0.306
1000.0	50	4.10	10.00	2.00	3.934	-4.043	4.118	0.448
1000.0	50	4.10	10.00	10.00	3.935	-4.036	4.187	2.121
1000.0	50	5.00	0.50	0.75	4.639	-7.216	5.049	0.988
1000.0	50	5.00	0.50	2.00	4.639	-7.229	5.056	1.119
1000.0	50	5.00	0.50	10.00	4.639	-7.224	5.152	3.040
1000.0	50	5.00	1.40	0.75	4.683	-6.338	5.041	0.824
1000.0	50	5.00	1.40	2.00	4.683	-6.345	5.046	0.914
1000.0	50	5.00	1.40	10.00	4.683	-6.337	5.141	2.828
1000.0	50	5.00	3.20	0.75	4.742	-5.152	5.027	0.542
1000.0	50	5.00	3.20	2.00	4.742	-5.154	5.032	0.649
1000.0	50	5.00	3.20	10.00	4.743	-5.145	5.121	2.417
1000.0	50	5.00	4.10	0.75	4.763	-4.735	5.024	0.481
1000.0	50	5.00	4.10	2.00	4.763	-4.735	5.028	0.560
1000.0	50	5.00	4.10	10.00	4.764	-4.728	5.112	2.241
1000.0	50	5.00	5.00	0.75	4.780	-4.394	5.021	0.418
1000.0	50	5.00	5.00	2.00	4.780	-4.394	5.025	0.496
1000.0	50	5.00	5.00	10.00	4.781	-4.388	5.106	2.115
1000.0	50	5.00	10.00	0.75	4.834	-3.327	5.008	0.170
1000.0	50	5.00	10.00	2.00	4.834	-3.328	5.013	0.261
1000.0	50	5.00	10.00	10.00	4.834	-3.323	5.073	1.469
1000.0	50	10.00	0.50	0.75	9.744	-2.559	9.984	-0.160
1000.0	50	10.00	0.50	2.00	9.744	-2.558	9.989	-0.113
1000.0	50	10.00	0.50	10.00	9.745	-2.551	10.039	0.389

1000.0	50	10.00	1.40	0.75	9.757	-2.426	9.982	-0.184
1000.0	50	10.00	1.40	2.00	9.758	-2.425	9.986	-0.136
1000.0	50	10.00	1.40	10.00	9.758	-2.419	10.034	0.345
1000.0	50	10.00	3.20	0.75	9.778	-2.216	9.978	-0.215
1000.0	50	10.00	3.20	2.00	9.779	-2.215	9.982	-0.181
1000.0	50	10.00	3.20	10.00	9.779	-2.210	10.026	0.262
1000.0	50	10.00	4.10	0.75	9.787	-2.132	9.978	-0.225
1000.0	50	10.00	4.10	2.00	9.787	-2.131	9.980	-0.197
1000.0	50	10.00	4.10	10.00	9.787	-2.127	10.023	0.231
1000.0	50	10.00	5.00	0.75	9.794	-2.059	9.976	-0.236
1000.0	50	10.00	5.00	2.00	9.794	-2.058	9.977	-0.225
1000.0	50	10.00	5.00	10.00	9.794	-2.055	10.018	0.184
1000.0	50	10.00	10.00	0.75	9.820	-1.796	9.971	-0.288
1000.0	50	10.00	10.00	2.00	9.820	-1.796	9.972	-0.277
1000.0	50	10.00	10.00	10.00	9.820	-1.798	9.999	-0.006

Table A.3: Simulations for an electric field of 50 kV/m and proton beam kinetic energy of 1000 MeV.

A.2 Electric field: 100 kV/m

A.2.1 Proton energy: 90 MeV

E_p MeV	E kV/m	σ_{x_0} mm	σ_{y_0} mm	σ_{z_0} mm	$\sigma_{x_{el}}$ mm	$\frac{\sigma_{x_{el}}-\sigma_{x_0}}{\sigma_{x_0}}$ %	$\sigma_{x_{H_2^+}}$ mm	$\frac{\sigma_{x_{H_2^+}}-\sigma_{x_0}}{\sigma_{x_0}}$ %
90.0	100	0.50	0.50	0.75	3.102	520.412	1.244	148.866
90.0	100	0.50	0.50	2.00	2.697	439.417	1.245	148.971
90.0	100	0.50	0.50	10.00	2.264	352.899	1.245	149.034
90.0	100	0.50	1.40	0.75	1.447	189.498	1.038	107.545
90.0	100	0.50	1.40	2.00	1.241	148.144	1.039	107.777
90.0	100	0.50	1.40	10.00	1.015	102.957	1.039	107.882
90.0	100	0.50	3.20	0.75	0.616	23.142	0.858	71.608
90.0	100	0.50	3.20	2.00	0.499	-0.258	0.866	73.271
90.0	100	0.50	3.20	10.00	0.364	-27.277	0.870	74.054
90.0	100	0.50	4.10	0.75	0.469	-6.282	0.802	60.473
90.0	100	0.50	4.10	2.00	0.371	-25.793	0.817	63.482
90.0	100	0.50	4.10	10.00	0.257	-48.602	0.825	65.034
90.0	100	0.50	5.00	0.75	0.386	-22.734	0.755	51.009
90.0	100	0.50	5.00	2.00	0.305	-38.958	0.779	55.891
90.0	100	0.50	5.00	10.00	0.213	-57.450	0.791	58.256
90.0	100	0.50	10.00	0.75	0.319	-36.234	0.616	23.221
90.0	100	0.50	10.00	2.00	0.295	-40.983	0.662	32.451
90.0	100	0.50	10.00	10.00	0.277	-44.676	0.690	37.951
90.0	100	1.40	0.50	0.75	1.025	-26.814	1.865	33.208
90.0	100	1.40	0.50	2.00	0.828	-40.868	1.866	33.296
90.0	100	1.40	0.50	10.00	0.573	-59.102	1.867	33.325
90.0	100	1.40	1.40	0.75	0.782	-44.170	1.787	27.650
90.0	100	1.40	1.40	2.00	0.696	-50.297	1.789	27.791
90.0	100	1.40	1.40	10.00	0.598	-57.278	1.790	27.853
90.0	100	1.40	3.20	0.75	0.901	-35.649	1.687	20.529
90.0	100	1.40	3.20	2.00	0.880	-37.111	1.695	21.081
90.0	100	1.40	3.20	10.00	0.863	-38.353	1.698	21.315
90.0	100	1.40	4.10	0.75	0.966	-31.028	1.650	17.850
90.0	100	1.40	4.10	2.00	0.953	-31.913	1.664	18.834
90.0	100	1.40	4.10	10.00	0.944	-32.540	1.668	19.140
90.0	100	1.40	5.00	0.75	1.018	-27.313	1.619	15.647
90.0	100	1.40	5.00	2.00	1.009	-27.899	1.639	17.088
90.0	100	1.40	5.00	10.00	1.005	-28.226	1.644	17.420
90.0	100	1.40	10.00	0.75	1.174	-16.158	1.528	9.167
90.0	100	1.40	10.00	2.00	1.172	-16.294	1.566	11.875
90.0	100	1.40	10.00	10.00	1.173	-16.239	1.567	11.905
90.0	100	3.20	0.50	0.75	2.514	-21.423	3.486	8.941
90.0	100	3.20	0.50	2.00	2.506	-21.681	3.488	9.013
90.0	100	3.20	0.50	10.00	2.505	-21.710	3.490	9.062
90.0	100	3.20	1.40	0.75	2.636	-17.628	3.459	8.088
90.0	100	3.20	1.40	2.00	2.633	-17.734	3.463	8.204

90.0	100	3.20	1.40	10.00	2.635	-17.664	3.464	8.254
90.0	100	3.20	3.20	0.75	2.787	-12.911	3.411	6.580
90.0	100	3.20	3.20	2.00	2.786	-12.942	3.419	6.856
90.0	100	3.20	3.20	10.00	2.789	-12.844	3.422	6.927
90.0	100	3.20	4.10	0.75	2.836	-11.387	3.391	5.980
90.0	100	3.20	4.10	2.00	2.835	-11.407	3.404	6.375
90.0	100	3.20	4.10	10.00	2.838	-11.308	3.405	6.392
90.0	100	3.20	5.00	0.75	2.874	-10.187	3.376	5.508
90.0	100	3.20	5.00	2.00	2.874	-10.201	3.390	5.949
90.0	100	3.20	5.00	10.00	2.877	-10.106	3.390	5.947
90.0	100	3.20	10.00	0.75	2.993	-6.464	3.327	3.965
90.0	100	3.20	10.00	2.00	2.993	-6.466	3.341	4.405
90.0	100	3.20	10.00	10.00	2.995	-6.398	3.338	4.308
90.0	100	4.10	0.50	0.75	3.529	-13.924	4.341	5.878
90.0	100	4.10	0.50	2.00	3.526	-13.988	4.344	5.949
90.0	100	4.10	0.50	10.00	3.530	-13.892	4.345	5.984
90.0	100	4.10	1.40	0.75	3.617	-11.782	4.322	5.413
90.0	100	4.10	1.40	2.00	3.616	-11.809	4.326	5.507
90.0	100	4.10	1.40	10.00	3.620	-11.709	4.327	5.541
90.0	100	4.10	3.20	0.75	3.731	-8.993	4.286	4.535
90.0	100	4.10	3.20	2.00	3.731	-9.000	4.295	4.747
90.0	100	4.10	3.20	10.00	3.734	-8.915	4.295	4.760
90.0	100	4.10	4.10	0.75	3.770	-8.045	4.272	4.186
90.0	100	4.10	4.10	2.00	3.770	-8.049	4.283	4.454
90.0	100	4.10	4.10	10.00	3.773	-7.972	4.282	4.439
90.0	100	4.10	5.00	0.75	3.801	-7.284	4.260	3.911
90.0	100	4.10	5.00	2.00	3.801	-7.286	4.272	4.183
90.0	100	4.10	5.00	10.00	3.804	-7.214	4.270	4.156
90.0	100	4.10	10.00	0.75	3.903	-4.812	4.220	2.923
90.0	100	4.10	10.00	2.00	3.903	-4.811	4.228	3.130
90.0	100	4.10	10.00	10.00	3.905	-4.761	4.226	3.076
90.0	100	5.00	0.50	0.75	4.513	-9.742	5.208	4.152
90.0	100	5.00	0.50	2.00	4.512	-9.761	5.211	4.211
90.0	100	5.00	0.50	10.00	4.517	-9.668	5.212	4.241
90.0	100	5.00	1.40	0.75	4.578	-8.441	5.193	3.865
90.0	100	5.00	1.40	2.00	4.578	-8.448	5.198	3.951
90.0	100	5.00	1.40	10.00	4.582	-8.365	5.199	3.978
90.0	100	5.00	3.20	0.75	4.667	-6.665	5.166	3.318
90.0	100	5.00	3.20	2.00	4.667	-6.666	5.174	3.485
90.0	100	5.00	3.20	10.00	4.670	-6.600	5.174	3.474
90.0	100	5.00	4.10	0.75	4.698	-6.036	5.155	3.104
90.0	100	5.00	4.10	2.00	4.698	-6.037	5.164	3.285
90.0	100	5.00	4.10	10.00	4.701	-5.977	5.163	3.260
90.0	100	5.00	5.00	0.75	4.724	-5.520	5.146	2.919
90.0	100	5.00	5.00	2.00	4.724	-5.520	5.155	3.100
90.0	100	5.00	5.00	10.00	4.727	-5.466	5.153	3.070
90.0	100	5.00	10.00	0.75	4.811	-3.780	5.112	2.233
90.0	100	5.00	10.00	2.00	4.811	-3.779	5.117	2.348
90.0	100	5.00	10.00	10.00	4.813	-3.741	5.115	2.307
90.0	100	10.00	0.50	0.75	9.720	-2.800	10.106	1.060

90.0	100	10.00	0.50	2.00	9.720	-2.799	10.108	1.083
90.0	100	10.00	0.50	10.00	9.723	-2.771	10.110	1.095
90.0	100	10.00	1.40	0.75	9.740	-2.601	10.102	1.019
90.0	100	10.00	1.40	2.00	9.740	-2.600	10.106	1.058
90.0	100	10.00	1.40	10.00	9.742	-2.576	10.105	1.053
90.0	100	10.00	3.20	0.75	9.771	-2.285	10.094	0.938
90.0	100	10.00	3.20	2.00	9.772	-2.284	10.098	0.976
90.0	100	10.00	3.20	10.00	9.774	-2.265	10.096	0.962
90.0	100	10.00	4.10	0.75	9.784	-2.158	10.090	0.899
90.0	100	10.00	4.10	2.00	9.784	-2.157	10.093	0.932
90.0	100	10.00	4.10	10.00	9.786	-2.139	10.092	0.917
90.0	100	10.00	5.00	0.75	9.795	-2.046	10.086	0.861
90.0	100	10.00	5.00	2.00	9.796	-2.045	10.089	0.890
90.0	100	10.00	5.00	10.00	9.797	-2.028	10.087	0.874
90.0	100	10.00	10.00	0.75	9.839	-1.608	10.069	0.686
90.0	100	10.00	10.00	2.00	9.839	-1.608	10.070	0.695
90.0	100	10.00	10.00	10.00	9.840	-1.597	10.068	0.675

Table A.4: Simulations for an electric field of 100 kV/m and proton beam kinetic energy of 90 MeV.

A.2.2 Proton energy: 200 MeV

E_p MeV	E kV/m	σ_{x_0} mm	σ_{y_0} mm	σ_{z_0} mm	$\sigma_{x_{el}}$ mm	$\frac{\sigma_{x_{el}}-\sigma_{x_0}}{\sigma_{x_0}}$ %	$\sigma_{x_{H_2^+}}$ mm	$\frac{\sigma_{x_{H_2^+}}-\sigma_{x_0}}{\sigma_{x_0}}$ %
200.0	100	0.50	0.50	0.75	2.180	336.012	1.022	104.357
200.0	100	0.50	0.50	2.00	1.867	273.359	1.026	105.124
200.0	100	0.50	0.50	10.00	1.555	211.100	1.030	105.943
200.0	100	0.50	1.40	0.75	0.987	97.443	0.864	72.853
200.0	100	0.50	1.40	2.00	0.817	63.367	0.873	74.659
200.0	100	0.50	1.40	10.00	0.643	28.665	0.884	76.708
200.0	100	0.50	3.20	0.75	0.428	-14.402	0.708	41.644
200.0	100	0.50	3.20	2.00	0.332	-33.656	0.725	45.006
200.0	100	0.50	3.20	10.00	0.225	-55.021	0.765	53.002
200.0	100	0.50	4.10	0.75	0.352	-29.531	0.664	32.721
200.0	100	0.50	4.10	2.00	0.279	-44.130	0.681	36.203
200.0	100	0.50	4.10	10.00	0.203	-59.395	0.733	46.502
200.0	100	0.50	5.00	0.75	0.323	-35.417	0.632	26.320
200.0	100	0.50	5.00	2.00	0.269	-46.108	0.649	29.834
200.0	100	0.50	5.00	10.00	0.219	-56.249	0.709	41.788
200.0	100	0.50	10.00	0.75	0.350	-30.085	0.556	11.284
200.0	100	0.50	10.00	2.00	0.337	-32.506	0.575	14.922
200.0	100	0.50	10.00	10.00	0.329	-34.181	0.636	27.296
200.0	100	1.40	0.50	0.75	0.853	-39.089	1.718	22.691
200.0	100	1.40	0.50	2.00	0.720	-48.601	1.724	23.160
200.0	100	1.40	0.50	10.00	0.577	-58.807	1.735	23.906
200.0	100	1.40	1.40	0.75	0.855	-38.907	1.655	18.219
200.0	100	1.40	1.40	2.00	0.810	-42.122	1.664	18.865
200.0	100	1.40	1.40	10.00	0.768	-45.147	1.680	19.979
200.0	100	1.40	3.20	0.75	1.017	-27.354	1.568	12.003
200.0	100	1.40	3.20	2.00	1.006	-28.132	1.582	12.969
200.0	100	1.40	3.20	10.00	0.998	-28.724	1.614	15.305
200.0	100	1.40	4.10	0.75	1.072	-23.441	1.540	9.975
200.0	100	1.40	4.10	2.00	1.065	-23.925	1.553	10.937
200.0	100	1.40	4.10	10.00	1.061	-24.239	1.593	13.775
200.0	100	1.40	5.00	0.75	1.113	-20.465	1.519	8.497
200.0	100	1.40	5.00	2.00	1.109	-20.794	1.534	9.537
200.0	100	1.40	5.00	10.00	1.106	-20.966	1.576	12.583
200.0	100	1.40	10.00	0.75	1.233	-11.958	1.468	4.847
200.0	100	1.40	10.00	2.00	1.231	-12.041	1.484	5.976
200.0	100	1.40	10.00	10.00	1.232	-12.020	1.520	8.562
200.0	100	3.20	0.50	0.75	2.691	-15.917	3.386	5.823
200.0	100	3.20	0.50	2.00	2.686	-16.064	3.393	6.016
200.0	100	3.20	0.50	10.00	2.685	-16.089	3.407	6.456
200.0	100	3.20	1.40	0.75	2.783	-13.030	3.363	5.105
200.0	100	3.20	1.40	2.00	2.781	-13.094	3.371	5.351
200.0	100	3.20	1.40	10.00	2.782	-13.066	3.388	5.885
200.0	100	3.20	3.20	0.75	2.895	-9.533	3.326	3.940

200.0	100	3.20	3.20	2.00	2.894	-9.554	3.335	4.209
200.0	100	3.20	3.20	10.00	2.896	-9.509	3.358	4.943
200.0	100	3.20	4.10	0.75	2.931	-8.413	3.313	3.544
200.0	100	3.20	4.10	2.00	2.930	-8.427	3.323	3.845
200.0	100	3.20	4.10	10.00	2.932	-8.380	3.346	4.557
200.0	100	3.20	5.00	0.75	2.959	-7.534	3.304	3.244
200.0	100	3.20	5.00	2.00	2.959	-7.543	3.314	3.548
200.0	100	3.20	5.00	10.00	2.960	-7.498	3.336	4.245
200.0	100	3.20	10.00	0.75	3.046	-4.811	3.273	2.295
200.0	100	3.20	10.00	2.00	3.046	-4.813	3.284	2.628
200.0	100	3.20	10.00	10.00	3.047	-4.778	3.298	3.050
200.0	100	4.10	0.50	0.75	3.678	-10.295	4.254	3.748
200.0	100	4.10	0.50	2.00	3.676	-10.334	4.260	3.903
200.0	100	4.10	0.50	10.00	3.678	-10.292	4.274	4.247
200.0	100	4.10	1.40	0.75	3.743	-8.707	4.239	3.384
200.0	100	4.10	1.40	2.00	3.742	-8.724	4.245	3.541
200.0	100	4.10	1.40	10.00	3.744	-8.677	4.262	3.946
200.0	100	4.10	3.20	0.75	3.827	-6.659	4.213	2.747
200.0	100	4.10	3.20	2.00	3.827	-6.665	4.220	2.932
200.0	100	4.10	3.20	10.00	3.828	-6.624	4.238	3.373
200.0	100	4.10	4.10	0.75	3.855	-5.966	4.203	2.518
200.0	100	4.10	4.10	2.00	3.855	-5.969	4.212	2.730
200.0	100	4.10	4.10	10.00	3.857	-5.932	4.229	3.144
200.0	100	4.10	5.00	0.75	3.878	-5.410	4.196	2.336
200.0	100	4.10	5.00	2.00	3.878	-5.413	4.205	2.556
200.0	100	4.10	5.00	10.00	3.880	-5.377	4.220	2.923
200.0	100	4.10	10.00	0.75	3.952	-3.606	4.171	1.729
200.0	100	4.10	10.00	2.00	3.952	-3.606	4.180	1.961
200.0	100	4.10	10.00	10.00	3.953	-3.580	4.188	2.154
200.0	100	5.00	0.50	0.75	4.639	-7.213	5.131	2.618
200.0	100	5.00	0.50	2.00	4.639	-7.225	5.136	2.720
200.0	100	5.00	0.50	10.00	4.641	-7.181	5.150	2.993
200.0	100	5.00	1.40	0.75	4.687	-6.257	5.120	2.398
200.0	100	5.00	1.40	2.00	4.687	-6.263	5.126	2.513
200.0	100	5.00	1.40	10.00	4.689	-6.222	5.140	2.800
200.0	100	5.00	3.20	0.75	4.752	-4.959	5.101	2.021
200.0	100	5.00	3.20	2.00	4.752	-4.960	5.108	2.157
200.0	100	5.00	3.20	10.00	4.754	-4.928	5.122	2.437
200.0	100	5.00	4.10	0.75	4.775	-4.500	5.094	1.880
200.0	100	5.00	4.10	2.00	4.775	-4.501	5.101	2.027
200.0	100	5.00	4.10	10.00	4.776	-4.471	5.114	2.275
200.0	100	5.00	5.00	0.75	4.794	-4.123	5.088	1.762
200.0	100	5.00	5.00	2.00	4.794	-4.123	5.097	1.930
200.0	100	5.00	5.00	10.00	4.795	-4.097	5.107	2.137
200.0	100	5.00	10.00	0.75	4.857	-2.854	5.068	1.353
200.0	100	5.00	10.00	2.00	4.857	-2.854	5.075	1.492
200.0	100	5.00	10.00	10.00	4.858	-2.834	5.079	1.587
200.0	100	10.00	0.50	0.75	9.786	-2.140	10.061	0.605
200.0	100	10.00	0.50	2.00	9.786	-2.139	10.063	0.628
200.0	100	10.00	0.50	10.00	9.787	-2.125	10.071	0.706

200.0	100	10.00	1.40	0.75	9.800	-1.995	10.058	0.581
200.0	100	10.00	1.40	2.00	9.801	-1.995	10.062	0.618
200.0	100	10.00	1.40	10.00	9.802	-1.982	10.068	0.675
200.0	100	10.00	3.20	0.75	9.823	-1.765	10.053	0.532
200.0	100	10.00	3.20	2.00	9.824	-1.765	10.057	0.571
200.0	100	10.00	3.20	10.00	9.825	-1.755	10.061	0.608
200.0	100	10.00	4.10	0.75	9.833	-1.672	10.051	0.507
200.0	100	10.00	4.10	2.00	9.833	-1.672	10.055	0.550
200.0	100	10.00	4.10	10.00	9.834	-1.663	10.058	0.575
200.0	100	10.00	5.00	0.75	9.841	-1.591	10.049	0.488
200.0	100	10.00	5.00	2.00	9.841	-1.590	10.052	0.522
200.0	100	10.00	5.00	10.00	9.842	-1.582	10.054	0.544
200.0	100	10.00	10.00	0.75	9.873	-1.271	10.038	0.380
200.0	100	10.00	10.00	2.00	9.873	-1.271	10.040	0.397
200.0	100	10.00	10.00	10.00	9.873	-1.265	10.040	0.402

Table A.5: Simulations for an electric field of 100 kV/m and proton beam kinetic energy of 200 MeV.

A.2.3 Proton energy: 1000 MeV

E_p MeV	E kV/m	σ_{x_0} mm	σ_{y_0} mm	σ_{z_0} mm	$\sigma_{x_{el}}$ mm	$\frac{\sigma_{x_{el}}-\sigma_{x_0}}{\sigma_{x_0}}$ %	$\sigma_{x_{H_2^+}}$ mm	$\frac{\sigma_{x_{H_2^+}}-\sigma_{x_0}}{\sigma_{x_0}}$ %
1000.0	100	0.50	0.50	0.75	1.360	171.927	0.651	30.100
1000.0	100	0.50	0.50	2.00	1.104	120.755	0.676	35.100
1000.0	100	0.50	0.50	10.00	0.419	-16.234	0.723	44.563
1000.0	100	0.50	1.40	0.75	0.610	22.054	0.580	15.987
1000.0	100	0.50	1.40	2.00	0.458	-8.473	0.590	18.055
1000.0	100	0.50	1.40	10.00	0.304	-39.286	0.732	46.301
1000.0	100	0.50	3.20	0.75	0.342	-31.589	0.540	7.918
1000.0	100	0.50	3.20	2.00	0.276	-44.725	0.545	9.090
1000.0	100	0.50	3.20	10.00	0.221	-55.826	0.653	30.543
1000.0	100	0.50	4.10	0.75	0.332	-33.528	0.531	6.188
1000.0	100	0.50	4.10	2.00	0.291	-41.838	0.536	7.184
1000.0	100	0.50	4.10	10.00	0.259	-48.159	0.634	26.827
1000.0	100	0.50	5.00	0.75	0.339	-32.194	0.525	5.053
1000.0	100	0.50	5.00	2.00	0.311	-37.708	0.530	5.938
1000.0	100	0.50	5.00	10.00	0.292	-41.640	0.620	23.983
1000.0	100	0.50	10.00	0.75	0.395	-21.099	0.512	2.383
1000.0	100	0.50	10.00	2.00	0.388	-22.334	0.515	3.041
1000.0	100	0.50	10.00	10.00	0.385	-23.011	0.582	16.313
1000.0	100	1.40	0.50	0.75	0.922	-34.164	1.479	5.643
1000.0	100	1.40	0.50	2.00	0.848	-39.439	1.490	6.395
1000.0	100	1.40	0.50	10.00	0.792	-43.461	1.605	14.674
1000.0	100	1.40	1.40	0.75	1.014	-27.576	1.455	3.939
1000.0	100	1.40	1.40	2.00	0.988	-29.431	1.463	4.515
1000.0	100	1.40	1.40	10.00	0.969	-30.759	1.566	11.877
1000.0	100	1.40	3.20	0.75	1.144	-18.307	1.433	2.388
1000.0	100	1.40	3.20	2.00	1.136	-18.833	1.438	2.695
1000.0	100	1.40	3.20	10.00	1.132	-19.170	1.524	8.879
1000.0	100	1.40	4.10	0.75	1.182	-15.594	1.428	1.970
1000.0	100	1.40	4.10	2.00	1.177	-15.937	1.431	2.246
1000.0	100	1.40	4.10	10.00	1.174	-16.141	1.513	8.079
1000.0	100	1.40	5.00	0.75	1.210	-13.577	1.424	1.694
1000.0	100	1.40	5.00	2.00	1.207	-13.817	1.428	1.977
1000.0	100	1.40	5.00	10.00	1.205	-13.949	1.503	7.349
1000.0	100	1.40	10.00	0.75	1.289	-7.929	1.414	0.979
1000.0	100	1.40	10.00	2.00	1.288	-7.997	1.416	1.166
1000.0	100	1.40	10.00	10.00	1.288	-8.012	1.473	5.196
1000.0	100	3.20	0.50	0.75	2.863	-10.546	3.243	1.346
1000.0	100	3.20	0.50	2.00	2.859	-10.662	3.248	1.502
1000.0	100	3.20	0.50	10.00	2.857	-10.705	3.321	3.790
1000.0	100	3.20	1.40	0.75	2.924	-8.626	3.235	1.101
1000.0	100	3.20	1.40	2.00	2.922	-8.687	3.239	1.205
1000.0	100	3.20	1.40	10.00	2.922	-8.698	3.310	3.428
1000.0	100	3.20	3.20	0.75	2.997	-6.335	3.226	0.806

1000.0	100	3.20	3.20	2.00	2.996	-6.361	3.229	0.907
1000.0	100	3.20	3.20	10.00	2.997	-6.355	3.293	2.896
1000.0	100	3.20	4.10	0.75	3.021	-5.605	3.223	0.726
1000.0	100	3.20	4.10	2.00	3.020	-5.622	3.227	0.841
1000.0	100	3.20	4.10	10.00	3.020	-5.614	3.286	2.690
1000.0	100	3.20	5.00	0.75	3.039	-5.032	3.221	0.659
1000.0	100	3.20	5.00	2.00	3.039	-5.045	3.224	0.745
1000.0	100	3.20	5.00	10.00	3.039	-5.035	3.280	2.486
1000.0	100	3.20	10.00	0.75	3.096	-3.258	3.214	0.442
1000.0	100	3.20	10.00	2.00	3.096	-3.262	3.217	0.538
1000.0	100	3.20	10.00	10.00	3.096	-3.251	3.258	1.809
1000.0	100	4.10	0.50	0.75	3.819	-6.842	4.135	0.842
1000.0	100	4.10	0.50	2.00	3.818	-6.877	4.138	0.939
1000.0	100	4.10	0.50	10.00	3.818	-6.874	4.200	2.447
1000.0	100	4.10	1.40	0.75	3.862	-5.799	4.130	0.721
1000.0	100	4.10	1.40	2.00	3.861	-5.818	4.133	0.813
1000.0	100	4.10	1.40	10.00	3.862	-5.809	4.193	2.272
1000.0	100	4.10	3.20	0.75	3.917	-4.463	4.123	0.565
1000.0	100	4.10	3.20	2.00	3.917	-4.472	4.127	0.651
1000.0	100	4.10	3.20	10.00	3.917	-4.461	4.181	1.986
1000.0	100	4.10	4.10	0.75	3.936	-4.012	4.120	0.499
1000.0	100	4.10	4.10	2.00	3.935	-4.018	4.123	0.569
1000.0	100	4.10	4.10	10.00	3.936	-4.008	4.174	1.811
1000.0	100	4.10	5.00	0.75	3.950	-3.650	4.120	0.484
1000.0	100	4.10	5.00	2.00	3.950	-3.655	4.123	0.550
1000.0	100	4.10	5.00	10.00	3.951	-3.644	4.171	1.735
1000.0	100	4.10	10.00	0.75	3.999	-2.475	4.114	0.332
1000.0	100	4.10	10.00	2.00	3.998	-2.476	4.117	0.409
1000.0	100	4.10	10.00	10.00	3.999	-2.467	4.151	1.241
1000.0	100	5.00	0.50	0.75	4.759	-4.827	5.029	0.571
1000.0	100	5.00	0.50	2.00	4.758	-4.840	5.032	0.633
1000.0	100	5.00	0.50	10.00	4.759	-4.829	5.085	1.704
1000.0	100	5.00	1.40	0.75	4.790	-4.202	5.025	0.509
1000.0	100	5.00	1.40	2.00	4.790	-4.210	5.028	0.562
1000.0	100	5.00	1.40	10.00	4.790	-4.198	5.080	1.606
1000.0	100	5.00	3.20	0.75	4.832	-3.356	5.020	0.406
1000.0	100	5.00	3.20	2.00	4.832	-3.360	5.023	0.462
1000.0	100	5.00	3.20	10.00	4.833	-3.350	5.069	1.382
1000.0	100	5.00	4.10	0.75	4.847	-3.058	5.019	0.381
1000.0	100	5.00	4.10	2.00	4.847	-3.060	5.022	0.432
1000.0	100	5.00	4.10	10.00	4.847	-3.051	5.065	1.305
1000.0	100	5.00	5.00	0.75	4.859	-2.812	5.018	0.355
1000.0	100	5.00	5.00	2.00	4.859	-2.814	5.021	0.412
1000.0	100	5.00	5.00	10.00	4.860	-2.806	5.062	1.242
1000.0	100	5.00	10.00	0.75	4.901	-1.985	5.013	0.255
1000.0	100	5.00	10.00	2.00	4.901	-1.986	5.016	0.328
1000.0	100	5.00	10.00	10.00	4.901	-1.979	5.044	0.874
1000.0	100	10.00	0.50	0.75	9.848	-1.520	10.006	0.055
1000.0	100	10.00	0.50	2.00	9.848	-1.520	10.007	0.071
1000.0	100	10.00	0.50	10.00	9.849	-1.514	10.033	0.327

1000.0	100	10.00	1.40	0.75	9.857	-1.426	10.005	0.051
1000.0	100	10.00	1.40	2.00	9.857	-1.426	10.006	0.061
1000.0	100	10.00	1.40	10.00	9.858	-1.421	10.031	0.314
1000.0	100	10.00	3.20	0.75	9.872	-1.276	10.003	0.033
1000.0	100	10.00	3.20	2.00	9.872	-1.276	10.005	0.052
1000.0	100	10.00	3.20	10.00	9.873	-1.272	10.027	0.268
1000.0	100	10.00	4.10	0.75	9.878	-1.215	10.002	0.024
1000.0	100	10.00	4.10	2.00	9.878	-1.215	10.005	0.047
1000.0	100	10.00	4.10	10.00	9.879	-1.212	10.025	0.253
1000.0	100	10.00	5.00	0.75	9.884	-1.162	10.002	0.021
1000.0	100	10.00	5.00	2.00	9.884	-1.162	10.004	0.041
1000.0	100	10.00	5.00	10.00	9.884	-1.159	10.024	0.244
1000.0	100	10.00	10.00	0.75	9.905	-0.953	10.000	-0.001
1000.0	100	10.00	10.00	2.00	9.905	-0.953	10.003	0.033
1000.0	100	10.00	10.00	10.00	9.905	-0.951	10.019	0.187

Table A.6: Simulations for an electric field of 100 kV/m and proton beam kinetic energy of 1000 MeV.

A.3 Electric field: 200 kV/m

A.3.1 Proton energy: 90 MeV

E_p MeV	E kV/m	σ_{x_0} mm	σ_{y_0} mm	σ_{z_0} mm	$\sigma_{x_{el}}$ mm	$\frac{\sigma_{x_{el}}-\sigma_{x_0}}{\sigma_{x_0}}$ %	$\sigma_{x_{H_2^+}}$ mm	$\frac{\sigma_{x_{H_2^+}}-\sigma_{x_0}}{\sigma_{x_0}}$ %
90.0	200	0.50	0.50	0.75	2.088	317.653	0.861	72.256
90.0	200	0.50	0.50	2.00	1.786	257.170	0.862	72.378
90.0	200	0.50	0.50	10.00	1.425	185.017	0.862	72.417
90.0	200	0.50	1.40	0.75	0.938	87.573	0.759	51.820
90.0	200	0.50	1.40	2.00	0.776	55.160	0.761	52.128
90.0	200	0.50	1.40	10.00	0.586	17.289	0.761	52.263
90.0	200	0.50	3.20	0.75	0.407	-18.580	0.665	33.079
90.0	200	0.50	3.20	2.00	0.317	-36.532	0.675	34.961
90.0	200	0.50	3.20	10.00	0.213	-57.459	0.679	35.833
90.0	200	0.50	4.10	0.75	0.340	-32.094	0.634	26.775
90.0	200	0.50	4.10	2.00	0.273	-45.423	0.649	29.900
90.0	200	0.50	4.10	10.00	0.204	-59.275	0.657	31.412
90.0	200	0.50	5.00	0.75	0.316	-36.832	0.610	21.926
90.0	200	0.50	5.00	2.00	0.268	-46.397	0.629	25.794
90.0	200	0.50	5.00	10.00	0.225	-55.038	0.640	28.056
90.0	200	0.50	10.00	0.75	0.351	-29.717	0.551	10.188
90.0	200	0.50	10.00	2.00	0.341	-31.802	0.579	15.803
90.0	200	0.50	10.00	10.00	0.336	-32.844	0.592	18.308
90.0	200	1.40	0.50	0.75	0.831	-40.636	1.627	16.211
90.0	200	1.40	0.50	2.00	0.714	-48.987	1.628	16.311
90.0	200	1.40	0.50	10.00	0.595	-57.499	1.629	16.373
90.0	200	1.40	1.40	0.75	0.857	-38.751	1.587	13.369
90.0	200	1.40	1.40	2.00	0.820	-41.408	1.590	13.543
90.0	200	1.40	1.40	10.00	0.792	-43.437	1.591	13.608
90.0	200	1.40	3.20	0.75	1.025	-26.781	1.533	9.531
90.0	200	1.40	3.20	2.00	1.016	-27.397	1.541	10.105
90.0	200	1.40	3.20	10.00	1.015	-27.531	1.545	10.349
90.0	200	1.40	4.10	0.75	1.080	-22.885	1.514	8.146
90.0	200	1.40	4.10	2.00	1.074	-23.261	1.526	8.989
90.0	200	1.40	4.10	10.00	1.075	-23.219	1.530	9.263
90.0	200	1.40	5.00	0.75	1.121	-19.944	1.499	7.088
90.0	200	1.40	5.00	2.00	1.117	-20.195	1.514	8.131
90.0	200	1.40	5.00	10.00	1.119	-20.076	1.518	8.410
90.0	200	1.40	10.00	0.75	1.238	-11.605	1.461	4.359
90.0	200	1.40	10.00	2.00	1.237	-11.662	1.479	5.673
90.0	200	1.40	10.00	10.00	1.239	-11.499	1.480	5.737
90.0	200	3.20	0.50	0.75	2.705	-15.466	3.336	4.238
90.0	200	3.20	0.50	2.00	2.702	-15.574	3.338	4.310
90.0	200	3.20	0.50	10.00	2.709	-15.338	3.339	4.353
90.0	200	3.20	1.40	0.75	2.796	-12.633	3.321	3.781
90.0	200	3.20	1.40	2.00	2.794	-12.674	3.325	3.896

90.0	200	3.20	1.40	10.00	2.801	-12.480	3.326	3.939
90.0	200	3.20	3.20	0.75	2.905	-9.219	3.297	3.037
90.0	200	3.20	3.20	2.00	2.905	-9.229	3.304	3.250
90.0	200	3.20	3.20	10.00	2.909	-9.080	3.305	3.268
90.0	200	3.20	4.10	0.75	2.940	-8.129	3.288	2.756
90.0	200	3.20	4.10	2.00	2.940	-8.134	3.296	3.004
90.0	200	3.20	4.10	10.00	2.944	-8.000	3.296	3.014
90.0	200	3.20	5.00	0.75	2.967	-7.274	3.281	2.538
90.0	200	3.20	5.00	2.00	2.967	-7.276	3.289	2.794
90.0	200	3.20	5.00	10.00	2.971	-7.156	3.289	2.794
90.0	200	3.20	10.00	0.75	3.052	-4.633	3.259	1.836
90.0	200	3.20	10.00	2.00	3.052	-4.631	3.264	2.005
90.0	200	3.20	10.00	10.00	3.054	-4.555	3.263	1.980
90.0	200	4.10	0.50	0.75	3.691	-9.969	4.212	2.721
90.0	200	4.10	0.50	2.00	3.690	-9.992	4.214	2.782
90.0	200	4.10	0.50	10.00	3.698	-9.804	4.215	2.815
90.0	200	4.10	1.40	0.75	3.755	-8.417	4.202	2.479
90.0	200	4.10	1.40	2.00	3.755	-8.425	4.205	2.567
90.0	200	4.10	1.40	10.00	3.761	-8.279	4.206	2.590
90.0	200	4.10	3.20	0.75	3.837	-6.424	4.184	2.058
90.0	200	4.10	3.20	2.00	3.837	-6.424	4.191	2.209
90.0	200	4.10	3.20	10.00	3.841	-6.317	4.190	2.206
90.0	200	4.10	4.10	0.75	3.864	-5.751	4.178	1.901
90.0	200	4.10	4.10	2.00	3.864	-5.750	4.184	2.056
90.0	200	4.10	4.10	10.00	3.868	-5.656	4.184	2.047
90.0	200	4.10	5.00	0.75	3.886	-5.212	4.173	1.773
90.0	200	4.10	5.00	2.00	3.886	-5.210	4.179	1.921
90.0	200	4.10	5.00	10.00	3.890	-5.125	4.178	1.908
90.0	200	4.10	10.00	0.75	3.958	-3.464	4.153	1.303
90.0	200	4.10	10.00	2.00	3.958	-3.463	4.157	1.391
90.0	200	4.10	10.00	10.00	3.960	-3.409	4.156	1.366
90.0	200	5.00	0.50	0.75	4.652	-6.968	5.094	1.872
90.0	200	5.00	0.50	2.00	4.651	-6.973	5.096	1.919
90.0	200	5.00	0.50	10.00	4.658	-6.837	5.097	1.946
90.0	200	5.00	1.40	0.75	4.698	-6.036	5.086	1.725
90.0	200	5.00	1.40	2.00	4.698	-6.036	5.090	1.801
90.0	200	5.00	1.40	10.00	4.703	-5.930	5.091	1.814
90.0	200	5.00	3.20	0.75	4.761	-4.774	5.074	1.474
90.0	200	5.00	3.20	2.00	4.761	-4.772	5.079	1.571
90.0	200	5.00	3.20	10.00	4.765	-4.695	5.078	1.567
90.0	200	5.00	4.10	0.75	4.784	-4.329	5.069	1.373
90.0	200	5.00	4.10	2.00	4.784	-4.327	5.073	1.468
90.0	200	5.00	4.10	10.00	4.787	-4.259	5.073	1.461
90.0	200	5.00	5.00	0.75	4.802	-3.964	5.065	1.292
90.0	200	5.00	5.00	2.00	4.802	-3.962	5.069	1.376
90.0	200	5.00	5.00	10.00	4.805	-3.901	5.068	1.366
90.0	200	5.00	10.00	0.75	4.863	-2.737	5.048	0.963
90.0	200	5.00	10.00	2.00	4.863	-2.735	5.051	1.013
90.0	200	5.00	10.00	10.00	4.865	-2.695	5.049	0.983
90.0	200	10.00	0.50	0.75	9.795	-2.051	10.035	0.355

90.0	200	10.00	0.50	2.00	9.795	-2.050	10.037	0.373
90.0	200	10.00	0.50	10.00	9.798	-2.018	10.038	0.380
90.0	200	10.00	1.40	0.75	9.809	-1.911	10.034	0.339
90.0	200	10.00	1.40	2.00	9.809	-1.910	10.036	0.362
90.0	200	10.00	1.40	10.00	9.812	-1.883	10.036	0.359
90.0	200	10.00	3.20	0.75	9.831	-1.688	10.030	0.303
90.0	200	10.00	3.20	2.00	9.831	-1.688	10.032	0.321
90.0	200	10.00	3.20	10.00	9.833	-1.666	10.031	0.312
90.0	200	10.00	4.10	0.75	9.840	-1.599	10.029	0.286
90.0	200	10.00	4.10	2.00	9.840	-1.598	10.030	0.300
90.0	200	10.00	4.10	10.00	9.842	-1.579	10.029	0.290
90.0	200	10.00	5.00	0.75	9.848	-1.520	10.027	0.268
90.0	200	10.00	5.00	2.00	9.848	-1.519	10.028	0.280
90.0	200	10.00	5.00	10.00	9.850	-1.502	10.027	0.268
90.0	200	10.00	10.00	0.75	9.879	-1.213	10.019	0.193
90.0	200	10.00	10.00	2.00	9.879	-1.212	10.020	0.201
90.0	200	10.00	10.00	10.00	9.880	-1.200	10.017	0.169

Table A.7: Simulations for an electric field of 200 kV/m and proton beam kinetic energy of 90 MeV.

A.3.2 Proton energy: 200 MeV

E_p MeV	E kV/m	σ_{x_0} mm	σ_{y_0} mm	σ_{z_0} mm	$\sigma_{x_{el}}$ mm	$\frac{\sigma_{x_{el}}-\sigma_{x_0}}{\sigma_{x_0}}$ %	$\sigma_{x_{H_2^+}}$ mm	$\frac{\sigma_{x_{H_2^+}}-\sigma_{x_0}}{\sigma_{x_0}}$ %
200.0	200	0.50	0.50	0.75	1.447	189.447	0.747	49.488
200.0	200	0.50	0.50	2.00	1.209	141.752	0.753	50.559
200.0	200	0.50	0.50	10.00	0.956	91.242	0.758	51.685
200.0	200	0.50	1.40	0.75	0.634	26.747	0.663	32.640
200.0	200	0.50	1.40	2.00	0.498	-0.418	0.673	34.664
200.0	200	0.50	1.40	10.00	0.349	-30.121	0.687	37.335
200.0	200	0.50	3.20	0.75	0.330	-34.016	0.587	17.358
200.0	200	0.50	3.20	2.00	0.269	-46.225	0.597	19.430
200.0	200	0.50	3.20	10.00	0.211	-57.855	0.628	25.670
200.0	200	0.50	4.10	0.75	0.317	-36.630	0.567	13.339
200.0	200	0.50	4.10	2.00	0.278	-44.373	0.578	15.543
200.0	200	0.50	4.10	10.00	0.246	-50.743	0.613	22.633
200.0	200	0.50	5.00	0.75	0.323	-35.316	0.553	10.656
200.0	200	0.50	5.00	2.00	0.298	-40.406	0.564	12.847
200.0	200	0.50	5.00	10.00	0.279	-44.159	0.601	20.258
200.0	200	0.50	10.00	0.75	0.385	-23.088	0.525	4.960
200.0	200	0.50	10.00	2.00	0.379	-24.174	0.537	7.493
200.0	200	0.50	10.00	10.00	0.377	-24.660	0.567	13.350
200.0	200	1.40	0.50	0.75	0.868	-38.032	1.548	10.542
200.0	200	1.40	0.50	2.00	0.805	-42.476	1.553	10.942
200.0	200	1.40	0.50	10.00	0.755	-46.103	1.564	11.716
200.0	200	1.40	1.40	0.75	0.972	-30.574	1.514	8.119
200.0	200	1.40	1.40	2.00	0.953	-31.952	1.520	8.592
200.0	200	1.40	1.40	10.00	0.940	-32.855	1.537	9.761
200.0	200	1.40	3.20	0.75	1.119	-20.089	1.471	5.069
200.0	200	1.40	3.20	2.00	1.114	-20.434	1.480	5.744
200.0	200	1.40	3.20	10.00	1.113	-20.504	1.505	7.477
200.0	200	1.40	4.10	0.75	1.161	-17.062	1.459	4.246
200.0	200	1.40	4.10	2.00	1.158	-17.278	1.469	4.897
200.0	200	1.40	4.10	10.00	1.158	-17.263	1.493	6.613
200.0	200	1.40	5.00	0.75	1.192	-14.822	1.452	3.681
200.0	200	1.40	5.00	2.00	1.190	-14.969	1.460	4.280
200.0	200	1.40	5.00	10.00	1.191	-14.915	1.484	5.993
200.0	200	1.40	10.00	0.75	1.280	-8.598	1.432	2.260
200.0	200	1.40	10.00	2.00	1.279	-8.634	1.441	2.911
200.0	200	1.40	10.00	10.00	1.280	-8.554	1.457	4.091
200.0	200	3.20	0.50	0.75	2.833	-11.463	3.282	2.557
200.0	200	3.20	0.50	2.00	2.831	-11.527	3.286	2.703
200.0	200	3.20	0.50	10.00	2.834	-11.428	3.298	3.069
200.0	200	3.20	1.40	0.75	2.901	-9.351	3.270	2.195
200.0	200	3.20	1.40	2.00	2.900	-9.377	3.276	2.376
200.0	200	3.20	1.40	10.00	2.903	-9.285	3.289	2.767
200.0	200	3.20	3.20	0.75	2.981	-6.839	3.254	1.700

200.0	200	3.20	3.20	2.00	2.981	-6.846	3.260	1.874
200.0	200	3.20	3.20	10.00	2.983	-6.772	3.273	2.283
200.0	200	3.20	4.10	0.75	3.007	-6.040	3.249	1.529
200.0	200	3.20	4.10	2.00	3.007	-6.044	3.255	1.718
200.0	200	3.20	4.10	10.00	3.009	-5.977	3.268	2.122
200.0	200	3.20	5.00	0.75	3.027	-5.415	3.245	1.410
200.0	200	3.20	5.00	2.00	3.027	-5.417	3.251	1.605
200.0	200	3.20	5.00	10.00	3.029	-5.356	3.262	1.953
200.0	200	3.20	10.00	0.75	3.089	-3.484	3.233	1.023
200.0	200	3.20	10.00	2.00	3.089	-3.484	3.238	1.174
200.0	200	3.20	10.00	10.00	3.090	-3.444	3.244	1.372
200.0	200	4.10	0.50	0.75	3.797	-7.394	4.166	1.604
200.0	200	4.10	0.50	2.00	3.796	-7.410	4.170	1.706
200.0	200	4.10	0.50	10.00	3.800	-7.324	4.180	1.952
200.0	200	4.10	1.40	0.75	3.844	-6.252	4.159	1.429
200.0	200	4.10	1.40	2.00	3.843	-6.258	4.163	1.531
200.0	200	4.10	1.40	10.00	3.846	-6.187	4.173	1.780
200.0	200	4.10	3.20	0.75	3.903	-4.794	4.147	1.151
200.0	200	4.10	3.20	2.00	3.903	-4.795	4.152	1.270
200.0	200	4.10	3.20	10.00	3.906	-4.741	4.163	1.526
200.0	200	4.10	4.10	0.75	3.924	-4.302	4.143	1.059
200.0	200	4.10	4.10	2.00	3.924	-4.302	4.148	1.177
200.0	200	4.10	4.10	10.00	3.926	-4.255	4.157	1.402
200.0	200	4.10	5.00	0.75	3.940	-3.908	4.141	0.989
200.0	200	4.10	5.00	2.00	3.940	-3.908	4.145	1.105
200.0	200	4.10	5.00	10.00	3.942	-3.864	4.153	1.292
200.0	200	4.10	10.00	0.75	3.992	-2.632	4.130	0.731
200.0	200	4.10	10.00	2.00	3.992	-2.631	4.134	0.828
200.0	200	4.10	10.00	10.00	3.993	-2.603	4.138	0.916
200.0	200	5.00	0.50	0.75	4.740	-5.193	5.054	1.077
200.0	200	5.00	0.50	2.00	4.740	-5.196	5.057	1.145
200.0	200	5.00	0.50	10.00	4.743	-5.132	5.066	1.319
200.0	200	5.00	1.40	0.75	4.774	-4.510	5.049	0.975
200.0	200	5.00	1.40	2.00	4.774	-4.511	5.052	1.045
200.0	200	5.00	1.40	10.00	4.777	-4.458	5.061	1.229
200.0	200	5.00	3.20	0.75	4.821	-3.589	5.041	0.818
200.0	200	5.00	3.20	2.00	4.821	-3.588	5.045	0.903
200.0	200	5.00	3.20	10.00	4.823	-3.549	5.053	1.050
200.0	200	5.00	4.10	0.75	4.837	-3.264	5.038	0.762
200.0	200	5.00	4.10	2.00	4.837	-3.263	5.042	0.842
200.0	200	5.00	4.10	10.00	4.839	-3.228	5.048	0.966
200.0	200	5.00	5.00	0.75	4.850	-2.997	5.036	0.720
200.0	200	5.00	5.00	2.00	4.850	-2.997	5.040	0.806
200.0	200	5.00	5.00	10.00	4.852	-2.965	5.045	0.907
200.0	200	5.00	10.00	0.75	4.895	-2.101	5.026	0.529
200.0	200	5.00	10.00	2.00	4.895	-2.100	5.029	0.584
200.0	200	5.00	10.00	10.00	4.896	-2.079	5.032	0.632
200.0	200	10.00	0.50	0.75	9.840	-1.600	10.013	0.130
200.0	200	10.00	0.50	2.00	9.840	-1.599	10.014	0.144
200.0	200	10.00	0.50	10.00	9.842	-1.583	10.019	0.186

200.0	200	10.00	1.40	0.75	9.850	-1.497	10.012	0.120
200.0	200	10.00	1.40	2.00	9.850	-1.497	10.014	0.141
200.0	200	10.00	1.40	10.00	9.852	-1.483	10.017	0.171
200.0	200	10.00	3.20	0.75	9.866	-1.335	10.010	0.101
200.0	200	10.00	3.20	2.00	9.867	-1.335	10.012	0.121
200.0	200	10.00	3.20	10.00	9.868	-1.324	10.014	0.138
200.0	200	10.00	4.10	0.75	9.873	-1.270	10.009	0.092
200.0	200	10.00	4.10	2.00	9.873	-1.269	10.011	0.111
200.0	200	10.00	4.10	10.00	9.874	-1.259	10.012	0.121
200.0	200	10.00	5.00	0.75	9.879	-1.212	10.008	0.083
200.0	200	10.00	5.00	2.00	9.879	-1.212	10.010	0.098
200.0	200	10.00	5.00	10.00	9.880	-1.202	10.011	0.105
200.0	200	10.00	10.00	0.75	9.901	-0.987	10.004	0.041
200.0	200	10.00	10.00	2.00	9.901	-0.987	10.006	0.062
200.0	200	10.00	10.00	10.00	9.902	-0.980	10.003	0.032

Table A.8: Simulations for an electric field of 200 kV/m and proton beam kinetic energy of 200 MeV.

A.3.3 Proton energy: 1000 MeV

E_p MeV	E kV/m	σ_{x_0} mm	σ_{y_0} mm	σ_{z_0} mm	$\sigma_{x_{el}}$ mm	$\frac{\sigma_{x_{el}}-\sigma_{x_0}}{\sigma_{x_0}}$ %	$\sigma_{x_{H_2^+}}$ mm	$\frac{\sigma_{x_{H_2^+}}-\sigma_{x_0}}{\sigma_{x_0}}$ %
1000.0	200	0.50	0.50	0.75	0.888	77.665	0.573	14.533
1000.0	200	0.50	0.50	2.00	0.688	37.674	0.579	15.809
1000.0	200	0.50	0.50	10.00	0.233	-53.403	0.608	21.587
1000.0	200	0.50	1.40	0.75	0.418	-16.329	0.538	7.542
1000.0	200	0.50	1.40	2.00	0.306	-38.890	0.545	8.944
1000.0	200	0.50	1.40	10.00	0.192	-61.534	0.611	22.271
1000.0	200	0.50	3.20	0.75	0.337	-32.644	0.518	3.612
1000.0	200	0.50	3.20	2.00	0.305	-38.998	0.521	4.249
1000.0	200	0.50	3.20	10.00	0.283	-43.393	0.575	14.954
1000.0	200	0.50	4.10	0.75	0.352	-29.645	0.514	2.866
1000.0	200	0.50	4.10	2.00	0.333	-33.446	0.517	3.436
1000.0	200	0.50	4.10	10.00	0.321	-35.870	0.566	13.256
1000.0	200	0.50	5.00	0.75	0.368	-26.483	0.511	2.246
1000.0	200	0.50	5.00	2.00	0.355	-28.978	0.515	2.948
1000.0	200	0.50	5.00	10.00	0.348	-30.472	0.560	11.963
1000.0	200	0.50	10.00	0.75	0.422	-15.696	0.506	1.134
1000.0	200	0.50	10.00	2.00	0.419	-16.276	0.509	1.783
1000.0	200	0.50	10.00	10.00	0.418	-16.479	0.542	8.386
1000.0	200	1.40	0.50	0.75	1.009	-27.895	1.436	2.600
1000.0	200	1.40	0.50	2.00	0.977	-30.246	1.441	2.961
1000.0	200	1.40	0.50	10.00	0.956	-31.733	1.499	7.079
1000.0	200	1.40	1.40	0.75	1.109	-20.752	1.425	1.813
1000.0	200	1.40	1.40	2.00	1.098	-21.596	1.428	2.029
1000.0	200	1.40	1.40	10.00	1.091	-22.054	1.480	5.719
1000.0	200	1.40	3.20	0.75	1.213	-13.348	1.414	1.029
1000.0	200	1.40	3.20	2.00	1.210	-13.597	1.418	1.251
1000.0	200	1.40	3.20	10.00	1.209	-13.677	1.461	4.332
1000.0	200	1.40	4.10	0.75	1.242	-11.319	1.412	0.856
1000.0	200	1.40	4.10	2.00	1.239	-11.482	1.415	1.052
1000.0	200	1.40	4.10	10.00	1.239	-11.515	1.456	3.973
1000.0	200	1.40	5.00	0.75	1.262	-9.831	1.410	0.735
1000.0	200	1.40	5.00	2.00	1.261	-9.947	1.413	0.906
1000.0	200	1.40	5.00	10.00	1.261	-9.955	1.451	3.650
1000.0	200	1.40	10.00	0.75	1.320	-5.736	1.406	0.435
1000.0	200	1.40	10.00	2.00	1.319	-5.769	1.408	0.603
1000.0	200	1.40	10.00	10.00	1.320	-5.747	1.438	2.720
1000.0	200	3.20	0.50	0.75	2.956	-7.621	3.217	0.520
1000.0	200	3.20	0.50	2.00	2.954	-7.676	3.220	0.614
1000.0	200	3.20	0.50	10.00	2.955	-7.653	3.255	1.725
1000.0	200	3.20	1.40	0.75	3.001	-6.229	3.213	0.415
1000.0	200	3.20	1.40	2.00	3.000	-6.258	3.216	0.502
1000.0	200	3.20	1.40	10.00	3.001	-6.230	3.251	1.583
1000.0	200	3.20	3.20	0.75	3.053	-4.588	3.209	0.286

1000.0	200	3.20	3.20	2.00	3.053	-4.600	3.211	0.339
1000.0	200	3.20	3.20	10.00	3.054	-4.574	3.243	1.336
1000.0	200	3.20	4.10	0.75	3.070	-4.067	3.208	0.250
1000.0	200	3.20	4.10	2.00	3.070	-4.075	3.210	0.314
1000.0	200	3.20	4.10	10.00	3.070	-4.051	3.239	1.208
1000.0	200	3.20	5.00	0.75	3.083	-3.659	3.207	0.221
1000.0	200	3.20	5.00	2.00	3.083	-3.665	3.209	0.272
1000.0	200	3.20	5.00	10.00	3.083	-3.643	3.234	1.067
1000.0	200	3.20	10.00	0.75	3.123	-2.400	3.203	0.108
1000.0	200	3.20	10.00	2.00	3.123	-2.402	3.205	0.166
1000.0	200	3.20	10.00	10.00	3.124	-2.386	3.229	0.895
1000.0	200	4.10	0.50	0.75	3.897	-4.953	4.112	0.288
1000.0	200	4.10	0.50	2.00	3.896	-4.970	4.114	0.338
1000.0	200	4.10	0.50	10.00	3.897	-4.942	4.145	1.088
1000.0	200	4.10	1.40	0.75	3.928	-4.206	4.109	0.228
1000.0	200	4.10	1.40	2.00	3.927	-4.215	4.111	0.278
1000.0	200	4.10	1.40	10.00	3.928	-4.190	4.141	1.009
1000.0	200	4.10	3.20	0.75	3.967	-3.255	4.107	0.166
1000.0	200	4.10	3.20	2.00	3.966	-3.259	4.108	0.201
1000.0	200	4.10	3.20	10.00	3.967	-3.239	4.135	0.847
1000.0	200	4.10	4.10	0.75	3.980	-2.935	4.106	0.136
1000.0	200	4.10	4.10	2.00	3.980	-2.937	4.107	0.167
1000.0	200	4.10	4.10	10.00	3.980	-2.920	4.130	0.722
1000.0	200	4.10	5.00	0.75	3.990	-2.678	4.105	0.117
1000.0	200	4.10	5.00	2.00	3.990	-2.680	4.107	0.175
1000.0	200	4.10	5.00	10.00	3.991	-2.663	4.130	0.726
1000.0	200	4.10	10.00	0.75	4.024	-1.845	4.102	0.043
1000.0	200	4.10	10.00	2.00	4.024	-1.846	4.104	0.090
1000.0	200	4.10	10.00	10.00	4.025	-1.834	4.123	0.564
1000.0	200	5.00	0.50	0.75	4.824	-3.516	5.008	0.152
1000.0	200	5.00	0.50	2.00	4.824	-3.521	5.009	0.185
1000.0	200	5.00	0.50	10.00	4.825	-3.498	5.036	0.712
1000.0	200	5.00	1.40	0.75	4.846	-3.071	5.006	0.122
1000.0	200	5.00	1.40	2.00	4.846	-3.074	5.008	0.157
1000.0	200	5.00	1.40	10.00	4.847	-3.054	5.033	0.651
1000.0	200	5.00	3.20	0.75	4.876	-2.470	5.004	0.076
1000.0	200	5.00	3.20	2.00	4.876	-2.471	5.005	0.107
1000.0	200	5.00	3.20	10.00	4.877	-2.456	5.026	0.520
1000.0	200	5.00	4.10	0.75	4.887	-2.258	5.003	0.056
1000.0	200	5.00	4.10	2.00	4.887	-2.259	5.005	0.106
1000.0	200	5.00	4.10	10.00	4.888	-2.245	5.027	0.534
1000.0	200	5.00	5.00	0.75	4.896	-2.084	5.002	0.047
1000.0	200	5.00	5.00	2.00	4.896	-2.085	5.004	0.088
1000.0	200	5.00	5.00	10.00	4.896	-2.073	5.027	0.541
1000.0	200	5.00	10.00	0.75	4.925	-1.499	4.999	-0.020
1000.0	200	5.00	10.00	2.00	4.925	-1.499	5.004	0.082
1000.0	200	5.00	10.00	10.00	4.925	-1.490	5.017	0.344
1000.0	200	10.00	0.50	0.75	9.883	-1.171	9.988	-0.124
1000.0	200	10.00	0.50	2.00	9.883	-1.171	9.988	-0.125
1000.0	200	10.00	0.50	10.00	9.884	-1.164	10.002	0.021

1000.0	200	10.00	1.40	0.75	9.890	-1.104	9.987	-0.126
1000.0	200	10.00	1.40	2.00	9.890	-1.104	9.987	-0.129
1000.0	200	10.00	1.40	10.00	9.890	-1.098	10.002	0.019
1000.0	200	10.00	3.20	0.75	9.900	-0.998	9.986	-0.142
1000.0	200	10.00	3.20	2.00	9.900	-0.998	9.989	-0.112
1000.0	200	10.00	3.20	10.00	9.901	-0.994	10.000	-0.005
1000.0	200	10.00	4.10	0.75	9.904	-0.956	9.986	-0.142
1000.0	200	10.00	4.10	2.00	9.904	-0.955	9.989	-0.113
1000.0	200	10.00	4.10	10.00	9.905	-0.951	9.998	-0.021
1000.0	200	10.00	5.00	0.75	9.908	-0.918	9.986	-0.137
1000.0	200	10.00	5.00	2.00	9.908	-0.918	9.989	-0.107
1000.0	200	10.00	5.00	10.00	9.909	-0.914	9.998	-0.022
1000.0	200	10.00	10.00	0.75	9.923	-0.770	9.985	-0.147
1000.0	200	10.00	10.00	2.00	9.923	-0.770	9.988	-0.120
1000.0	200	10.00	10.00	10.00	9.923	-0.768	9.994	-0.059

Table A.9: Simulations for an electric field of 200 kV/m and proton beam kinetic energy of 1000 MeV.

A.4 Electric field: 300 kV/m

A.4.1 Proton energy: 90 MeV

E_p MeV	E kV/m	σ_{x_0} mm	σ_{y_0} mm	σ_{z_0} mm	$\sigma_{x_{el}}$ mm	$\frac{\sigma_{x_{el}}-\sigma_{x_0}}{\sigma_{x_0}}$ %	$\sigma_{x_{H_2^+}}$ mm	$\frac{\sigma_{x_{H_2^+}}-\sigma_{x_0}}{\sigma_{x_0}}$ %
90.0	300	0.50	0.50	0.75	1.643	228.558	0.728	45.692
90.0	300	0.50	0.50	2.00	1.385	177.015	0.729	45.812
90.0	300	0.50	0.50	10.00	1.045	108.908	0.729	45.842
90.0	300	0.50	1.40	0.75	0.721	44.275	0.661	32.153
90.0	300	0.50	1.40	2.00	0.579	15.843	0.662	32.473
90.0	300	0.50	1.40	10.00	0.404	-19.154	0.663	32.658
90.0	300	0.50	3.20	0.75	0.343	-31.315	0.596	19.265
90.0	300	0.50	3.20	2.00	0.273	-45.314	0.605	21.065
90.0	300	0.50	3.20	10.00	0.201	-59.816	0.610	21.992
90.0	300	0.50	4.10	0.75	0.315	-36.997	0.576	15.228
90.0	300	0.50	4.10	2.00	0.269	-46.267	0.589	17.751
90.0	300	0.50	4.10	10.00	0.229	-54.167	0.596	19.115
90.0	300	0.50	5.00	0.75	0.314	-37.108	0.561	12.252
90.0	300	0.50	5.00	2.00	0.284	-43.292	0.576	15.226
90.0	300	0.50	5.00	10.00	0.261	-47.731	0.585	17.038
90.0	300	0.50	10.00	0.75	0.373	-25.459	0.528	5.652
90.0	300	0.50	10.00	2.00	0.366	-26.741	0.548	9.510
90.0	300	0.50	10.00	10.00	0.365	-27.038	0.554	10.899
90.0	300	1.40	0.50	0.75	0.836	-40.288	1.537	9.808
90.0	300	1.40	0.50	2.00	0.761	-45.617	1.539	9.922
90.0	300	1.40	0.50	10.00	0.708	-49.421	1.540	9.984
90.0	300	1.40	1.40	0.75	0.929	-33.646	1.510	7.833
90.0	300	1.40	1.40	2.00	0.907	-35.234	1.512	8.029
90.0	300	1.40	1.40	10.00	0.898	-35.854	1.514	8.123
90.0	300	1.40	3.20	0.75	1.088	-22.318	1.474	5.254
90.0	300	1.40	3.20	2.00	1.082	-22.688	1.480	5.690
90.0	300	1.40	3.20	10.00	1.085	-22.496	1.483	5.931
90.0	300	1.40	4.10	0.75	1.134	-18.969	1.461	4.361
90.0	300	1.40	4.10	2.00	1.131	-19.194	1.470	4.997
90.0	300	1.40	4.10	10.00	1.135	-18.949	1.474	5.260
90.0	300	1.40	5.00	0.75	1.169	-16.481	1.452	3.701
90.0	300	1.40	5.00	2.00	1.167	-16.630	1.463	4.520
90.0	300	1.40	5.00	10.00	1.171	-16.373	1.466	4.719
90.0	300	1.40	10.00	0.75	1.266	-9.546	1.430	2.157
90.0	300	1.40	10.00	2.00	1.266	-9.578	1.440	2.823
90.0	300	1.40	10.00	10.00	1.269	-9.379	1.441	2.963
90.0	300	3.20	0.50	0.75	2.793	-12.734	3.266	2.057
90.0	300	3.20	0.50	2.00	2.791	-12.794	3.268	2.116
90.0	300	3.20	0.50	10.00	2.802	-12.438	3.269	2.156
90.0	300	3.20	1.40	0.75	2.868	-10.376	3.255	1.731
90.0	300	3.20	1.40	2.00	2.867	-10.396	3.258	1.825

90.0	300	3.20	1.40	10.00	2.875	-10.150	3.260	1.875
90.0	300	3.20	3.20	0.75	2.958	-7.567	3.240	1.258
90.0	300	3.20	3.20	2.00	2.958	-7.570	3.245	1.407
90.0	300	3.20	3.20	10.00	2.963	-7.401	3.246	1.426
90.0	300	3.20	4.10	0.75	2.986	-6.674	3.235	1.084
90.0	300	3.20	4.10	2.00	2.986	-6.674	3.240	1.241
90.0	300	3.20	4.10	10.00	2.991	-6.527	3.240	1.255
90.0	300	3.20	5.00	0.75	3.009	-5.976	3.230	0.948
90.0	300	3.20	5.00	2.00	3.009	-5.974	3.235	1.101
90.0	300	3.20	5.00	10.00	3.013	-5.844	3.235	1.109
90.0	300	3.20	10.00	0.75	3.078	-3.821	3.216	0.509
90.0	300	3.20	10.00	2.00	3.078	-3.819	3.219	0.607
90.0	300	3.20	10.00	10.00	3.080	-3.740	3.218	0.574
90.0	300	4.10	0.50	0.75	3.764	-8.190	4.144	1.076
90.0	300	4.10	0.50	2.00	3.764	-8.201	4.146	1.124
90.0	300	4.10	0.50	10.00	3.774	-7.963	4.147	1.158
90.0	300	4.10	1.40	0.75	3.817	-6.912	4.137	0.907
90.0	300	4.10	1.40	2.00	3.817	-6.914	4.140	0.980
90.0	300	4.10	1.40	10.00	3.823	-6.745	4.141	1.005
90.0	300	4.10	3.20	0.75	3.883	-5.281	4.126	0.640
90.0	300	4.10	3.20	2.00	3.884	-5.278	4.130	0.721
90.0	300	4.10	3.20	10.00	3.888	-5.162	4.130	0.739
90.0	300	4.10	4.10	0.75	3.906	-4.732	4.122	0.547
90.0	300	4.10	4.10	2.00	3.906	-4.729	4.126	0.634
90.0	300	4.10	4.10	10.00	3.910	-4.628	4.126	0.632
90.0	300	4.10	5.00	0.75	3.924	-4.292	4.119	0.459
90.0	300	4.10	5.00	2.00	3.924	-4.289	4.122	0.549
90.0	300	4.10	5.00	10.00	3.928	-4.199	4.122	0.539
90.0	300	4.10	10.00	0.75	3.982	-2.869	4.107	0.162
90.0	300	4.10	10.00	2.00	3.982	-2.867	4.109	0.216
90.0	300	4.10	10.00	10.00	3.985	-2.812	4.107	0.182
90.0	300	5.00	0.50	0.75	4.714	-5.730	5.026	0.524
90.0	300	5.00	0.50	2.00	4.714	-5.730	5.028	0.565
90.0	300	5.00	0.50	10.00	4.722	-5.568	5.030	0.591
90.0	300	5.00	1.40	0.75	4.752	-4.966	5.021	0.418
90.0	300	5.00	1.40	2.00	4.752	-4.963	5.024	0.485
90.0	300	5.00	1.40	10.00	4.758	-4.845	5.025	0.497
90.0	300	5.00	3.20	0.75	4.803	-3.935	5.013	0.260
90.0	300	5.00	3.20	2.00	4.803	-3.932	5.017	0.334
90.0	300	5.00	3.20	10.00	4.808	-3.849	5.016	0.326
90.0	300	5.00	4.10	0.75	4.821	-3.572	5.010	0.201
90.0	300	5.00	4.10	2.00	4.822	-3.570	5.014	0.271
90.0	300	5.00	4.10	10.00	4.825	-3.497	5.013	0.255
90.0	300	5.00	5.00	0.75	4.836	-3.275	5.008	0.154
90.0	300	5.00	5.00	2.00	4.836	-3.273	5.010	0.206
90.0	300	5.00	5.00	10.00	4.840	-3.208	5.010	0.191
90.0	300	5.00	10.00	0.75	4.886	-2.277	4.997	-0.052
90.0	300	5.00	10.00	2.00	4.886	-2.275	4.999	-0.011
90.0	300	5.00	10.00	10.00	4.888	-2.235	4.997	-0.063
90.0	300	10.00	0.50	0.75	9.828	-1.721	9.954	-0.456

90.0	300	10.00	0.50	2.00	9.828	-1.720	9.956	-0.442
90.0	300	10.00	0.50	10.00	9.832	-1.685	9.956	-0.439
90.0	300	10.00	1.40	0.75	9.839	-1.607	9.953	-0.467
90.0	300	10.00	1.40	2.00	9.839	-1.606	9.955	-0.450
90.0	300	10.00	1.40	10.00	9.842	-1.577	9.955	-0.455
90.0	300	10.00	3.20	0.75	9.857	-1.426	9.951	-0.488
90.0	300	10.00	3.20	2.00	9.858	-1.425	9.952	-0.476
90.0	300	10.00	3.20	10.00	9.860	-1.403	9.951	-0.487
90.0	300	10.00	4.10	0.75	9.865	-1.353	9.950	-0.498
90.0	300	10.00	4.10	2.00	9.865	-1.352	9.951	-0.487
90.0	300	10.00	4.10	10.00	9.867	-1.332	9.950	-0.503
90.0	300	10.00	5.00	0.75	9.871	-1.289	9.949	-0.509
90.0	300	10.00	5.00	2.00	9.871	-1.288	9.950	-0.498
90.0	300	10.00	5.00	10.00	9.873	-1.270	9.948	-0.517
90.0	300	10.00	10.00	0.75	9.896	-1.040	9.944	-0.558
90.0	300	10.00	10.00	2.00	9.896	-1.039	9.944	-0.560
90.0	300	10.00	10.00	10.00	9.897	-1.027	9.942	-0.585

Table A.10: Simulations for an electric field of 300 kV/m and proton beam kinetic energy of 90 MeV.

A.4.2 Proton energy: 200 MeV

E_p MeV	E kV/m	σ_{x_0} mm	σ_{y_0} mm	σ_{z_0} mm	$\sigma_{x_{el}}$ mm	$\frac{\sigma_{x_{el}}-\sigma_{x_0}}{\sigma_{x_0}}$ %	$\sigma_{x_{H_2^+}}$ mm	$\frac{\sigma_{x_{H_2^+}}-\sigma_{x_0}}{\sigma_{x_0}}$ %
200.0	300	0.50	0.50	0.75	1.128	125.604	0.651	30.221
200.0	300	0.50	0.50	2.00	0.922	84.434	0.657	31.451
200.0	300	0.50	0.50	10.00	0.691	38.206	0.663	32.654
200.0	300	0.50	1.40	0.75	0.493	-1.308	0.594	18.815
200.0	300	0.50	1.40	2.00	0.376	-24.866	0.603	20.503
200.0	300	0.50	1.40	10.00	0.242	-51.518	0.616	23.191
200.0	300	0.50	3.20	0.75	0.318	-36.490	0.547	9.392
200.0	300	0.50	3.20	2.00	0.277	-44.671	0.554	10.895
200.0	300	0.50	3.20	10.00	0.244	-51.220	0.578	15.646
200.0	300	0.50	4.10	0.75	0.326	-34.900	0.536	7.171
200.0	300	0.50	4.10	2.00	0.301	-39.783	0.543	8.630
200.0	300	0.50	4.10	10.00	0.284	-43.132	0.567	13.496
200.0	300	0.50	5.00	0.75	0.341	-31.893	0.528	5.685
200.0	300	0.50	5.00	2.00	0.325	-35.049	0.536	7.280
200.0	300	0.50	5.00	10.00	0.315	-36.939	0.560	12.075
200.0	300	0.50	10.00	0.75	0.403	-19.422	0.512	2.452
200.0	300	0.50	10.00	2.00	0.399	-20.104	0.522	4.366
200.0	300	0.50	10.00	10.00	0.399	-20.241	0.539	7.769
200.0	300	1.40	0.50	0.75	0.924	-34.029	1.482	5.849
200.0	300	1.40	0.50	2.00	0.886	-36.746	1.487	6.246
200.0	300	1.40	0.50	10.00	0.862	-38.402	1.498	6.967
200.0	300	1.40	1.40	0.75	1.038	-25.842	1.460	4.268
200.0	300	1.40	1.40	2.00	1.026	-26.686	1.465	4.635
200.0	300	1.40	1.40	10.00	1.022	-26.984	1.479	5.671
200.0	300	1.40	3.20	0.75	1.167	-16.648	1.434	2.407
200.0	300	1.40	3.20	2.00	1.164	-16.860	1.439	2.815
200.0	300	1.40	3.20	10.00	1.165	-16.772	1.456	4.025
200.0	300	1.40	4.10	0.75	1.203	-14.100	1.427	1.932
200.0	300	1.40	4.10	2.00	1.201	-14.234	1.432	2.319
200.0	300	1.40	4.10	10.00	1.202	-14.116	1.451	3.629
200.0	300	1.40	5.00	0.75	1.229	-12.231	1.422	1.581
200.0	300	1.40	5.00	2.00	1.227	-12.322	1.429	2.104
200.0	300	1.40	5.00	10.00	1.229	-12.196	1.445	3.203
200.0	300	1.40	10.00	0.75	1.301	-7.088	1.411	0.759
200.0	300	1.40	10.00	2.00	1.300	-7.110	1.417	1.247
200.0	300	1.40	10.00	10.00	1.302	-7.009	1.428	1.974
200.0	300	3.20	0.50	0.75	2.898	-9.445	3.230	0.923
200.0	300	3.20	0.50	2.00	2.897	-9.483	3.233	1.027
200.0	300	3.20	0.50	10.00	2.901	-9.334	3.242	1.306
200.0	300	3.20	1.40	0.75	2.954	-7.699	3.222	0.700
200.0	300	3.20	1.40	2.00	2.953	-7.713	3.226	0.822
200.0	300	3.20	1.40	10.00	2.957	-7.597	3.236	1.124
200.0	300	3.20	3.20	0.75	3.020	-5.636	3.213	0.399

200.0	300	3.20	3.20	2.00	3.020	-5.639	3.217	0.542
200.0	300	3.20	3.20	10.00	3.022	-5.555	3.225	0.785
200.0	300	3.20	4.10	0.75	3.041	-4.983	3.210	0.300
200.0	300	3.20	4.10	2.00	3.041	-4.984	3.213	0.402
200.0	300	3.20	4.10	10.00	3.043	-4.909	3.221	0.662
200.0	300	3.20	5.00	0.75	3.057	-4.472	3.207	0.211
200.0	300	3.20	5.00	2.00	3.057	-4.472	3.211	0.338
200.0	300	3.20	5.00	10.00	3.059	-4.405	3.219	0.580
200.0	300	3.20	10.00	0.75	3.107	-2.896	3.200	-0.005
200.0	300	3.20	10.00	2.00	3.107	-2.895	3.202	0.060
200.0	300	3.20	10.00	10.00	3.109	-2.853	3.206	0.185
200.0	300	4.10	0.50	0.75	3.850	-6.096	4.114	0.338
200.0	300	4.10	0.50	2.00	3.850	-6.103	4.117	0.404
200.0	300	4.10	0.50	10.00	3.854	-5.998	4.125	0.598
200.0	300	4.10	1.40	0.75	3.889	-5.157	4.109	0.212
200.0	300	4.10	1.40	2.00	3.888	-5.159	4.112	0.295
200.0	300	4.10	1.40	10.00	3.892	-5.078	4.120	0.488
200.0	300	4.10	3.20	0.75	3.937	-3.964	4.103	0.067
200.0	300	4.10	3.20	2.00	3.938	-3.963	4.106	0.135
200.0	300	4.10	3.20	10.00	3.940	-3.905	4.112	0.296
200.0	300	4.10	4.10	0.75	3.954	-3.562	4.100	-0.009
200.0	300	4.10	4.10	2.00	3.954	-3.561	4.103	0.069
200.0	300	4.10	4.10	10.00	3.956	-3.510	4.109	0.226
200.0	300	4.10	5.00	0.75	3.967	-3.241	4.098	-0.044
200.0	300	4.10	5.00	2.00	3.967	-3.240	4.101	0.014
200.0	300	4.10	5.00	10.00	3.969	-3.194	4.106	0.158
200.0	300	4.10	10.00	0.75	4.010	-2.201	4.093	-0.179
200.0	300	4.10	10.00	2.00	4.010	-2.200	4.094	-0.143
200.0	300	4.10	10.00	10.00	4.011	-2.170	4.096	-0.107
200.0	300	5.00	0.50	0.75	4.785	-4.292	5.000	0.004
200.0	300	5.00	0.50	2.00	4.785	-4.293	5.002	0.040
200.0	300	5.00	0.50	10.00	4.789	-4.219	5.009	0.184
200.0	300	5.00	1.40	0.75	4.813	-3.733	4.997	-0.065
200.0	300	5.00	1.40	2.00	4.813	-3.733	5.000	-0.010
200.0	300	5.00	1.40	10.00	4.816	-3.675	5.006	0.113
200.0	300	5.00	3.20	0.75	4.851	-2.980	4.993	-0.144
200.0	300	5.00	3.20	2.00	4.851	-2.979	4.995	-0.103
200.0	300	5.00	3.20	10.00	4.853	-2.937	5.000	-0.000
200.0	300	5.00	4.10	0.75	4.864	-2.715	4.990	-0.192
200.0	300	5.00	4.10	2.00	4.864	-2.714	4.992	-0.162
200.0	300	5.00	4.10	10.00	4.866	-2.677	4.997	-0.053
200.0	300	5.00	5.00	0.75	4.875	-2.498	4.989	-0.218
200.0	300	5.00	5.00	2.00	4.875	-2.497	4.992	-0.162
200.0	300	5.00	5.00	10.00	4.877	-2.464	4.995	-0.101
200.0	300	5.00	10.00	0.75	4.912	-1.768	4.984	-0.323
200.0	300	5.00	10.00	2.00	4.912	-1.767	4.986	-0.280
200.0	300	5.00	10.00	10.00	4.913	-1.746	4.986	-0.289
200.0	300	10.00	0.50	0.75	9.864	-1.361	9.940	-0.602
200.0	300	10.00	0.50	2.00	9.864	-1.360	9.941	-0.591
200.0	300	10.00	0.50	10.00	9.866	-1.343	9.943	-0.566

200.0	300	10.00	1.40	0.75	9.872	-1.277	9.939	-0.607
200.0	300	10.00	1.40	2.00	9.872	-1.277	9.941	-0.591
200.0	300	10.00	1.40	10.00	9.874	-1.262	9.942	-0.577
200.0	300	10.00	3.20	0.75	9.885	-1.145	9.938	-0.616
200.0	300	10.00	3.20	2.00	9.886	-1.144	9.939	-0.605
200.0	300	10.00	3.20	10.00	9.887	-1.133	9.940	-0.601
200.0	300	10.00	4.10	0.75	9.891	-1.092	9.938	-0.621
200.0	300	10.00	4.10	2.00	9.891	-1.091	9.939	-0.611
200.0	300	10.00	4.10	10.00	9.892	-1.081	9.939	-0.612
200.0	300	10.00	5.00	0.75	9.896	-1.045	9.937	-0.627
200.0	300	10.00	5.00	2.00	9.896	-1.044	9.939	-0.611
200.0	300	10.00	5.00	10.00	9.897	-1.035	9.938	-0.623
200.0	300	10.00	10.00	0.75	9.914	-0.862	9.937	-0.634
200.0	300	10.00	10.00	2.00	9.914	-0.862	9.938	-0.624
200.0	300	10.00	10.00	10.00	9.914	-0.855	9.933	-0.673

Table A.11: Simulations for an electric field of 300 kV/m and proton beam kinetic energy of 200 MeV.

A.4.3 Proton energy: 1000 MeV

E_p MeV	E kV/m	σ_{x_0} mm	σ_{y_0} mm	σ_{z_0} mm	$\sigma_{x_{el}}$ mm	$\frac{\sigma_{x_{el}}-\sigma_{x_0}}{\sigma_{x_0}}$ %	$\sigma_{x_{H_2^+}}$ mm	$\frac{\sigma_{x_{H_2^+}}-\sigma_{x_0}}{\sigma_{x_0}}$ %
1000.0	300	0.50	0.50	0.75	0.690	38.060	0.546	9.163
1000.0	300	0.50	0.50	2.00	0.516	3.203	0.553	10.597
1000.0	300	0.50	0.50	10.00	0.199	-60.281	0.601	20.191
1000.0	300	0.50	1.40	0.75	0.361	-27.795	0.522	4.375
1000.0	300	0.50	1.40	2.00	0.275	-44.914	0.526	5.254
1000.0	300	0.50	1.40	10.00	0.200	-60.040	0.568	13.572
1000.0	300	0.50	3.20	0.75	0.351	-29.848	0.508	1.623
1000.0	300	0.50	3.20	2.00	0.331	-33.841	0.511	2.252
1000.0	300	0.50	3.20	10.00	0.319	-36.274	0.546	9.136
1000.0	300	0.50	4.10	0.75	0.370	-26.012	0.506	1.147
1000.0	300	0.50	4.10	2.00	0.358	-28.397	0.509	1.713
1000.0	300	0.50	4.10	10.00	0.351	-29.717	0.540	8.088
1000.0	300	0.50	5.00	0.75	0.386	-22.771	0.504	0.744
1000.0	300	0.50	5.00	2.00	0.378	-24.346	0.507	1.392
1000.0	300	0.50	5.00	10.00	0.374	-25.140	0.536	7.227
1000.0	300	0.50	10.00	0.75	0.435	-13.092	0.500	0.058
1000.0	300	0.50	10.00	2.00	0.433	-13.469	0.503	0.580
1000.0	300	0.50	10.00	10.00	0.432	-13.524	0.527	5.384
1000.0	300	1.40	0.50	0.75	1.065	-23.911	1.416	1.142
1000.0	300	1.40	0.50	2.00	1.045	-25.383	1.420	1.404
1000.0	300	1.40	0.50	10.00	1.034	-26.142	1.455	3.903
1000.0	300	1.40	1.40	0.75	1.157	-17.357	1.408	0.547
1000.0	300	1.40	1.40	2.00	1.149	-17.895	1.411	0.771
1000.0	300	1.40	1.40	10.00	1.147	-18.089	1.442	2.995
1000.0	300	1.40	3.20	0.75	1.245	-11.056	1.400	0.016
1000.0	300	1.40	3.20	2.00	1.243	-11.216	1.403	0.234
1000.0	300	1.40	3.20	10.00	1.243	-11.214	1.431	2.204
1000.0	300	1.40	4.10	0.75	1.269	-9.364	1.398	-0.107
1000.0	300	1.40	4.10	2.00	1.267	-9.469	1.400	0.035
1000.0	300	1.40	4.10	10.00	1.268	-9.447	1.426	1.864
1000.0	300	1.40	5.00	0.75	1.286	-8.130	1.397	-0.185
1000.0	300	1.40	5.00	2.00	1.285	-8.204	1.399	-0.054
1000.0	300	1.40	5.00	10.00	1.286	-8.172	1.423	1.664
1000.0	300	1.40	10.00	0.75	1.333	-4.754	1.395	-0.365
1000.0	300	1.40	10.00	2.00	1.333	-4.775	1.396	-0.276
1000.0	300	1.40	10.00	10.00	1.334	-4.740	1.417	1.223
1000.0	300	3.20	0.50	0.75	2.998	-6.303	3.190	-0.309
1000.0	300	3.20	0.50	2.00	2.997	-6.338	3.192	-0.246
1000.0	300	3.20	0.50	10.00	2.999	-6.292	3.216	0.489
1000.0	300	3.20	1.40	0.75	3.035	-5.155	3.188	-0.384
1000.0	300	3.20	1.40	2.00	3.034	-5.174	3.190	-0.325
1000.0	300	3.20	1.40	10.00	3.036	-5.132	3.212	0.372
1000.0	300	3.20	3.20	0.75	3.078	-3.808	3.184	-0.499

1000.0	300	3.20	3.20	2.00	3.078	-3.816	3.186	-0.423
1000.0	300	3.20	3.20	10.00	3.079	-3.784	3.207	0.226
1000.0	300	3.20	4.10	0.75	3.092	-3.382	3.183	-0.516
1000.0	300	3.20	4.10	2.00	3.092	-3.387	3.185	-0.463
1000.0	300	3.20	4.10	10.00	3.093	-3.358	3.206	0.194
1000.0	300	3.20	5.00	0.75	3.102	-3.049	3.183	-0.524
1000.0	300	3.20	5.00	2.00	3.102	-3.052	3.183	-0.520
1000.0	300	3.20	5.00	10.00	3.103	-3.026	3.204	0.127
1000.0	300	3.20	10.00	0.75	3.135	-2.020	3.181	-0.583
1000.0	300	3.20	10.00	2.00	3.135	-2.020	3.185	-0.461
1000.0	300	3.20	10.00	10.00	3.136	-2.003	3.197	-0.080
1000.0	300	4.10	0.50	0.75	3.932	-4.110	4.080	-0.486
1000.0	300	4.10	0.50	2.00	3.931	-4.119	4.082	-0.433
1000.0	300	4.10	0.50	10.00	3.933	-4.083	4.102	0.047
1000.0	300	4.10	1.40	0.75	3.957	-3.497	4.078	-0.526
1000.0	300	4.10	1.40	2.00	3.956	-3.502	4.080	-0.481
1000.0	300	4.10	1.40	10.00	3.958	-3.471	4.098	-0.044
1000.0	300	4.10	3.20	0.75	3.989	-2.718	4.076	-0.574
1000.0	300	4.10	3.20	2.00	3.988	-2.720	4.077	-0.565
1000.0	300	4.10	3.20	10.00	3.989	-2.697	4.097	-0.081
1000.0	300	4.10	4.10	0.75	3.999	-2.456	4.076	-0.593
1000.0	300	4.10	4.10	2.00	3.999	-2.457	4.075	-0.598
1000.0	300	4.10	4.10	10.00	4.000	-2.437	4.096	-0.088
1000.0	300	4.10	5.00	0.75	4.008	-2.246	4.075	-0.608
1000.0	300	4.10	5.00	2.00	4.008	-2.247	4.074	-0.636
1000.0	300	4.10	5.00	10.00	4.009	-2.228	4.095	-0.132
1000.0	300	4.10	10.00	0.75	4.036	-1.566	4.076	-0.580
1000.0	300	4.10	10.00	2.00	4.036	-1.566	4.077	-0.562
1000.0	300	4.10	10.00	10.00	4.036	-1.554	4.089	-0.270
1000.0	300	5.00	0.50	0.75	4.853	-2.932	4.971	-0.576
1000.0	300	5.00	0.50	2.00	4.853	-2.935	4.973	-0.543
1000.0	300	5.00	0.50	10.00	4.855	-2.907	4.989	-0.212
1000.0	300	5.00	1.40	0.75	4.872	-2.567	4.970	-0.608
1000.0	300	5.00	1.40	2.00	4.872	-2.569	4.971	-0.588
1000.0	300	5.00	1.40	10.00	4.873	-2.546	4.989	-0.216
1000.0	300	5.00	3.20	0.75	4.896	-2.076	4.968	-0.640
1000.0	300	5.00	3.20	2.00	4.896	-2.077	4.968	-0.644
1000.0	300	5.00	3.20	10.00	4.897	-2.059	4.987	-0.254
1000.0	300	5.00	4.10	0.75	4.905	-1.903	4.968	-0.637
1000.0	300	5.00	4.10	2.00	4.905	-1.904	4.967	-0.659
1000.0	300	5.00	4.10	10.00	4.906	-1.888	4.985	-0.292
1000.0	300	5.00	5.00	0.75	4.912	-1.761	4.967	-0.651
1000.0	300	5.00	5.00	2.00	4.912	-1.761	4.969	-0.615
1000.0	300	5.00	5.00	10.00	4.913	-1.748	4.983	-0.333
1000.0	300	5.00	10.00	0.75	4.936	-1.284	4.969	-0.619
1000.0	300	5.00	10.00	2.00	4.936	-1.284	4.968	-0.641
1000.0	300	5.00	10.00	10.00	4.936	-1.274	4.979	-0.420
1000.0	300	10.00	0.50	0.75	9.898	-1.016	9.924	-0.765
1000.0	300	10.00	0.50	2.00	9.898	-1.016	9.925	-0.754
1000.0	300	10.00	0.50	10.00	9.899	-1.009	9.934	-0.660

1000.0	300	10.00	1.40	0.75	9.904	-0.962	9.923	-0.766
1000.0	300	10.00	1.40	2.00	9.904	-0.962	9.925	-0.746
1000.0	300	10.00	1.40	10.00	9.904	-0.955	9.934	-0.664
1000.0	300	10.00	3.20	0.75	9.912	-0.875	9.924	-0.755
1000.0	300	10.00	3.20	2.00	9.912	-0.875	9.925	-0.750
1000.0	300	10.00	3.20	10.00	9.913	-0.870	9.932	-0.675
1000.0	300	10.00	4.10	0.75	9.916	-0.841	9.925	-0.748
1000.0	300	10.00	4.10	2.00	9.916	-0.840	9.924	-0.756
1000.0	300	10.00	4.10	10.00	9.916	-0.836	9.932	-0.684
1000.0	300	10.00	5.00	0.75	9.919	-0.810	9.924	-0.758
1000.0	300	10.00	5.00	2.00	9.919	-0.810	9.925	-0.749
1000.0	300	10.00	5.00	10.00	9.919	-0.805	9.931	-0.693
1000.0	300	10.00	10.00	0.75	9.931	-0.689	9.926	-0.741
1000.0	300	10.00	10.00	2.00	9.931	-0.689	9.927	-0.734
1000.0	300	10.00	10.00	10.00	9.931	-0.686	9.927	-0.732

Table A.12: Simulations for an electric field of 300 kV/m and proton beam kinetic energy of 1000 MeV.

A.5 Electric field: 600 kV/m

A.5.1 Proton energy: 90 MeV

E_p MeV	E kV/m	σ_{x_0} mm	σ_{y_0} mm	σ_{z_0} mm	$\sigma_{x_{el}}$ mm	$\frac{\sigma_{x_{el}}-\sigma_{x_0}}{\sigma_{x_0}}$ %	$\sigma_{x_{H_2^+}}$ mm	$\frac{\sigma_{x_{H_2^+}}-\sigma_{x_0}}{\sigma_{x_0}}$ %
90.0	600	0.50	0.50	0.75	1.071	114.235	0.615	23.088
90.0	600	0.50	0.50	2.00	0.870	74.075	0.616	23.244
90.0	600	0.50	0.50	10.00	0.539	7.803	0.617	23.355
90.0	600	0.50	1.40	0.75	0.466	-6.733	0.580	15.975
90.0	600	0.50	1.40	2.00	0.354	-29.111	0.583	16.518
90.0	600	0.50	1.40	10.00	0.210	-58.089	0.584	16.760
90.0	600	0.50	3.20	0.75	0.314	-37.161	0.544	8.857
90.0	600	0.50	3.20	2.00	0.278	-44.328	0.553	10.505
90.0	600	0.50	3.20	10.00	0.256	-48.885	0.557	11.422
90.0	600	0.50	4.10	0.75	0.326	-34.847	0.535	6.999
90.0	600	0.50	4.10	2.00	0.305	-39.044	0.544	8.762
90.0	600	0.50	4.10	10.00	0.295	-40.905	0.550	9.993
90.0	600	0.50	5.00	0.75	0.342	-31.540	0.529	5.752
90.0	600	0.50	5.00	2.00	0.329	-34.219	0.539	7.823
90.0	600	0.50	5.00	10.00	0.325	-34.954	0.545	8.924
90.0	600	0.50	10.00	0.75	0.405	-18.929	0.517	3.312
90.0	600	0.50	10.00	2.00	0.403	-19.481	0.527	5.345
90.0	600	0.50	10.00	10.00	0.404	-19.116	0.529	5.763
90.0	600	1.40	0.50	0.75	0.929	-33.628	1.470	4.996
90.0	600	1.40	0.50	2.00	0.898	-35.864	1.472	5.123
90.0	600	1.40	0.50	10.00	0.912	-34.860	1.473	5.191
90.0	600	1.40	1.40	0.75	1.047	-25.213	1.455	3.940
90.0	600	1.40	1.40	2.00	1.038	-25.861	1.458	4.171
90.0	600	1.40	1.40	10.00	1.049	-25.084	1.460	4.285
90.0	600	1.40	3.20	0.75	1.174	-16.125	1.437	2.624
90.0	600	1.40	3.20	2.00	1.172	-16.269	1.442	3.017
90.0	600	1.40	3.20	10.00	1.180	-15.739	1.445	3.197
90.0	600	1.40	4.10	0.75	1.209	-13.635	1.432	2.251
90.0	600	1.40	4.10	2.00	1.208	-13.720	1.438	2.708
90.0	600	1.40	4.10	10.00	1.214	-13.264	1.440	2.849
90.0	600	1.40	5.00	0.75	1.235	-11.814	1.428	1.995
90.0	600	1.40	5.00	2.00	1.234	-11.867	1.434	2.446
90.0	600	1.40	5.00	10.00	1.239	-11.467	1.436	2.572
90.0	600	1.40	10.00	0.75	1.304	-6.826	1.419	1.392
90.0	600	1.40	10.00	2.00	1.304	-6.832	1.425	1.753
90.0	600	1.40	10.00	10.00	1.308	-6.597	1.423	1.674
90.0	600	3.20	0.50	0.75	2.909	-9.098	3.236	1.128
90.0	600	3.20	0.50	2.00	2.908	-9.112	3.238	1.186
90.0	600	3.20	0.50	10.00	2.926	-8.548	3.239	1.223
90.0	600	3.20	1.40	0.75	2.963	-7.397	3.231	0.973
90.0	600	3.20	1.40	2.00	2.963	-7.396	3.234	1.053

90.0	600	3.20	1.40	10.00	2.974	-7.062	3.235	1.086
90.0	600	3.20	3.20	0.75	3.027	-5.399	3.224	0.756
90.0	600	3.20	3.20	2.00	3.027	-5.394	3.227	0.852
90.0	600	3.20	3.20	10.00	3.034	-5.195	3.228	0.864
90.0	600	3.20	4.10	0.75	3.047	-4.768	3.222	0.682
90.0	600	3.20	4.10	2.00	3.048	-4.763	3.225	0.769
90.0	600	3.20	4.10	10.00	3.053	-4.595	3.225	0.778
90.0	600	3.20	5.00	0.75	3.063	-4.275	3.220	0.634
90.0	600	3.20	5.00	2.00	3.063	-4.270	3.223	0.715
90.0	600	3.20	5.00	10.00	3.068	-4.125	3.223	0.704
90.0	600	3.20	10.00	0.75	3.112	-2.762	3.215	0.473
90.0	600	3.20	10.00	2.00	3.112	-2.758	3.218	0.575
90.0	600	3.20	10.00	10.00	3.114	-2.675	3.214	0.433
90.0	600	4.10	0.50	0.75	3.860	-5.849	4.127	0.648
90.0	600	4.10	0.50	2.00	3.860	-5.846	4.128	0.689
90.0	600	4.10	0.50	10.00	3.874	-5.511	4.129	0.714
90.0	600	4.10	1.40	0.75	3.898	-4.938	4.123	0.572
90.0	600	4.10	1.40	2.00	3.898	-4.933	4.126	0.629
90.0	600	4.10	1.40	10.00	3.906	-4.721	4.126	0.640
90.0	600	4.10	3.20	0.75	3.945	-3.785	4.119	0.456
90.0	600	4.10	3.20	2.00	3.945	-3.780	4.121	0.506
90.0	600	4.10	3.20	10.00	3.950	-3.648	4.121	0.510
90.0	600	4.10	4.10	0.75	3.961	-3.398	4.117	0.414
90.0	600	4.10	4.10	2.00	3.961	-3.394	4.119	0.472
90.0	600	4.10	4.10	10.00	3.965	-3.281	4.119	0.456
90.0	600	4.10	5.00	0.75	3.973	-3.089	4.116	0.388
90.0	600	4.10	5.00	2.00	3.974	-3.085	4.118	0.431
90.0	600	4.10	5.00	10.00	3.978	-2.987	4.117	0.410
90.0	600	4.10	10.00	0.75	4.014	-2.093	4.113	0.307
90.0	600	4.10	10.00	2.00	4.014	-2.090	4.115	0.357
90.0	600	4.10	10.00	10.00	4.017	-2.033	4.109	0.229
90.0	600	5.00	0.50	0.75	4.795	-4.106	5.019	0.378
90.0	600	5.00	0.50	2.00	4.795	-4.101	5.020	0.410
90.0	600	5.00	0.50	10.00	4.806	-3.885	5.021	0.425
90.0	600	5.00	1.40	0.75	4.822	-3.565	5.017	0.337
90.0	600	5.00	1.40	2.00	4.822	-3.559	5.019	0.377
90.0	600	5.00	1.40	10.00	4.829	-3.417	5.019	0.380
90.0	600	5.00	3.20	0.75	4.858	-2.838	5.014	0.273
90.0	600	5.00	3.20	2.00	4.858	-2.834	5.016	0.311
90.0	600	5.00	3.20	10.00	4.863	-2.741	5.015	0.297
90.0	600	5.00	4.10	0.75	4.871	-2.584	5.012	0.248
90.0	600	5.00	4.10	2.00	4.871	-2.580	5.014	0.281
90.0	600	5.00	4.10	10.00	4.875	-2.500	5.013	0.261
90.0	600	5.00	5.00	0.75	4.881	-2.375	5.011	0.228
90.0	600	5.00	5.00	2.00	4.881	-2.372	5.013	0.266
90.0	600	5.00	5.00	10.00	4.885	-2.302	5.011	0.230
90.0	600	5.00	10.00	0.75	4.916	-1.678	5.009	0.190
90.0	600	5.00	10.00	2.00	4.916	-1.676	5.009	0.186
90.0	600	5.00	10.00	10.00	4.918	-1.634	5.005	0.102
90.0	600	10.00	0.50	0.75	9.871	-1.291	9.990	-0.104

90.0	600	10.00	0.50	2.00	9.871	-1.289	9.991	-0.092
90.0	600	10.00	0.50	10.00	9.875	-1.247	9.990	-0.098
90.0	600	10.00	1.40	0.75	9.879	-1.210	9.989	-0.105
90.0	600	10.00	1.40	2.00	9.879	-1.209	9.991	-0.093
90.0	600	10.00	1.40	10.00	9.882	-1.177	9.989	-0.105
90.0	600	10.00	3.20	0.75	9.892	-1.084	9.989	-0.107
90.0	600	10.00	3.20	2.00	9.892	-1.082	9.990	-0.100
90.0	600	10.00	3.20	10.00	9.894	-1.059	9.988	-0.121
90.0	600	10.00	4.10	0.75	9.897	-1.033	9.989	-0.109
90.0	600	10.00	4.10	2.00	9.897	-1.032	9.989	-0.108
90.0	600	10.00	4.10	10.00	9.899	-1.011	9.987	-0.129
90.0	600	10.00	5.00	0.75	9.901	-0.988	9.989	-0.114
90.0	600	10.00	5.00	2.00	9.901	-0.987	9.988	-0.116
90.0	600	10.00	5.00	10.00	9.903	-0.968	9.986	-0.136
90.0	600	10.00	10.00	0.75	9.918	-0.816	9.985	-0.150
90.0	600	10.00	10.00	2.00	9.918	-0.815	9.984	-0.155
90.0	600	10.00	10.00	10.00	9.920	-0.803	9.983	-0.169

Table A.13: Simulations for an electric field of 600 kV/m and proton beam kinetic energy of 90 MeV.

A.5.2 Proton energy: 200 MeV

E_p MeV	E kV/m	σ_{x_0} mm	σ_{y_0} mm	σ_{z_0} mm	$\sigma_{x_{el}}$ mm	$\frac{\sigma_{x_{el}}-\sigma_{x_0}}{\sigma_{x_0}}$ %	$\sigma_{x_{H_2^+}}$ mm	$\frac{\sigma_{x_{H_2^+}}-\sigma_{x_0}}{\sigma_{x_0}}$ %
200.0	600	0.50	0.50	0.75	0.727	45.364	0.571	14.221
200.0	600	0.50	0.50	2.00	0.564	12.715	0.577	15.360
200.0	600	0.50	0.50	10.00	0.352	-29.551	0.584	16.715
200.0	600	0.50	1.40	0.75	0.355	-29.097	0.543	8.501
200.0	600	0.50	1.40	2.00	0.273	-45.317	0.549	9.818
200.0	600	0.50	1.40	10.00	0.194	-61.235	0.560	11.912
200.0	600	0.50	3.20	0.75	0.337	-32.658	0.521	4.184
200.0	600	0.50	3.20	2.00	0.318	-36.322	0.526	5.225
200.0	600	0.50	3.20	10.00	0.309	-38.166	0.541	8.238
200.0	600	0.50	4.10	0.75	0.358	-28.443	0.516	3.247
200.0	600	0.50	4.10	2.00	0.347	-30.579	0.522	4.358
200.0	600	0.50	4.10	10.00	0.343	-31.338	0.536	7.195
200.0	600	0.50	5.00	0.75	0.376	-24.868	0.513	2.679
200.0	600	0.50	5.00	2.00	0.369	-26.249	0.520	3.922
200.0	600	0.50	5.00	10.00	0.367	-26.542	0.533	6.535
200.0	600	0.50	10.00	0.75	0.429	-14.220	0.509	1.785
200.0	600	0.50	10.00	2.00	0.427	-14.526	0.515	2.994
200.0	600	0.50	10.00	10.00	0.428	-14.339	0.521	4.237
200.0	600	1.40	0.50	0.75	1.032	-26.256	1.439	2.791
200.0	600	1.40	0.50	2.00	1.016	-27.416	1.444	3.107
200.0	600	1.40	0.50	10.00	1.020	-27.163	1.451	3.633
200.0	600	1.40	1.40	0.75	1.135	-18.963	1.428	2.025
200.0	600	1.40	1.40	2.00	1.129	-19.325	1.432	2.317
200.0	600	1.40	1.40	10.00	1.133	-19.036	1.443	3.052
200.0	600	1.40	3.20	0.75	1.232	-11.993	1.418	1.253
200.0	600	1.40	3.20	2.00	1.231	-12.081	1.421	1.509
200.0	600	1.40	3.20	10.00	1.234	-11.833	1.432	2.277
200.0	600	1.40	4.10	0.75	1.258	-10.134	1.415	1.058
200.0	600	1.40	4.10	2.00	1.257	-10.187	1.419	1.375
200.0	600	1.40	4.10	10.00	1.260	-9.966	1.429	2.039
200.0	600	1.40	5.00	0.75	1.277	-8.782	1.413	0.944
200.0	600	1.40	5.00	2.00	1.277	-8.817	1.417	1.238
200.0	600	1.40	5.00	10.00	1.279	-8.619	1.426	1.832
200.0	600	1.40	10.00	0.75	1.329	-5.102	1.410	0.734
200.0	600	1.40	10.00	2.00	1.328	-5.108	1.414	0.985
200.0	600	1.40	10.00	10.00	1.330	-4.987	1.416	1.162
200.0	600	3.20	0.50	0.75	2.983	-6.779	3.217	0.538
200.0	600	3.20	0.50	2.00	2.983	-6.790	3.220	0.613
200.0	600	3.20	0.50	10.00	2.990	-6.562	3.226	0.803
200.0	600	3.20	1.40	0.75	3.023	-5.527	3.214	0.451
200.0	600	3.20	1.40	2.00	3.023	-5.528	3.217	0.521
200.0	600	3.20	1.40	10.00	3.028	-5.379	3.223	0.717
200.0	600	3.20	3.20	0.75	3.070	-4.062	3.211	0.334

200.0	600	3.20	3.20	2.00	3.070	-4.060	3.213	0.402
200.0	600	3.20	3.20	10.00	3.073	-3.962	3.218	0.551
200.0	600	3.20	4.10	0.75	3.085	-3.599	3.210	0.301
200.0	600	3.20	4.10	2.00	3.085	-3.597	3.212	0.373
200.0	600	3.20	4.10	10.00	3.088	-3.513	3.216	0.487
200.0	600	3.20	5.00	0.75	3.096	-3.238	3.209	0.276
200.0	600	3.20	5.00	2.00	3.096	-3.236	3.211	0.335
200.0	600	3.20	5.00	10.00	3.099	-3.162	3.214	0.433
200.0	600	3.20	10.00	0.75	3.132	-2.128	3.208	0.235
200.0	600	3.20	10.00	2.00	3.132	-2.126	3.211	0.346
200.0	600	3.20	10.00	10.00	3.133	-2.082	3.207	0.232
200.0	600	4.10	0.50	0.75	3.920	-4.391	4.111	0.274
200.0	600	4.10	0.50	2.00	3.920	-4.391	4.113	0.314
200.0	600	4.10	0.50	10.00	3.926	-4.251	4.118	0.438
200.0	600	4.10	1.40	0.75	3.947	-3.724	4.109	0.227
200.0	600	4.10	1.40	2.00	3.947	-3.722	4.111	0.275
200.0	600	4.10	1.40	10.00	3.951	-3.625	4.116	0.385
200.0	600	4.10	3.20	0.75	3.982	-2.879	4.107	0.168
200.0	600	4.10	3.20	2.00	3.982	-2.877	4.109	0.219
200.0	600	4.10	3.20	10.00	3.985	-2.812	4.112	0.287
200.0	600	4.10	4.10	0.75	3.994	-2.596	4.106	0.153
200.0	600	4.10	4.10	2.00	3.994	-2.594	4.108	0.202
200.0	600	4.10	4.10	10.00	3.996	-2.538	4.110	0.248
200.0	600	4.10	5.00	0.75	4.003	-2.370	4.106	0.142
200.0	600	4.10	5.00	2.00	4.003	-2.368	4.108	0.195
200.0	600	4.10	5.00	10.00	4.005	-2.318	4.109	0.213
200.0	600	4.10	10.00	0.75	4.033	-1.638	4.106	0.139
200.0	600	4.10	10.00	2.00	4.033	-1.637	4.111	0.263
200.0	600	4.10	10.00	10.00	4.034	-1.606	4.103	0.080
200.0	600	5.00	0.50	0.75	4.844	-3.114	5.006	0.120
200.0	600	5.00	0.50	2.00	4.844	-3.112	5.007	0.148
200.0	600	5.00	0.50	10.00	4.849	-3.019	5.011	0.225
200.0	600	5.00	1.40	0.75	4.864	-2.718	5.005	0.097
200.0	600	5.00	1.40	2.00	4.864	-2.715	5.007	0.132
200.0	600	5.00	1.40	10.00	4.868	-2.649	5.010	0.192
200.0	600	5.00	3.20	0.75	4.891	-2.186	5.003	0.064
200.0	600	5.00	3.20	2.00	4.891	-2.184	5.005	0.099
200.0	600	5.00	3.20	10.00	4.893	-2.138	5.006	0.129
200.0	600	5.00	4.10	0.75	4.900	-2.000	5.003	0.056
200.0	600	5.00	4.10	2.00	4.900	-1.998	5.005	0.093
200.0	600	5.00	4.10	10.00	4.902	-1.958	5.005	0.103
200.0	600	5.00	5.00	0.75	4.908	-1.847	5.002	0.049
200.0	600	5.00	5.00	2.00	4.908	-1.845	5.004	0.080
200.0	600	5.00	5.00	10.00	4.910	-1.810	5.004	0.080
200.0	600	5.00	10.00	0.75	4.933	-1.334	5.004	0.082
200.0	600	5.00	10.00	2.00	4.933	-1.333	5.007	0.131
200.0	600	5.00	10.00	10.00	4.934	-1.311	4.999	-0.015
200.0	600	10.00	0.50	0.75	9.895	-1.049	9.983	-0.172
200.0	600	10.00	0.50	2.00	9.895	-1.048	9.984	-0.162
200.0	600	10.00	0.50	10.00	9.897	-1.029	9.984	-0.162

200.0	600	10.00	1.40	0.75	9.901	-0.990	9.983	-0.171
200.0	600	10.00	1.40	2.00	9.901	-0.989	9.984	-0.155
200.0	600	10.00	1.40	10.00	9.903	-0.974	9.983	-0.168
200.0	600	10.00	3.20	0.75	9.910	-0.897	9.983	-0.165
200.0	600	10.00	3.20	2.00	9.910	-0.897	9.985	-0.145
200.0	600	10.00	3.20	10.00	9.912	-0.885	9.982	-0.179
200.0	600	10.00	4.10	0.75	9.914	-0.860	9.984	-0.161
200.0	600	10.00	4.10	2.00	9.914	-0.859	9.985	-0.146
200.0	600	10.00	4.10	10.00	9.915	-0.848	9.982	-0.185
200.0	600	10.00	5.00	0.75	9.917	-0.827	9.984	-0.156
200.0	600	10.00	5.00	2.00	9.917	-0.827	9.985	-0.153
200.0	600	10.00	5.00	10.00	9.918	-0.817	9.981	-0.190
200.0	600	10.00	10.00	0.75	9.930	-0.699	9.982	-0.182
200.0	600	10.00	10.00	2.00	9.930	-0.699	9.981	-0.188
200.0	600	10.00	10.00	10.00	9.931	-0.692	9.979	-0.214

Table A.14: Simulations for an electric field of 600 kV/m and proton beam kinetic energy of 200 MeV.

A.5.3 Proton energy: 1000 MeV

E_p MeV	E kV/m	σ_{x_0} mm	σ_{y_0} mm	σ_{z_0} mm	$\sigma_{x_{el}}$ mm	$\frac{\sigma_{x_{el}}-\sigma_{x_0}}{\sigma_{x_0}}$ %	$\sigma_{x_{H_2^+}}$ mm	$\frac{\sigma_{x_{H_2^+}}-\sigma_{x_0}}{\sigma_{x_0}}$ %
1000.0	600	0.50	0.50	0.75	0.462	-7.604	0.525	4.950
1000.0	600	0.50	0.50	2.00	0.329	-34.156	0.530	6.039
1000.0	600	0.50	0.50	10.00	0.236	-52.888	0.534	6.895
1000.0	600	0.50	1.40	0.75	0.334	-33.212	0.512	2.385
1000.0	600	0.50	1.40	2.00	0.290	-41.927	0.514	2.865
1000.0	600	0.50	1.40	10.00	0.263	-47.438	0.536	7.277
1000.0	600	0.50	3.20	0.75	0.382	-23.611	0.505	0.906
1000.0	600	0.50	3.20	2.00	0.373	-25.409	0.506	1.287
1000.0	600	0.50	3.20	10.00	0.369	-26.152	0.526	5.155
1000.0	600	0.50	4.10	0.75	0.401	-19.848	0.503	0.625
1000.0	600	0.50	4.10	2.00	0.395	-20.935	0.505	0.965
1000.0	600	0.50	4.10	10.00	0.394	-21.278	0.525	5.098
1000.0	600	0.50	5.00	0.75	0.415	-17.058	0.502	0.452
1000.0	600	0.50	5.00	2.00	0.411	-17.784	0.504	0.812
1000.0	600	0.50	5.00	10.00	0.410	-17.942	0.523	4.699
1000.0	600	0.50	10.00	0.75	0.452	-9.531	0.502	0.455
1000.0	600	0.50	10.00	2.00	0.451	-9.710	0.507	1.324
1000.0	600	0.50	10.00	10.00	0.452	-9.627	0.517	3.437
1000.0	600	1.40	0.50	0.75	1.150	-17.843	1.410	0.707
1000.0	600	1.40	0.50	2.00	1.141	-18.510	1.412	0.866
1000.0	600	1.40	0.50	10.00	1.140	-18.579	1.431	2.201
1000.0	600	1.40	1.40	0.75	1.223	-12.652	1.406	0.399
1000.0	600	1.40	1.40	2.00	1.219	-12.900	1.408	0.560
1000.0	600	1.40	1.40	10.00	1.220	-12.841	1.424	1.733
1000.0	600	1.40	3.20	0.75	1.288	-7.990	1.402	0.118
1000.0	600	1.40	3.20	2.00	1.287	-8.064	1.403	0.206
1000.0	600	1.40	3.20	10.00	1.288	-7.981	1.421	1.535
1000.0	600	1.40	4.10	0.75	1.305	-6.765	1.401	0.056
1000.0	600	1.40	4.10	2.00	1.305	-6.813	1.402	0.122
1000.0	600	1.40	4.10	10.00	1.306	-6.735	1.420	1.398
1000.0	600	1.40	5.00	0.75	1.318	-5.877	1.400	0.032
1000.0	600	1.40	5.00	2.00	1.317	-5.911	1.402	0.108
1000.0	600	1.40	5.00	10.00	1.318	-5.837	1.417	1.232
1000.0	600	1.40	10.00	0.75	1.352	-3.464	1.402	0.117
1000.0	600	1.40	10.00	2.00	1.351	-3.473	1.404	0.307
1000.0	600	1.40	10.00	10.00	1.352	-3.424	1.413	0.894
1000.0	600	3.20	0.50	0.75	3.054	-4.567	3.199	-0.030
1000.0	600	3.20	0.50	2.00	3.053	-4.582	3.200	-0.006
1000.0	600	3.20	0.50	10.00	3.056	-4.508	3.214	0.440
1000.0	600	3.20	1.40	0.75	3.080	-3.746	3.197	-0.080
1000.0	600	3.20	1.40	2.00	3.080	-3.753	3.198	-0.063
1000.0	600	3.20	1.40	10.00	3.082	-3.697	3.214	0.427
1000.0	600	3.20	3.20	0.75	3.111	-2.789	3.197	-0.101

1000.0	600	3.20	3.20	2.00	3.111	-2.791	3.199	-0.032
1000.0	600	3.20	3.20	10.00	3.112	-2.751	3.210	0.301
1000.0	600	3.20	4.10	0.75	3.120	-2.486	3.196	-0.112
1000.0	600	3.20	4.10	2.00	3.120	-2.488	3.200	0.015
1000.0	600	3.20	4.10	10.00	3.122	-2.453	3.211	0.329
1000.0	600	3.20	5.00	0.75	3.128	-2.250	3.197	-0.099
1000.0	600	3.20	5.00	2.00	3.128	-2.251	3.199	-0.028
1000.0	600	3.20	5.00	10.00	3.129	-2.220	3.209	0.284
1000.0	600	3.20	10.00	0.75	3.151	-1.523	3.199	-0.040
1000.0	600	3.20	10.00	2.00	3.151	-1.522	3.202	0.059
1000.0	600	3.20	10.00	10.00	3.152	-1.503	3.204	0.120
1000.0	600	4.10	0.50	0.75	3.977	-3.004	4.095	-0.113
1000.0	600	4.10	0.50	2.00	3.977	-3.007	4.095	-0.111
1000.0	600	4.10	0.50	10.00	3.979	-2.958	4.109	0.213
1000.0	600	4.10	1.40	0.75	3.995	-2.568	4.095	-0.129
1000.0	600	4.10	1.40	2.00	3.995	-2.569	4.095	-0.127
1000.0	600	4.10	1.40	10.00	3.996	-2.531	4.107	0.174
1000.0	600	4.10	3.20	0.75	4.017	-2.016	4.094	-0.147
1000.0	600	4.10	3.20	2.00	4.017	-2.016	4.097	-0.069
1000.0	600	4.10	3.20	10.00	4.018	-1.989	4.107	0.163
1000.0	600	4.10	4.10	0.75	4.025	-1.831	4.095	-0.125
1000.0	600	4.10	4.10	2.00	4.025	-1.831	4.095	-0.110
1000.0	600	4.10	4.10	10.00	4.026	-1.807	4.105	0.131
1000.0	600	4.10	5.00	0.75	4.031	-1.682	4.096	-0.098
1000.0	600	4.10	5.00	2.00	4.031	-1.682	4.096	-0.097
1000.0	600	4.10	5.00	10.00	4.032	-1.661	4.104	0.103
1000.0	600	4.10	10.00	0.75	4.051	-1.202	4.098	-0.054
1000.0	600	4.10	10.00	2.00	4.051	-1.202	4.101	0.026
1000.0	600	4.10	10.00	10.00	4.051	-1.188	4.100	-0.006
1000.0	600	5.00	0.50	0.75	4.892	-2.168	4.992	-0.155
1000.0	600	5.00	0.50	2.00	4.892	-2.169	4.993	-0.147
1000.0	600	5.00	0.50	10.00	4.893	-2.135	5.003	0.064
1000.0	600	5.00	1.40	0.75	4.905	-1.910	4.992	-0.165
1000.0	600	5.00	1.40	2.00	4.905	-1.910	4.994	-0.120
1000.0	600	5.00	1.40	10.00	4.906	-1.883	5.003	0.068
1000.0	600	5.00	3.20	0.75	4.922	-1.562	4.993	-0.149
1000.0	600	5.00	3.20	2.00	4.922	-1.562	4.993	-0.137
1000.0	600	5.00	3.20	10.00	4.923	-1.542	5.002	0.033
1000.0	600	5.00	4.10	0.75	4.928	-1.440	4.994	-0.128
1000.0	600	5.00	4.10	2.00	4.928	-1.440	4.993	-0.136
1000.0	600	5.00	4.10	10.00	4.929	-1.422	5.001	0.012
1000.0	600	5.00	5.00	0.75	4.933	-1.340	4.993	-0.149
1000.0	600	5.00	5.00	2.00	4.933	-1.339	4.993	-0.134
1000.0	600	5.00	5.00	10.00	4.934	-1.324	5.000	-0.007
1000.0	600	5.00	10.00	0.75	4.950	-1.003	4.997	-0.068
1000.0	600	5.00	10.00	2.00	4.950	-1.003	5.000	0.000
1000.0	600	5.00	10.00	10.00	4.950	-0.992	4.996	-0.084
1000.0	600	10.00	0.50	0.75	9.919	-0.814	9.976	-0.237
1000.0	600	10.00	0.50	2.00	9.919	-0.814	9.977	-0.227
1000.0	600	10.00	0.50	10.00	9.919	-0.806	9.980	-0.204

1000.0	600	10.00	1.40	0.75	9.922	-0.776	9.977	-0.234
1000.0	600	10.00	1.40	2.00	9.922	-0.776	9.978	-0.220
1000.0	600	10.00	1.40	10.00	9.923	-0.769	9.979	-0.208
1000.0	600	10.00	3.20	0.75	9.928	-0.715	9.978	-0.220
1000.0	600	10.00	3.20	2.00	9.929	-0.715	9.980	-0.201
1000.0	600	10.00	3.20	10.00	9.929	-0.709	9.978	-0.217
1000.0	600	10.00	4.10	0.75	9.931	-0.690	9.979	-0.213
1000.0	600	10.00	4.10	2.00	9.931	-0.690	9.982	-0.177
1000.0	600	10.00	4.10	10.00	9.931	-0.685	9.978	-0.222
1000.0	600	10.00	5.00	0.75	9.933	-0.669	9.980	-0.203
1000.0	600	10.00	5.00	2.00	9.933	-0.669	9.984	-0.156
1000.0	600	10.00	5.00	10.00	9.934	-0.664	9.977	-0.226
1000.0	600	10.00	10.00	0.75	9.942	-0.584	9.984	-0.160
1000.0	600	10.00	10.00	2.00	9.942	-0.584	9.982	-0.175
1000.0	600	10.00	10.00	10.00	9.942	-0.581	9.975	-0.245

Table A.15: Simulations for an electric field of 600 kV/m and proton beam kinetic energy of 1000 MeV.

A.6 Electric field: 1000 kV/m

A.6.1 Proton energy: 90 MeV

E_p MeV	E kV/m	σ_{x_0} mm	σ_{y_0} mm	σ_{z_0} mm	$\sigma_{x_{el}}$ mm	$\frac{\sigma_{x_{el}}-\sigma_{x_0}}{\sigma_{x_0}}$ %	$\sigma_{x_{H_2^+}}$ mm	$\frac{\sigma_{x_{H_2^+}}-\sigma_{x_0}}{\sigma_{x_0}}$ %
90.0	1000	0.50	0.50	0.75	0.771	54.248	0.567	13.421
90.0	1000	0.50	0.50	2.00	0.601	20.152	0.568	13.697
90.0	1000	0.50	0.50	10.00	0.281	-43.886	0.569	13.786
90.0	1000	0.50	1.40	0.75	0.362	-27.563	0.545	8.957
90.0	1000	0.50	1.40	2.00	0.277	-44.606	0.548	9.564
90.0	1000	0.50	1.40	10.00	0.193	-61.338	0.549	9.875
90.0	1000	0.50	3.20	0.75	0.330	-34.048	0.524	4.773
90.0	1000	0.50	3.20	2.00	0.310	-37.920	0.530	5.960
90.0	1000	0.50	3.20	10.00	0.307	-38.557	0.533	6.682
90.0	1000	0.50	4.10	0.75	0.351	-29.831	0.519	3.748
90.0	1000	0.50	4.10	2.00	0.340	-32.049	0.525	5.099
90.0	1000	0.50	4.10	10.00	0.341	-31.807	0.529	5.830
90.0	1000	0.50	5.00	0.75	0.369	-26.148	0.516	3.190
90.0	1000	0.50	5.00	2.00	0.362	-27.559	0.523	4.563
90.0	1000	0.50	5.00	10.00	0.365	-27.015	0.526	5.193
90.0	1000	0.50	10.00	0.75	0.425	-14.992	0.512	2.357
90.0	1000	0.50	10.00	2.00	0.424	-15.278	0.519	3.700
90.0	1000	0.50	10.00	10.00	0.427	-14.667	0.517	3.309
90.0	1000	1.40	0.50	0.75	1.013	-27.637	1.439	2.786
90.0	1000	1.40	0.50	2.00	0.997	-28.770	1.441	2.900
90.0	1000	1.40	0.50	10.00	1.041	-25.630	1.442	2.983
90.0	1000	1.40	1.40	0.75	1.120	-19.978	1.430	2.127
90.0	1000	1.40	1.40	2.00	1.116	-20.296	1.433	2.326
90.0	1000	1.40	1.40	10.00	1.137	-18.781	1.434	2.433
90.0	1000	1.40	3.20	0.75	1.224	-12.604	1.419	1.381
90.0	1000	1.40	3.20	2.00	1.223	-12.665	1.424	1.685
90.0	1000	1.40	3.20	10.00	1.233	-11.948	1.425	1.780
90.0	1000	1.40	4.10	0.75	1.251	-10.639	1.417	1.214
90.0	1000	1.40	4.10	2.00	1.251	-10.670	1.421	1.502
90.0	1000	1.40	4.10	10.00	1.259	-10.098	1.422	1.572
90.0	1000	1.40	5.00	0.75	1.271	-9.211	1.415	1.096
90.0	1000	1.40	5.00	2.00	1.271	-9.227	1.419	1.356
90.0	1000	1.40	5.00	10.00	1.277	-8.750	1.420	1.406
90.0	1000	1.40	10.00	0.75	1.325	-5.330	1.412	0.871
90.0	1000	1.40	10.00	2.00	1.325	-5.326	1.417	1.204
90.0	1000	1.40	10.00	10.00	1.329	-5.073	1.412	0.868
90.0	1000	3.20	0.50	0.75	2.973	-7.085	3.217	0.524
90.0	1000	3.20	0.50	2.00	2.973	-7.079	3.218	0.570
90.0	1000	3.20	0.50	10.00	2.997	-6.354	3.219	0.599
90.0	1000	3.20	1.40	0.75	3.016	-5.758	3.214	0.439
90.0	1000	3.20	1.40	2.00	3.016	-5.749	3.216	0.496

90.0	1000	3.20	1.40	10.00	3.029	-5.333	3.217	0.517
90.0	1000	3.20	3.20	0.75	3.065	-4.212	3.210	0.326
90.0	1000	3.20	3.20	2.00	3.065	-4.204	3.212	0.389
90.0	1000	3.20	3.20	10.00	3.073	-3.977	3.212	0.383
90.0	1000	3.20	4.10	0.75	3.081	-3.726	3.210	0.308
90.0	1000	3.20	4.10	2.00	3.081	-3.718	3.212	0.364
90.0	1000	3.20	4.10	10.00	3.087	-3.532	3.211	0.332
90.0	1000	3.20	5.00	0.75	3.093	-3.346	3.209	0.288
90.0	1000	3.20	5.00	2.00	3.093	-3.339	3.212	0.365
90.0	1000	3.20	5.00	10.00	3.098	-3.182	3.209	0.287
90.0	1000	3.20	10.00	0.75	3.130	-2.185	3.209	0.297
90.0	1000	3.20	10.00	2.00	3.130	-2.180	3.209	0.272
90.0	1000	3.20	10.00	10.00	3.133	-2.094	3.204	0.125
90.0	1000	4.10	0.50	0.75	3.913	-4.563	4.110	0.247
90.0	1000	4.10	0.50	2.00	3.913	-4.553	4.111	0.280
90.0	1000	4.10	0.50	10.00	3.930	-4.137	4.112	0.293
90.0	1000	4.10	1.40	0.75	3.942	-3.857	4.109	0.208
90.0	1000	4.10	1.40	2.00	3.942	-3.848	4.110	0.247
90.0	1000	4.10	1.40	10.00	3.953	-3.593	4.110	0.249
90.0	1000	4.10	3.20	0.75	3.978	-2.967	4.107	0.161
90.0	1000	4.10	3.20	2.00	3.979	-2.961	4.108	0.204
90.0	1000	4.10	3.20	10.00	3.985	-2.813	4.107	0.171
90.0	1000	4.10	4.10	0.75	3.991	-2.670	4.106	0.146
90.0	1000	4.10	4.10	2.00	3.991	-2.665	4.108	0.206
90.0	1000	4.10	4.10	10.00	3.996	-2.542	4.106	0.139
90.0	1000	4.10	5.00	0.75	4.000	-2.433	4.106	0.140
90.0	1000	4.10	5.00	2.00	4.000	-2.428	4.109	0.217
90.0	1000	4.10	5.00	10.00	4.005	-2.322	4.105	0.111
90.0	1000	4.10	10.00	0.75	4.032	-1.670	4.105	0.114
90.0	1000	4.10	10.00	2.00	4.032	-1.667	4.104	0.086
90.0	1000	4.10	10.00	10.00	4.034	-1.608	4.100	0.003
90.0	1000	5.00	0.50	0.75	4.839	-3.218	5.005	0.092
90.0	1000	5.00	0.50	2.00	4.840	-3.210	5.006	0.116
90.0	1000	5.00	0.50	10.00	4.853	-2.946	5.006	0.120
90.0	1000	5.00	1.40	0.75	4.860	-2.799	5.004	0.075
90.0	1000	5.00	1.40	2.00	4.860	-2.792	5.005	0.103
90.0	1000	5.00	1.40	10.00	4.869	-2.623	5.005	0.093
90.0	1000	5.00	3.20	0.75	4.888	-2.240	5.003	0.051
90.0	1000	5.00	3.20	2.00	4.888	-2.235	5.005	0.098
90.0	1000	5.00	3.20	10.00	4.893	-2.132	5.002	0.043
90.0	1000	5.00	4.10	0.75	4.898	-2.044	5.002	0.049
90.0	1000	5.00	4.10	2.00	4.898	-2.040	5.005	0.096
90.0	1000	5.00	4.10	10.00	4.902	-1.954	5.001	0.022
90.0	1000	5.00	5.00	0.75	4.906	-1.885	5.003	0.060
90.0	1000	5.00	5.00	2.00	4.906	-1.881	5.004	0.075
90.0	1000	5.00	5.00	10.00	4.910	-1.806	5.000	0.003
90.0	1000	5.00	10.00	0.75	4.932	-1.352	5.000	-0.003
90.0	1000	5.00	10.00	2.00	4.933	-1.350	4.999	-0.023
90.0	1000	5.00	10.00	10.00	4.935	-1.307	4.996	-0.074
90.0	1000	10.00	0.50	0.75	9.894	-1.056	9.981	-0.193

90.0	1000	10.00	0.50	2.00	9.895	-1.055	9.982	-0.182
90.0	1000	10.00	0.50	10.00	9.899	-1.005	9.981	-0.194
90.0	1000	10.00	1.40	0.75	9.901	-0.995	9.981	-0.190
90.0	1000	10.00	1.40	2.00	9.901	-0.993	9.982	-0.182
90.0	1000	10.00	1.40	10.00	9.904	-0.957	9.980	-0.198
90.0	1000	10.00	3.20	0.75	9.910	-0.897	9.981	-0.190
90.0	1000	10.00	3.20	2.00	9.910	-0.896	9.981	-0.193
90.0	1000	10.00	3.20	10.00	9.913	-0.871	9.979	-0.208
90.0	1000	10.00	4.10	0.75	9.914	-0.859	9.981	-0.195
90.0	1000	10.00	4.10	2.00	9.914	-0.858	9.980	-0.199
90.0	1000	10.00	4.10	10.00	9.916	-0.835	9.979	-0.212
90.0	1000	10.00	5.00	0.75	9.918	-0.825	9.980	-0.200
90.0	1000	10.00	5.00	2.00	9.918	-0.824	9.980	-0.205
90.0	1000	10.00	5.00	10.00	9.920	-0.804	9.978	-0.216
90.0	1000	10.00	10.00	0.75	9.931	-0.694	9.977	-0.225
90.0	1000	10.00	10.00	2.00	9.931	-0.694	9.977	-0.228
90.0	1000	10.00	10.00	10.00	9.932	-0.681	9.976	-0.236

Table A.16: Simulations for an electric field of 1000 kV/m and proton beam kinetic energy of 90 MeV.

A.6.2 Proton energy: 200 MeV

E_p MeV	E kV/m	σ_{x_0} mm	σ_{y_0} mm	σ_{z_0} mm	$\sigma_{x_{el}}$ mm	$\frac{\sigma_{x_{el}}-\sigma_{x_0}}{\sigma_{x_0}}$ %	$\sigma_{x_{H_2^+}}$ mm	$\frac{\sigma_{x_{H_2^+}}-\sigma_{x_0}}{\sigma_{x_0}}$ %
200.0	1000	0.50	0.50	0.75	0.528	5.585	0.540	8.097
200.0	1000	0.50	0.50	2.00	0.391	-21.838	0.543	8.698
200.0	1000	0.50	0.50	10.00	0.202	-59.540	0.549	9.764
200.0	1000	0.50	1.40	0.75	0.322	-35.658	0.523	4.663
200.0	1000	0.50	1.40	2.00	0.271	-45.870	0.527	5.322
200.0	1000	0.50	1.40	10.00	0.237	-52.607	0.536	7.129
200.0	1000	0.50	3.20	0.75	0.362	-27.579	0.511	2.293
200.0	1000	0.50	3.20	2.00	0.352	-29.550	0.515	3.052
200.0	1000	0.50	3.20	10.00	0.351	-29.795	0.525	4.922
200.0	1000	0.50	4.10	0.75	0.383	-23.304	0.509	1.803
200.0	1000	0.50	4.10	2.00	0.378	-24.456	0.513	2.696
200.0	1000	0.50	4.10	10.00	0.378	-24.323	0.521	4.285
200.0	1000	0.50	5.00	0.75	0.400	-20.068	0.508	1.586
200.0	1000	0.50	5.00	2.00	0.396	-20.816	0.512	2.455
200.0	1000	0.50	5.00	10.00	0.397	-20.545	0.519	3.809
200.0	1000	0.50	10.00	0.75	0.444	-11.215	0.506	1.295
200.0	1000	0.50	10.00	2.00	0.443	-11.379	0.512	2.421
200.0	1000	0.50	10.00	10.00	0.445	-11.069	0.512	2.397
200.0	1000	1.40	0.50	0.75	1.105	-21.079	1.421	1.495
200.0	1000	1.40	0.50	2.00	1.096	-21.692	1.423	1.665
200.0	1000	1.40	0.50	10.00	1.113	-20.506	1.429	2.079
200.0	1000	1.40	1.40	0.75	1.191	-14.943	1.415	1.047
200.0	1000	1.40	1.40	2.00	1.188	-15.131	1.417	1.182
200.0	1000	1.40	1.40	10.00	1.196	-14.547	1.424	1.729
200.0	1000	1.40	3.20	0.75	1.269	-9.388	1.409	0.657
200.0	1000	1.40	3.20	2.00	1.268	-9.428	1.412	0.857
200.0	1000	1.40	3.20	10.00	1.273	-9.104	1.417	1.242
200.0	1000	1.40	4.10	0.75	1.289	-7.930	1.408	0.592
200.0	1000	1.40	4.10	2.00	1.289	-7.952	1.411	0.758
200.0	1000	1.40	4.10	10.00	1.292	-7.682	1.415	1.086
200.0	1000	1.40	5.00	0.75	1.304	-6.873	1.407	0.520
200.0	1000	1.40	5.00	2.00	1.304	-6.887	1.410	0.728
200.0	1000	1.40	5.00	10.00	1.307	-6.655	1.413	0.962
200.0	1000	1.40	10.00	0.75	1.344	-4.012	1.408	0.545
200.0	1000	1.40	10.00	2.00	1.344	-4.012	1.413	0.917
200.0	1000	1.40	10.00	10.00	1.346	-3.882	1.408	0.561
200.0	1000	3.20	0.50	0.75	3.030	-5.311	3.206	0.198
200.0	1000	3.20	0.50	2.00	3.030	-5.312	3.208	0.240
200.0	1000	3.20	0.50	10.00	3.039	-5.016	3.211	0.356
200.0	1000	3.20	1.40	0.75	3.061	-4.336	3.205	0.153
200.0	1000	3.20	1.40	2.00	3.061	-4.332	3.206	0.195
200.0	1000	3.20	1.40	10.00	3.067	-4.156	3.209	0.295
200.0	1000	3.20	3.20	0.75	3.098	-3.201	3.203	0.089

200.0	1000	3.20	3.20	2.00	3.098	-3.197	3.205	0.152
200.0	1000	3.20	3.20	10.00	3.101	-3.090	3.206	0.195
200.0	1000	3.20	4.10	0.75	3.109	-2.844	3.203	0.081
200.0	1000	3.20	4.10	2.00	3.109	-2.840	3.204	0.129
200.0	1000	3.20	4.10	10.00	3.112	-2.750	3.205	0.157
200.0	1000	3.20	5.00	0.75	3.118	-2.565	3.203	0.092
200.0	1000	3.20	5.00	2.00	3.118	-2.562	3.204	0.140
200.0	1000	3.20	5.00	10.00	3.121	-2.483	3.204	0.124
200.0	1000	3.20	10.00	0.75	3.145	-1.709	3.207	0.223
200.0	1000	3.20	10.00	2.00	3.145	-1.707	3.207	0.232
200.0	1000	3.20	10.00	10.00	3.147	-1.662	3.200	0.004
200.0	1000	4.10	0.50	0.75	3.958	-3.458	4.102	0.038
200.0	1000	4.10	0.50	2.00	3.958	-3.454	4.103	0.066
200.0	1000	4.10	0.50	10.00	3.965	-3.281	4.105	0.129
200.0	1000	4.10	1.40	0.75	3.979	-2.940	4.101	0.021
200.0	1000	4.10	1.40	2.00	3.980	-2.936	4.102	0.050
200.0	1000	4.10	1.40	10.00	3.984	-2.826	4.104	0.095
200.0	1000	4.10	3.20	0.75	4.006	-2.288	4.100	-0.004
200.0	1000	4.10	3.20	2.00	4.006	-2.285	4.101	0.025
200.0	1000	4.10	3.20	10.00	4.009	-2.214	4.102	0.037
200.0	1000	4.10	4.10	0.75	4.015	-2.069	4.100	0.004
200.0	1000	4.10	4.10	2.00	4.015	-2.067	4.102	0.049
200.0	1000	4.10	4.10	10.00	4.018	-2.006	4.101	0.014
200.0	1000	4.10	5.00	0.75	4.022	-1.895	4.101	0.016
200.0	1000	4.10	5.00	2.00	4.022	-1.892	4.104	0.107
200.0	1000	4.10	5.00	10.00	4.025	-1.840	4.100	-0.007
200.0	1000	4.10	10.00	0.75	4.045	-1.332	4.103	0.084
200.0	1000	4.10	10.00	2.00	4.045	-1.330	4.102	0.048
200.0	1000	4.10	10.00	10.00	4.047	-1.299	4.096	-0.087
200.0	1000	5.00	0.50	0.75	4.876	-2.470	4.997	-0.052
200.0	1000	5.00	0.50	2.00	4.877	-2.467	4.998	-0.032
200.0	1000	5.00	0.50	10.00	4.882	-2.356	5.000	-0.000
200.0	1000	5.00	1.40	0.75	4.892	-2.164	4.997	-0.060
200.0	1000	5.00	1.40	2.00	4.892	-2.160	4.998	-0.036
200.0	1000	5.00	1.40	10.00	4.896	-2.086	4.999	-0.020
200.0	1000	5.00	3.20	0.75	4.912	-1.753	4.997	-0.061
200.0	1000	5.00	3.20	2.00	4.912	-1.751	4.999	-0.022
200.0	1000	5.00	3.20	10.00	4.915	-1.701	4.997	-0.057
200.0	1000	5.00	4.10	0.75	4.920	-1.610	4.997	-0.053
200.0	1000	5.00	4.10	2.00	4.920	-1.607	5.002	0.036
200.0	1000	5.00	4.10	10.00	4.922	-1.565	4.996	-0.073
200.0	1000	5.00	5.00	0.75	4.925	-1.492	4.998	-0.037
200.0	1000	5.00	5.00	2.00	4.925	-1.490	5.002	0.037
200.0	1000	5.00	5.00	10.00	4.927	-1.453	4.996	-0.087
200.0	1000	5.00	10.00	0.75	4.945	-1.098	4.998	-0.033
200.0	1000	5.00	10.00	2.00	4.945	-1.097	4.997	-0.057
200.0	1000	5.00	10.00	10.00	4.946	-1.074	4.993	-0.144
200.0	1000	10.00	0.50	0.75	9.912	-0.879	9.977	-0.230
200.0	1000	10.00	0.50	2.00	9.912	-0.878	9.979	-0.214
200.0	1000	10.00	0.50	10.00	9.914	-0.856	9.977	-0.233

200.0	1000	10.00	1.40	0.75	9.917	-0.834	9.978	-0.222
200.0	1000	10.00	1.40	2.00	9.917	-0.833	9.979	-0.209
200.0	1000	10.00	1.40	10.00	9.918	-0.816	9.976	-0.236
200.0	1000	10.00	3.20	0.75	9.924	-0.762	9.979	-0.213
200.0	1000	10.00	3.20	2.00	9.924	-0.762	9.978	-0.217
200.0	1000	10.00	3.20	10.00	9.925	-0.749	9.976	-0.243
200.0	1000	10.00	4.10	0.75	9.927	-0.734	9.978	-0.216
200.0	1000	10.00	4.10	2.00	9.927	-0.733	9.978	-0.222
200.0	1000	10.00	4.10	10.00	9.928	-0.722	9.975	-0.246
200.0	1000	10.00	5.00	0.75	9.929	-0.709	9.978	-0.222
200.0	1000	10.00	5.00	2.00	9.929	-0.708	9.977	-0.227
200.0	1000	10.00	5.00	10.00	9.930	-0.698	9.975	-0.249
200.0	1000	10.00	10.00	0.75	9.939	-0.611	9.976	-0.245
200.0	1000	10.00	10.00	2.00	9.939	-0.611	9.975	-0.248
200.0	1000	10.00	10.00	10.00	9.940	-0.604	9.974	-0.264

Table A.17: Simulations for an electric field of 1000 kV/m and proton beam kinetic energy of 200 MeV.

A.6.3 Proton energy: 1000 MeV

E_p MeV	E kV/m	σ_{x_0} mm	σ_{y_0} mm	σ_{z_0} mm	$\sigma_{x_{el}}$ mm	$\frac{\sigma_{x_{el}}-\sigma_{x_0}}{\sigma_{x_0}}$ %	$\sigma_{x_{H_2^+}}$ mm	$\frac{\sigma_{x_{H_2^+}}-\sigma_{x_0}}{\sigma_{x_0}}$ %
1000.0	1000	0.50	0.50	0.75	0.373	-25.474	0.514	2.777
1000.0	1000	0.50	0.50	2.00	0.276	-44.864	0.517	3.423
1000.0	1000	0.50	0.50	10.00	0.285	-43.028	0.520	3.964
1000.0	1000	0.50	1.40	0.75	0.346	-30.716	0.506	1.135
1000.0	1000	0.50	1.40	2.00	0.322	-35.573	0.507	1.477
1000.0	1000	0.50	1.40	10.00	0.312	-37.670	0.521	4.130
1000.0	1000	0.50	3.20	0.75	0.404	-19.199	0.501	0.284
1000.0	1000	0.50	3.20	2.00	0.399	-20.202	0.503	0.591
1000.0	1000	0.50	3.20	10.00	0.398	-20.350	0.517	3.432
1000.0	1000	0.50	4.10	0.75	0.420	-15.928	0.501	0.262
1000.0	1000	0.50	4.10	2.00	0.417	-16.540	0.503	0.539
1000.0	1000	0.50	4.10	10.00	0.417	-16.529	0.516	3.134
1000.0	1000	0.50	5.00	0.75	0.432	-13.594	0.501	0.220
1000.0	1000	0.50	5.00	2.00	0.430	-14.005	0.503	0.639
1000.0	1000	0.50	5.00	10.00	0.430	-13.928	0.515	3.079
1000.0	1000	0.50	10.00	0.75	0.462	-7.520	0.503	0.695
1000.0	1000	0.50	10.00	2.00	0.462	-7.622	0.508	1.600
1000.0	1000	0.50	10.00	10.00	0.463	-7.485	0.510	1.914
1000.0	1000	1.40	0.50	0.75	1.201	-14.190	1.403	0.248
1000.0	1000	1.40	0.50	2.00	1.196	-14.562	1.404	0.264
1000.0	1000	1.40	0.50	10.00	1.200	-14.320	1.416	1.176
1000.0	1000	1.40	1.40	0.75	1.260	-9.973	1.400	0.015
1000.0	1000	1.40	1.40	2.00	1.258	-10.111	1.402	0.155
1000.0	1000	1.40	1.40	10.00	1.261	-9.944	1.416	1.145
1000.0	1000	1.40	3.20	0.75	1.312	-6.288	1.400	-0.021
1000.0	1000	1.40	3.20	2.00	1.311	-6.328	1.401	0.085
1000.0	1000	1.40	3.20	10.00	1.313	-6.209	1.413	0.951
1000.0	1000	1.40	4.10	0.75	1.325	-5.328	1.399	-0.046
1000.0	1000	1.40	4.10	2.00	1.325	-5.354	1.402	0.162
1000.0	1000	1.40	4.10	10.00	1.326	-5.251	1.412	0.827
1000.0	1000	1.40	5.00	0.75	1.335	-4.635	1.399	-0.041
1000.0	1000	1.40	5.00	2.00	1.335	-4.652	1.402	0.148
1000.0	1000	1.40	5.00	10.00	1.336	-4.561	1.410	0.726
1000.0	1000	1.40	10.00	0.75	1.361	-2.757	1.403	0.233
1000.0	1000	1.40	10.00	2.00	1.361	-2.761	1.408	0.577
1000.0	1000	1.40	10.00	10.00	1.362	-2.707	1.406	0.398
1000.0	1000	3.20	0.50	0.75	3.084	-3.614	3.195	-0.145
1000.0	1000	3.20	0.50	2.00	3.084	-3.620	3.196	-0.133
1000.0	1000	3.20	0.50	10.00	3.087	-3.527	3.206	0.177
1000.0	1000	3.20	1.40	0.75	3.105	-2.975	3.195	-0.157
1000.0	1000	3.20	1.40	2.00	3.105	-2.977	3.197	-0.081
1000.0	1000	3.20	1.40	10.00	3.107	-2.912	3.205	0.171
1000.0	1000	3.20	3.20	0.75	3.129	-2.232	3.196	-0.138

1000.0	1000	3.20	3.20	2.00	3.129	-2.232	3.197	-0.099
1000.0	1000	3.20	3.20	10.00	3.130	-2.188	3.203	0.091
1000.0	1000	3.20	4.10	0.75	3.136	-1.998	3.196	-0.124
1000.0	1000	3.20	4.10	2.00	3.136	-1.997	3.197	-0.100
1000.0	1000	3.20	4.10	10.00	3.137	-1.959	3.202	0.060
1000.0	1000	3.20	5.00	0.75	3.142	-1.815	3.196	-0.126
1000.0	1000	3.20	5.00	2.00	3.142	-1.814	3.198	-0.048
1000.0	1000	3.20	5.00	10.00	3.143	-1.781	3.201	0.034
1000.0	1000	3.20	10.00	0.75	3.160	-1.252	3.202	0.077
1000.0	1000	3.20	10.00	2.00	3.160	-1.251	3.209	0.279
1000.0	1000	3.20	10.00	10.00	3.161	-1.231	3.198	-0.064
1000.0	1000	4.10	0.50	0.75	4.002	-2.399	4.093	-0.182
1000.0	1000	4.10	0.50	2.00	4.002	-2.400	4.094	-0.147
1000.0	1000	4.10	0.50	10.00	4.004	-2.342	4.101	0.031
1000.0	1000	4.10	1.40	0.75	4.016	-2.061	4.092	-0.188
1000.0	1000	4.10	1.40	2.00	4.016	-2.060	4.094	-0.153
1000.0	1000	4.10	1.40	10.00	4.017	-2.018	4.100	0.008
1000.0	1000	4.10	3.20	0.75	4.033	-1.633	4.093	-0.167
1000.0	1000	4.10	3.20	2.00	4.033	-1.633	4.095	-0.133
1000.0	1000	4.10	3.20	10.00	4.034	-1.603	4.098	-0.039
1000.0	1000	4.10	4.10	0.75	4.039	-1.490	4.094	-0.150
1000.0	1000	4.10	4.10	2.00	4.039	-1.489	4.096	-0.092
1000.0	1000	4.10	4.10	10.00	4.040	-1.463	4.098	-0.058
1000.0	1000	4.10	5.00	0.75	4.044	-1.375	4.095	-0.130
1000.0	1000	4.10	5.00	2.00	4.044	-1.374	4.098	-0.047
1000.0	1000	4.10	5.00	10.00	4.045	-1.351	4.097	-0.075
1000.0	1000	4.10	10.00	0.75	4.059	-1.004	4.102	0.057
1000.0	1000	4.10	10.00	2.00	4.059	-1.003	4.105	0.121
1000.0	1000	4.10	10.00	10.00	4.059	-0.989	4.094	-0.139
1000.0	1000	5.00	0.50	0.75	4.912	-1.752	4.990	-0.203
1000.0	1000	5.00	0.50	2.00	4.912	-1.751	4.991	-0.180
1000.0	1000	5.00	0.50	10.00	4.914	-1.713	4.996	-0.070
1000.0	1000	5.00	1.40	0.75	4.922	-1.551	4.990	-0.193
1000.0	1000	5.00	1.40	2.00	4.922	-1.550	4.991	-0.179
1000.0	1000	5.00	1.40	10.00	4.924	-1.521	4.996	-0.086
1000.0	1000	5.00	3.20	0.75	4.936	-1.282	4.991	-0.177
1000.0	1000	5.00	3.20	2.00	4.936	-1.282	4.994	-0.120
1000.0	1000	5.00	3.20	10.00	4.937	-1.260	4.994	-0.116
1000.0	1000	5.00	4.10	0.75	4.941	-1.188	4.992	-0.158
1000.0	1000	5.00	4.10	2.00	4.941	-1.187	4.995	-0.110
1000.0	1000	5.00	4.10	10.00	4.942	-1.168	4.994	-0.129
1000.0	1000	5.00	5.00	0.75	4.944	-1.110	4.993	-0.137
1000.0	1000	5.00	5.00	2.00	4.945	-1.110	4.996	-0.076
1000.0	1000	5.00	5.00	10.00	4.945	-1.093	4.993	-0.140
1000.0	1000	5.00	10.00	0.75	4.957	-0.850	5.001	0.025
1000.0	1000	5.00	10.00	2.00	4.958	-0.850	5.000	-0.007
1000.0	1000	5.00	10.00	10.00	4.958	-0.839	4.991	-0.186
1000.0	1000	10.00	0.50	0.75	9.930	-0.705	9.975	-0.251
1000.0	1000	10.00	0.50	2.00	9.930	-0.704	9.978	-0.223
1000.0	1000	10.00	0.50	10.00	9.930	-0.696	9.974	-0.258

1000.0	1000	10.00	1.40	0.75	9.933	-0.675	9.976	-0.242
1000.0	1000	10.00	1.40	2.00	9.933	-0.675	9.979	-0.210
1000.0	1000	10.00	1.40	10.00	9.933	-0.667	9.974	-0.260
1000.0	1000	10.00	3.20	0.75	9.937	-0.628	9.979	-0.212
1000.0	1000	10.00	3.20	2.00	9.937	-0.628	9.980	-0.204
1000.0	1000	10.00	3.20	10.00	9.938	-0.622	9.973	-0.266
1000.0	1000	10.00	4.10	0.75	9.939	-0.609	9.980	-0.203
1000.0	1000	10.00	4.10	2.00	9.939	-0.609	9.979	-0.210
1000.0	1000	10.00	4.10	10.00	9.940	-0.603	9.973	-0.268
1000.0	1000	10.00	5.00	0.75	9.941	-0.592	9.980	-0.203
1000.0	1000	10.00	5.00	2.00	9.941	-0.592	9.978	-0.216
1000.0	1000	10.00	5.00	10.00	9.941	-0.587	9.973	-0.271
1000.0	1000	10.00	10.00	0.75	9.947	-0.527	9.977	-0.232
1000.0	1000	10.00	10.00	2.00	9.947	-0.527	9.976	-0.241
1000.0	1000	10.00	10.00	10.00	9.948	-0.523	9.972	-0.282

Table A.18: Simulations for an electric field of 1000 kV/m and proton beam kinetic energy of 1000 MeV.

Appendix B

IPM 10 cm long, electrons/ions initially at rest

B.1 Electric field: 300 kV/m

B.1.1 Proton energy: 90 MeV

E_p MeV	E kV/m	σ_{x_0} mm	σ_{y_0} mm	σ_{z_0} mm	$\sigma_{x_{el}}$ mm	$\frac{\sigma_{x_{el}}-\sigma_{x_0}}{\sigma_{x_0}}$ %	$\sigma_{x_{H_2^+}}$ mm	$\frac{\sigma_{x_{H_2^+}}-\sigma_{x_0}}{\sigma_{x_0}}$ %
90.0	300	0.50	0.50	0.75	0.620	24.049	0.591	18.145
90.0	300	0.50	0.50	2.00	0.605	20.902	0.591	18.236
90.0	300	0.50	0.50	10.00	0.546	9.201	0.591	18.295
90.0	300	1.40	1.40	0.75	1.365	-2.491	1.439	2.798
90.0	300	1.40	1.40	2.00	1.365	-2.503	1.440	2.869
90.0	300	1.40	1.40	10.00	1.363	-2.654	1.441	2.946
90.0	300	3.20	3.20	0.75	3.164	-1.118	3.214	0.423
90.0	300	3.20	3.20	2.00	3.164	-1.117	3.215	0.480
90.0	300	3.20	3.20	10.00	3.164	-1.119	3.216	0.499
90.0	300	4.10	4.10	0.75	4.064	-0.866	4.107	0.166
90.0	300	4.10	4.10	2.00	4.065	-0.866	4.108	0.206
90.0	300	4.10	4.10	10.00	4.065	-0.866	4.109	0.211
90.0	300	5.00	5.00	0.75	4.964	-0.720	5.002	0.032
90.0	300	5.00	5.00	2.00	4.964	-0.720	5.002	0.050
90.0	300	5.00	5.00	10.00	4.964	-0.720	5.003	0.055
90.0	300	10.00	10.00	0.75	9.955	-0.454	9.978	-0.222
90.0	300	10.00	10.00	2.00	9.955	-0.454	9.978	-0.222
90.0	300	10.00	10.00	10.00	9.955	-0.454	9.978	-0.221

Table B.1: Simulations for an electric field of 300 kV/m and proton beam kinetic energy of 90 MeV when the ionization takes place all along the 10 cm of the IPM.

Appendix C

IPM 10 cm long, initial electron/ion speed distribution calculated with GARFIELD++

C.1 Electric field: 300 kV/m

C.1.1 Proton energy: 90 MeV

$\mathbf{E}_p$ MeV	E kV/m	σ_{x_0} mm	σ_{y_0} mm	σ_{z_0} mm	$\sigma_{x_{el}}$ mm	$\frac{\sigma_{x_{el}}-\sigma_{x_0}}{\sigma_{x_0}}$ %	$\sigma_{x_{H_2^+}}$ mm	$\frac{\sigma_{x_{H_2^+}}-\sigma_{x_0}}{\sigma_{x_0}}$ %
90.0	300	0.50	0.50	0.75	3.347	569.318	0.594	18.790
90.0	300	0.50	0.50	2.00	3.345	569.054	0.594	18.866
90.0	300	0.50	0.50	10.00	3.334	566.891	0.594	18.900
90.0	300	1.40	1.40	0.75	3.583	155.907	1.440	2.887
90.0	300	1.40	1.40	2.00	3.583	155.902	1.442	2.974
90.0	300	1.40	1.40	10.00	3.582	155.849	1.443	3.040
90.0	300	3.20	3.20	0.75	4.596	43.635	3.214	0.436
90.0	300	3.20	3.20	2.00	4.596	43.635	3.216	0.502
90.0	300	3.20	3.20	10.00	4.596	43.635	3.217	0.520
90.0	300	4.10	4.10	0.75	5.263	28.356	4.107	0.180
90.0	300	4.10	4.10	2.00	5.263	28.356	4.109	0.219
90.0	300	4.10	4.10	10.00	5.263	28.356	4.109	0.226
90.0	300	5.00	5.00	0.75	5.990	19.794	5.002	0.043
90.0	300	5.00	5.00	2.00	5.990	19.794	5.003	0.059
90.0	300	5.00	5.00	10.00	5.990	19.794	5.003	0.064
90.0	300	10.00	10.00	0.75	10.521	5.208	9.978	-0.219
90.0	300	10.00	10.00	2.00	10.521	5.208	9.978	-0.218
90.0	300	10.00	10.00	10.00	10.521	5.208	9.978	-0.217

Table C.1: Simulations for an electric field of 300 kV/m and proton beam kinetic energy of 90 MeV when the ionization takes place along the 10 cm of the IPM and the detected particles have non zero initial speed.

Appendix D

Range of ions in silicon

The studies summarized in this report show that ions are less affected by space charge effects. Should the decision to detect ions for reconstructing the beam profile be taken, the selected-read out system must be compatible with such choice. One of the investigated read-out systems is a pixelated silicon sensor bonded to a pixelated read-out chip (TimePix3). The sensor is a diode.

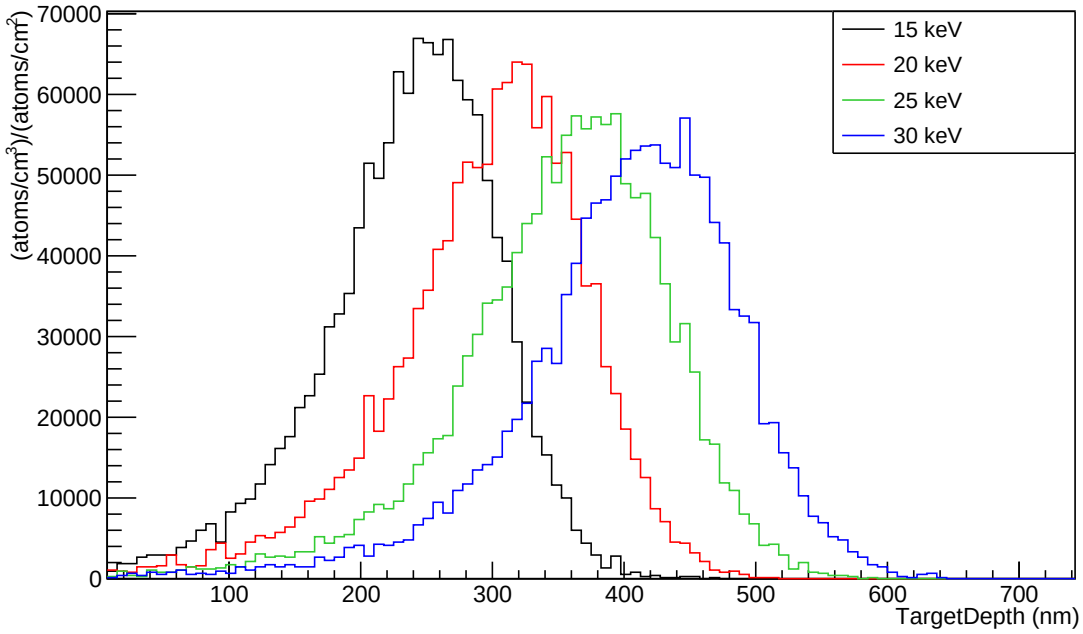

Figure D.1: Range of H_2^+ in a silicon layer 750 nm thick for different ionized molecule energies.

The SRIM [7] code was used to evaluate the range of H_2^+ in 750 nm of silicon. Due to the molecules break-up at a solids surface, the range of protons in silicon was also calculated. Studies have shown that typically full breakup usually occurs within 300A. So for energies above 10 keV, most molecules acts like independent ions. An attempt to calculate the range of ionized N_2 molecules in the silicon was performed, but the results are not conclusive. As a matter of fact, in SRIM the ions in the target are assumed to be stripped of all electrons which move slower than the ion. N_2 has the double of the mass of a nitrogen ion. By doubling the mass of the ion, with a constant energy, its velocity will change. This changes the electrons attached to the ion. Therefore the range of N_2 ionized molecules calculated can not be considered the real one and were not reported in

this document.

Each SRIM simulation consisted of 10000 ions (1% accuracy of the results).

D.1 Range of H_2^+

Fig. D.1 show the range of H_2^+ in a silicon layer 750 nm thick when a difference of potential of 30 kV, 40 kV, 50 kV and 60 kV is applied between the electrodes of the IPM. These values correspond to uniform electric fields of 300 kV/m, 400 kV/m, 500 kV/m, 600 kV/m. Since the ionized molecules are created in the middle of the detector, if only one electron has been stripped off, in the previously mentioned electric fields they reach kinetic energies of 15 keV, 20 keV, 25 keV and 30 keV respectively.

The ordinate units in fig. D.1 are (atoms/cm^3)/(atoms/cm^2). When multiplying this units by an incident flux (ions/cm^2), a plot of the impurity concentration (i.e. implanted ion concentration) in ions/cm^3 versus depth is obtain.

Table D.1 summarized the quantities of interest of fig.D.1 and therefore reports the range of H_2^+ of different energies in a silicon layer 750 nm thick and the peak value (ordinate value) corresponding to such range.

Ion	Energy (keV)	Range (nm)	Approximate Peak Value (atoms/cm^3)/(atoms/cm^2)
H_2^+	15	230.5	6.7 10^4
H_2^+	20	290.0	6.4 10^4
H_2^+	25	345.9	5.7 10^4
H_2^+	30	395.9	5.4 10^4

Table D.1: Range of H_2^+ of different energies in a silicon layer 750 nm thick and peak ordinate value for such range.

Table D.2 summarizes the same quantities for protons in silicon. The kinetic energy of protons is considered to be half of the kinetic energy of H_2^+ molecules. This assumption is based on the fact that the molecule would break into two ions of the same mass.

Ion	Energy (keV)	Range (nm)	Approximate Peak Value (atoms/cm^3)/(atoms/cm^2)
H^+	7.5	105.4	9.3 10^4
H^+	10	132.7	7.6 10^4
H^+	12.5	158.4	7.4 10^4
H^+	15	181.5	8.3 10^4

Table D.2: Range of H^+ of different energies in a silicon layer 750 nm thick and peak ordinate value for such range.

In the reality, the H_2^+ molecule enter the silicon, travels some distance while being slowed down and then breaks into two protons having each one half of the residual ionized molecule kinetic energy. Therefore all tables in this Appendix has to be considered preliminary.

The number of electron/ion pairs created per proton pulse in 1 cm of residual gas with which the IPM is filled was calculated for different beam energies and is reported in the section "Ion-Electron pairs production in the ESS Cold Linac". The amount of H_2^+ ions is just a fraction (around 30%) of the total number of ions produced, but for simplicity here it is assumed that all the ions produced are H_2^+. From the numbers reported in the section "Ion-Electron pairs production in the ESS Cold Linac", and considering the geometry of

the silicon pixelated detector, it is possible to compute the number of ions (or electrons) that are expected to hit every pixel. Being interested in the damage of the silicon detector induced by the ions, the pixel exposed to the higher ion flux is considered. Table D.3 reports the number of ions expected to hit such pixel during every pulse. This quantity is then converted into a flux of ions by considering the size of the pixel (square of 55 μm side) and translated into concentration of H_2^+ implanted in the silicon at the depth inside the semiconductor where most of such ions stop.

To obtain the maximum impurity concentration at the ion range depth for one year of irradiation time, each row of the last column of Table D.3 should be multiplied by $14 \times 3600 \times 24 \times 365 = 4.4\ 10^8$, where 14 is the number of pulses/second. In the worst case among those reported for H_2^+ (90 MeV protons and 15 keV kinetic energy) therefore the maximum impurity concentration will be $(9.4\ 10^9) \cdot (4.4\ 10^8) = 4.1\ 10^{18}$ atoms/cm^3/year at a depth of 230 nm. The same order of magnitude is obtained by considering H^+ ions. The density of silicon is $5\ 10^{22}$ atoms/cm^3, much higher than such number.

Proton beam energy (MeV)	H_2^+/pulse/cm (1/pulse/cm)	H_2^+/pulse/pixel (1/pulse/pixel)	H_2^+/pulse/cm^2 (1/pulse/cm^2)	max. impurity concentration/pulse for H_2^+ of 15 keV (atoms/cm^3/pulse)
90	105986	4.29	$1.4\ 10^5$	$9.4\ 10^9$
200	60159	2.42	$8.0\ 10^4$	$5.3\ 10^9$
500	36662	1.47	$4.9\ 10^4$	$3.3\ 10^9$
1000	29463	1.19	$3.9\ 10^4$	$2.6\ 10^9$
1500	27717	1.11	$3.6\ 10^4$	$2.4\ 10^9$
2000	27224	1.10	$3.4\ 10^4$	$2.3\ 10^9$

Table D.3: Maximum impurity concentration of 15 keV H_2^+ at the depth where most of such ions stop in the silicon as a function of the proton beam energy.

As already told, in the reality less than 30% of the produced ionized molecules are H_2^+, therefore the concentration of impurities due to the implantation of hydrogen ions reduces by 1/3 (but same order of magnitude). The damage due to the number of H_2^+ (or H^+) implanted into the silicon detector can therefore be considered negligible.

D.2 Preliminary conclusion

The range of ionized hydrogen molecules and protons in a silicon detector 750 nm thick been calculated with SRIM. Following such results it will be possible to foresee the amplitude of the signal induced and compare it to experimental results performed at IPHI. Unfortunately no conclusion can be drawn on the range of heavier ionized molecules/ions.

Bibliography

[1] C A Thomas, F Belloni, and J Marroncle. Space charge studies for the ionisation profile monitors for the ess cold linac. In *Ibic*, pages 6–9, 2016.

[2] R Wanzenberg. Nonlinear Motion of a Point Charge in the 3D Space Charge Field of a Gaussian Bunch. Technical Report May, DESY, 2010.

[3] Ess technical design report. Technical report, ESS, 2013.

[4] K. Baraka, S. Biagi, A. Folkestad, J. Renner, H. Schindler, N. Shiell, I. Smirnov, R. Veenhof, and K. Zenker. *Garfield++ simulation of tracking detectors*.

[5] I.B. Smirnov. Modeling of ionization produced by fast charged particles in gases. *Nuclear Instruments and Methods in Physics Research Section A: Accelerators, Spectrometers, Detectors and Associated Equipment*, 554(13):474 – 493, 2005.

[6] H Paul and M Berger. Atomic and Molecular Data for Radiotherapy and Radiation Research. Technical Report May, 1995.

[7] J. F. Ziegler, M. D. Ziegler, and J. P. Biersack. SRIM - The stopping and range of ions in matter (2010). *Nuclear Instruments and Methods in Physics Research B*, 268:1818–1823, June 2010.